MycoKeys 26: 1–11 (2017)
doi: 10.3897/mycokeys.26.14506
http://mycokeys.pensoft.net

RESEARCH ARTICLE

A peer-reviewed open-access journal
MycoKeys
Launched to accelerate biodiversity research

Chlorovibrissea korfii sp. nov. from northern hemisphere and *Vibrissea flavovirens* new to China

Huan-Di Zheng[1], Wen-Ying Zhuang[1,2]

1 *State Key Laboratory of Mycology, Institute of Microbiology, Chinese Academy of Sciences, Beijing 100101, China* **2** *University of Chinese Academy of Sciences, Beijing 100049, China*

Corresponding author: *Wen-Ying Zhuang* (zhuangwy@im.ac.cn)

Academic editor: *A. Miller* | Received 13 Julne 2017 | Accepted 7 July 2017 | Published 4 August 2017

Citation: Zheng H-D, Zhuang W-Y (2017) *Chlorovibrissea korfii* sp. nov. from northern hemisphere and *Vibrissea flavovirens* new to China. MycoKeys 26: 1–11. https://doi.org/10.3897/mycokeys.26.14506

Abstract

A new species, *Chlorovibrissea korfii*, is described and illustrated, which is distinct from other members of the genus by the overall pale greenish apothecia 0.8–2.0 mm in diam. and 0.6–1.5 mm high, J+ asci 70–83 × 4.5–5.5 µm, and non-septate ascospores 44–52 × 1.2–1.5 µm. This is the first species of *Chlorovibrissea* reported from northern hemisphere. *Vibrissea flavovirens* is reported from China for the first time. Sequence analyses of the internal transcribed spacer of nuclear ribosomal DNA are used to confirm the affinity of the two taxa.

Key words

morphology, sequence analysis, taxonomy, Vibrisseaceae

Introduction

Vibrisseaceae was erected by Korf in 1990 to accommodate the genera *Vibrissea* Fr., *Chlorovibrissea* L.M. Kohn and *Leucovibrissea* (A. Sánchez) Korf. Members of the family are characterized by aquatic or semi-aquatic habitat, apothecia sessile to long stipitate, disc color range from whitish, yellowish, brownish, olivaceous to blackish green, ectal excipulum composed of textura globosa, textura angularis to textura prismatica, and filiform ascospores (Korf 1990). The three genera are distinguishable by the color of apothecia, structure of ectal excipulum and ascal apex apparatus (Korf 1990; Sandoval-Leiva et al. 2014). Besides the above three genera, *Acephala* Grünig

Copyright *Huan-Di Zheng, Wen-Ying Zhuang*. This is an open access article distributed under the terms of the Creative Commons Attribution License (CC BY 4.0), which permits unrestricted use, distribution, and reproduction in any medium, provided the original author and source are credited.

& T.N. Sieber and *Phialocephala* W.B. Kendr. known only by asexual states, are also included in the family (Kirk et al. 2008; Johnston et al. 2014). *Acephala* was erected for the non-sporulating species of *Phialocephala* that contain a small group of dark septate root endophytes (Grünig and Sieber 2005; Grünig et al. 2008; Grünig et al. 2009; Münzenberger et al. 2009; Wang et al. 2009; Day et al. 2012). About 80 species are currently accepted in the family, among which two species are in *Acephala*, six in *Chlorovibrissea*, one in *Leucovibrissea*, 33 in *Phialocephala*, and 36 in *Vibrissea* (Grünig et al. 2008; Kirk et al. 2008; Grünig et al. 2009; Münzenberger et al. 2009; Wang et al. 2009; Day et al. 2012; Johnston et al. 2014; Sandoval-Leiva et al. 2014; Index Fungorum 2017). The previous phylogenetic studies on the vibrisseaceous fungi showed that *Chlorovibrissea* and *Vibrissea* are not closely related, and the family was presumably polyphyletic (Wang et al. 2006; Sandoval-Leiva et al. 2014).

In China, only two Vibrisseaceous fungi were recorded, i.e. *V.* cf. *sporogyra* (Ingold) A. Sánchez from Hainan Province (Zhuang et al. 2002) and *V. truncorum* (Alb. & Schwein.) Fr. from Guizhou Province (He 1988). During our studies of the helotialean fungi from China, two newly collected specimens fit the circumscription of Vibrisseaceae and represent two species. Based on morphology and molecular data, one is proposed as a new species of *Chlorovibrissea*, and the other is identified as *V. flavovirens* (Pers.) Korf & J.R. Dixon which is new to China.

Materials and methods

Specimens were collected from Beijing and Yunnan Province in 2016, and apothecial gross morphology when fresh was photographed by a Canon PowerShot G16 digital camera. Dried apothecia were rehydrated with distilled water and sectioned at a thickness of 15 μm with a Yidi YD-1508A freezing microtome (Jinhua, China). Measurements were taken from longitudinal sections and from squash mounts in lactophenol cotton blue solution using an Olympus BH-2 microscope (Tokyo, Japan). Iodine reactions of ascus apparatus were tested in Melzer's reagent and Lugol's solution with or without 3% KOH solution pretreatment according to Baral (2009). Images were captured using a Canon G5 digital camera (Tokyo, Japan) attached to a Zeiss Axioskop 2 Plus microscope (Göttingen, Germany) for anatomical structure. Voucher specimens were deposited in the Herbarium Mycologicum Academiae Sinicae (HMAS). Name of the new species was formally registered in the database Fungal Names, one of the three official nomenclatural repositories for fungal names (Redhead and Norvell 2012).

Genomic DNA was extracted from dried apothecia using Plant Genomic DNA Kit (TIANGEN Biotech. Co., Ltd., Beijing, China). Materials were crushed in liquid nitrogen before extraction. The internal transcribed spacer of nuclear ribosomal DNA (ITS) were amplified and sequenced using primer pair ITS1 and ITS4 (White et al. 1990) according to Zheng and Zhuang (2016). Newly generated sequences were deposited in GenBank, and other sequences used in the phylogenetic analyses were retrieved from GenBank (Table 1). *Holwaya mucida* (Schulzer) Korf & Abawi was selected as

Table 1. Sequences used in this study.

Species	Strain/specimen	ITS
Acephala applanata Grünig & T.N. Sieber	CBS 109314	AY078146
A. macrosclerotiorum Münzenb. & Bubner	BB11_301_Ah_Pi_150506 (DNA46)	HM189696
Ascocoryne cylichnium (Tul.) Korf	VL272	JF440583
A. sarcoides (Jacq.) J.W. Groves & D.E. Wilson	CBS:309.71	HM152550
Chlorovibrissea albofusca (G.W. Beaton) Sandoval-Leiva, A.I. Romero & P.R. Johnst.	PDD 75692	AY789384
C. albofusca	PDD:88457	JN809648
C. bicolor (G.W. Beaton & Weste) L.M. Kohn	ICMP19895	KF924737
C. chilensis Sandoval-Leiva, A.i. Romero & P.R. Johnst.	PDD 99891	NR_132892
C. phialophora Samuels & L.M. Kohn 1989	PDD:83226	KF429261
C. korfii H.D. Zheng & W.Y. Zhuang	HMAS 275652	**KY924871***
Chlorovibrissea sp.	PDD70070	DQ257353
Hyaloscypha aureliella (Nyl.) Huhtinen	M235	EU940229
H. vitreola (P. Karst.) Boud.	M39	EU940231
Lachnum bicolor (Bull.) P. Karst.	ARON3113.P	AJ430394
L. virgineum. (Batsch) P. Karst.	3706	JF937586
Phialocephala aylmerensis J.B. Tanney & B. Douglas	DAOM C 250106	NR_136124
P. catenospora J.B. Tanney & B. Douglas	DAOM C 250108	NR_136122
P. dimorphospora W.B. Kendr.	CBS 300.62	NR_135931
Vibrissea filisporia (Bonord.) Korf & A. Sánchez	JLF2084	JX415338
V. flavovirens (Pers.) Korf & J.R. Dixon	MBH39316	AY789427
V. flavovirens	N/A	KF429257
V. flavovirens	HMAS 275653	**KY924872**
V. truncorum (Alb. & Schwein.) Fr.	PDD 99892	KF429259
V. truncorum (Alb. & Schwein.) Fr.	PDD 99893	KF429260
Uncultured *Vibrissea*	WPD-OTU-39	KT581681
Uncultured *Vibrissea*	WPW-OTU-33	KT581735
Chlorociboria aeruginosa (Oeder) Seaver ex C.S. Ramamurthi, Korf & L.R. Batra	PDD 81292	AY755360
Chlorociboria sp.	HMAS 273905	KY498614
Cudoniella clavus (Alb. & Schwein.) Dennis	BM18#13	AY789374
Dicephalospora aurantiaca (W.Y. Zhuang) W.Y. Zhuang & Z.Q. Zeng	HMAS 81363	DQ986483
Holwaya mucida (Schulzer) Korf & Abawi	B 70 0009352	DQ257357
Hymenoscyphus scutula (Pers.) W. Phillips	MBH29259	AY789432
Hyphodiscus hymeniophilus (P. Karst.) Baral	TNS:F-31802	AB546951
Ombrophila violacea (Hedw.) Fr.	WZ0024	AY789366
Roseodiscus rhodoleucus (Fr.) Baral	ARON2329.P	AJ430395

* Numbers in bold indicate sequences produced by this study

outgroup taxon. Alignment was generated and manually edited with BioEdit 7.0.5.3 (Hall 1999). Maximum parsimony (MP) and Neighbor-joining (NJ) analyses were carried out using PAUP*4.0b10 with parameters used by Zheng and Zhuang (2014). The

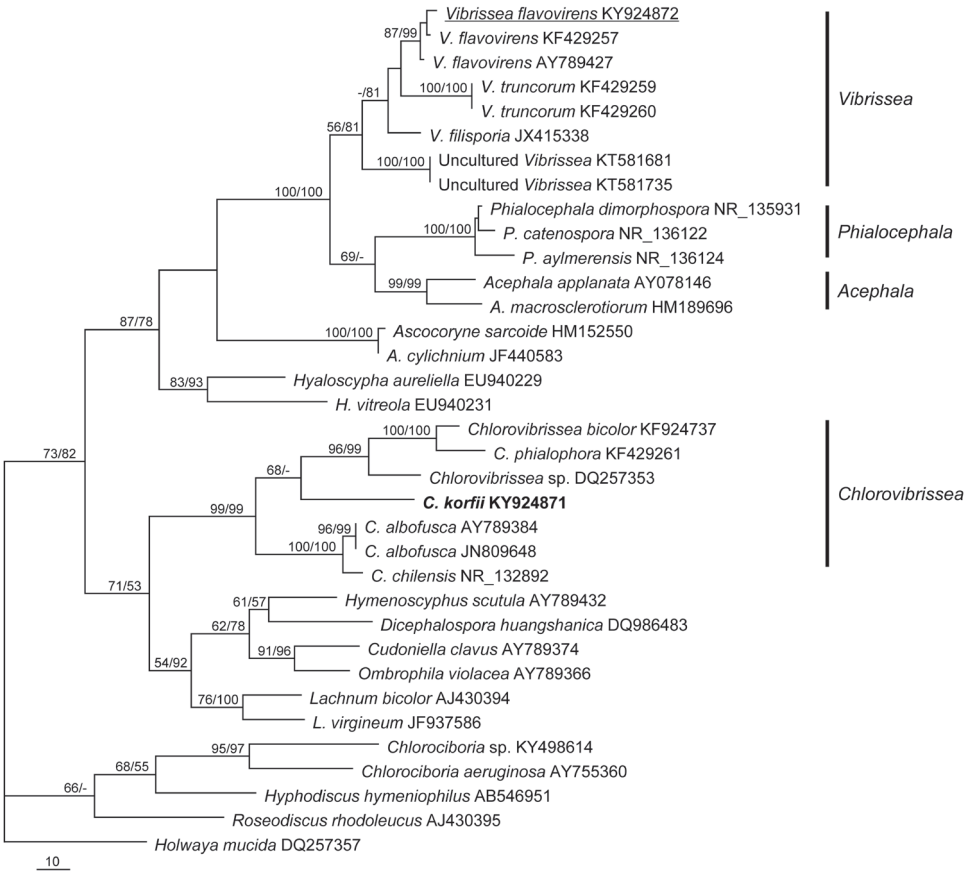

Figure 1. Phylogenetic affinity of *Chlorovibrissea korfii* and *Vibrissea flavovirens* inferred from maximum parsimony analysis of ITS sequences. Bootstrap values (≥50%) of MP and NJ are shown at nodes from left to right.

topological confidence of the NJ and MP trees was assessed with bootstrap analysis using 1,000 replications, each with 10 replicates of random stepwise addition of taxa. The resulting trees were viewed in TreeView 1.6.6 (Page 1996).

Results

Phylogenetic analyses

The ITS alignment consisted of 574 characters including gaps, of which 292 were constant, 52 were variable and parsimony-uninformative, and 230 were parsimony-informative. Forty-five equally most parsimonious trees were yielded by MP analysis (Tree length = 1085, Consistency index = 0.4719, Homoplasy index = 0.5281, Retention

index = 0.6739, Rescaled consistency index = 0.3180) and one of them was shown in Fig. 1. MP and NJ bootstrap proportions (BP) greater than 50% were labeled at the nodes. In the phylogenetic tree (Fig. 1), species of *Acephala*, *Chlorovibrissea*, *Phialocephala* and *Vibrissea* formed four well-supported clades corresponding to each genus, and three of them further clustered together with high supporting values except for *Chlorovibrissea*, which showed a distant relationship with others. The undescribed species appeared as a distinct terminal lineage within *Chlorovibrissea*. ITS sequences of *V. flavovirens* from the Chinese, North American and New Zealand materials were of high similarity (99%) and formed a well-supported terminal branch.

Taxonomy

Chlorovibrissea korfii **H.D. Zheng & W.Y. Zhuang, sp. nov.**
Fungal Names FN570451
Figure 2

Type. CHINA, Yunnan Province, Maguan County, 23°6.22'N, 104°19.75'E, alt. 1450 m, on moist rotten twig, 14 August 2016, X.H. Wang, S.H. Li, H.D. Zheng & S.C. Li YN16-151 (holotype: HMAS 275652).

Etymology. The specific epithet is in memory of the late distinguished mycologist Dr. R.P. Korf.

Description. Apothecia scattered or in cluster, discoid to slightly convex, stipitate, light greenish yellow, with hymenium and receptacle surface concolorous when fresh, 0.8–2.0 mm in diam. and 0.6–1.5 mm high, dried apothecial tissues with exudation of light yellow pigment in water; stipe cylindrical, with base dark, 0.4–1.0 mm high. Ectal excipulum of textura prismatica, non-gelatinous, 30–100 µm thick, hyphae parallel or lying at a low angle to receptacle surface, cells hyaline, with walls slightly thickened, terminal cells of external hyphae thin-walled, 8–25 × 3–7 µm. Medullary excipulum of textura porrecta to textura intricata, 30–300 µm thick, hyphae hyaline, 3–5 µm wide. Subhymenium not distinguishable. Hymenium 95–110 µm thick. Asci arising from simple septa, 8-spored, cylindrical, J+ in Melzer's reagent and Lugol's solution without KOH pretreatment, visible as two short blue lines, 70–83 × 4.5–5.5 µm. Ascospores filiform, tapering slightly from rounded apex to pointed base, hyaline, smooth, multiguttulate, non-septate, in fascicle, 44–52 × 1.2–1.5 µm. Paraphyses filiform, hyaline, unbranched, 1.5–2.0 µm wide, not exceeding the asci.

Notes. Six species have been recorded in the genus *Chlorovibrissea*. *Chlorovibrissea korfii* is different from any known species of the genus in both morphological and phylogenetic evidences. Morphologically, the diagnostic characteristic of the new species is the overall light greenish yellow apothecia. *Chlorovibrissea phialophora* Samuels & L.M. Kohn has ascospores of similar shape and size, but differs in apothecia stipitate-capitate, larger (2–5 mm in diam.) and dark green to nearly black, stipe longer (1–2.5 mm), asci larger (100–123 × 5–6 µm), and apical cells of ascospores forming subglobose to cylindrical phialides within the asci. The new fungus resembles *C. albofusca*

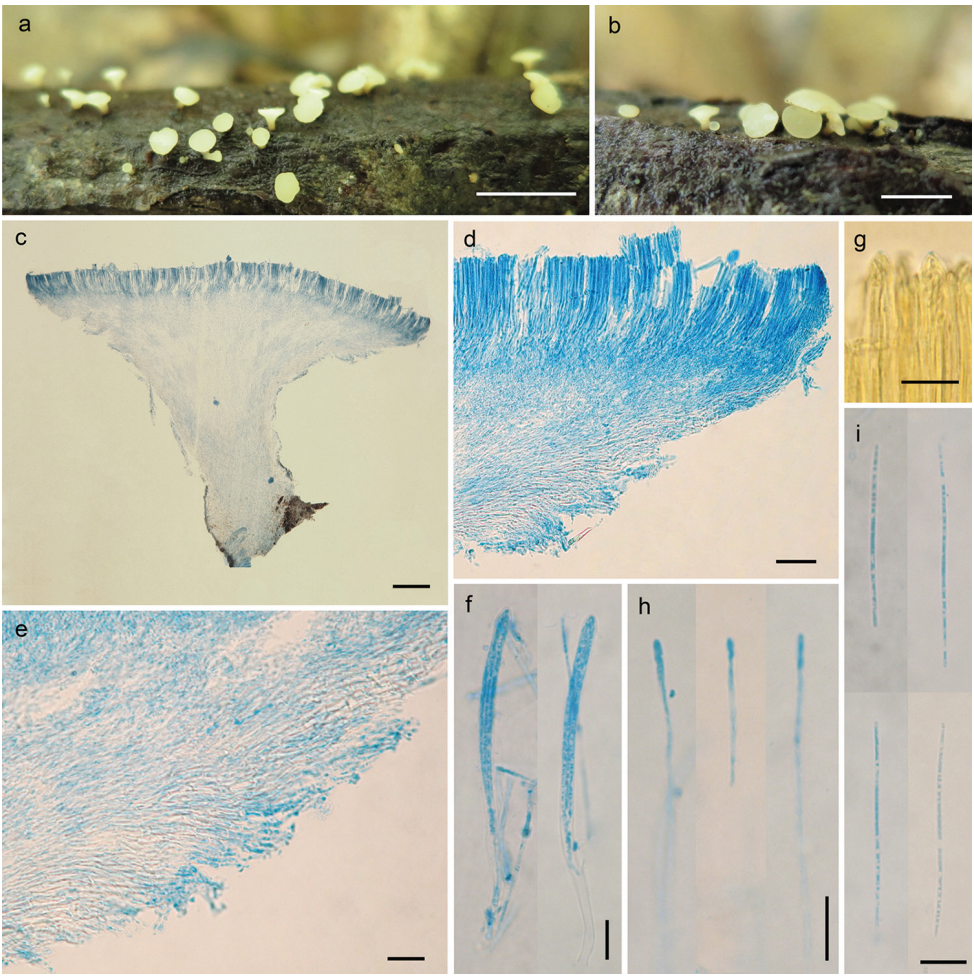

Figure 2. *Chlorovibrissea korfii* H.D. Zheng & W.Y. Zhuang (HMAS 275652, holotype). **a, b** Fresh apothecia on natural substrate **c** Longitudinal section of apothecium **d** Structure of margin, flank and hymenium **e** Excipular structure of flank **f** Asci **g** IKI reaction of apical rings **h** Paraphyses **i** Ascospores. Mouting media: **c–f, h, i** lactophenol cotton blue, **g** Lugol's solution. Scale bars: **a** = 5.0 mm, **b** = 2.0 mm, **c** = 200 μm, **d** = 40 μm, **e** = 20 μm, **f, h, i** = 10 μm, **g** = 5 μm.

(G.W. Beaton) Sandoval-Leiva, A.I. Romero & P.R. Johnst. in having pale colored apothecia, but the latter has larger apothecia (up to 4 mm diam. when dry) with hemispherical cap, larger ectal excipular cells (up to 35 × 15 μm) lying at a high angle to the outer surface, larger asci (195–225 × 7.5–8.5 μm), and larger ascospores (95–115 × 1.5–2 μm). Phylogenetically, *C. korfii* appeared to be related to *C. bicolor*, *C. phialophora* and *Chlorovibrissea* sp. (DQ257353) in the ITS tree (Fig. 1). *Chlorovibrissea bicolor* is different from the new species in apothecia with yellow, subglobose or lobed head up to 4 mm in diam. and a dark green tomentose stalk, larger asci (132–155 × 5–6.5 μm) and ascospores (53–60 × 1.5–2 μm).

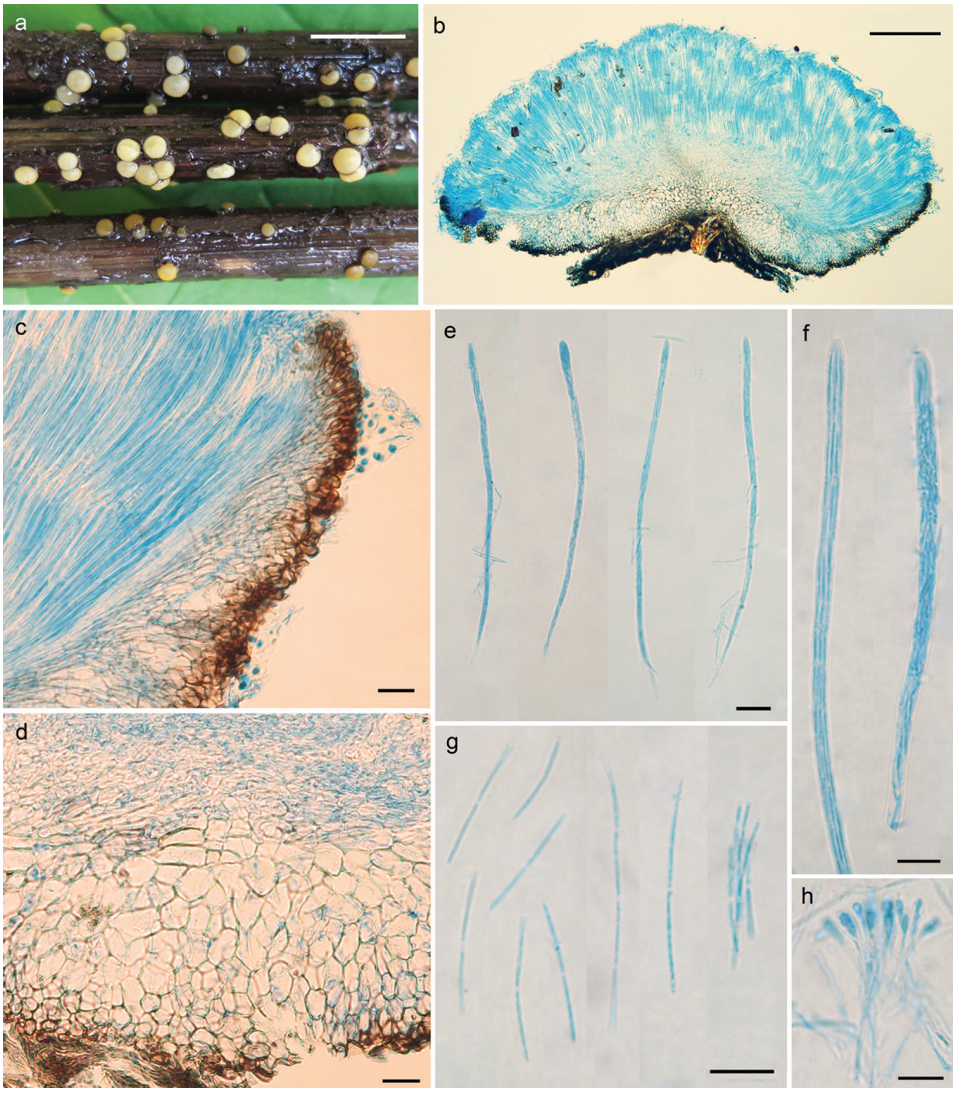

Figure 3. *Vibrissea flavovirens* (Pers.) Korf & J.R. Dixon (HMAS 275653). **a** Fresh apothecia on natural substrate **b** Longitudinal section of apothecium **c** Structure of margin and upper flank **d** Excipular structure of lower part and near base **e, f** Asci **g** Fragments of ascospores **h** Paraphyses. Mouting medium: **b–h** lactophenol cotton blue. Scale bars: **a** = 5.0 mm, **b** = 200 µm, **c–e** = 20 µm, **f–h** = 10 µm.

***Vibrissea flavovirens* (Pers.) Korf & J.R. Dixon, Mycotaxon 1(2): 134, 1974.**
Figure 3

≡ *Peziza flavovirens* Pers., Mycol. Eur. (Erlanga) 1: 323, 1822.

Description. Apothecia scattered or in cluster, slightly convex, sessile, hymenium surface light yellow, 0.5–1.5 mm in diam., receptacle surface brownish. Ectal excipulum

of textura angularis to textura prismatica, non-gelatinous, lying at a high angle to the outer surface, 30–140 μm thick, inner cells subhyaline to light brown and outer cells brown, 15–30 × 9–14 μm. Medullary excipulum of textura angularis to textura prismatica, 50–150 μm thick, cells hyaline, 5–16 × 4–6 μm. Subhymenium not distinguishable. Hymenium 280–290 μm thick. Asci arising from simple septa, 8-spored, cylindrical, J– in Melzer's reagent and Lugol's solution with or without KOH pretreatment, 227–241 × 5–6 μm. Ascospores filiform, hyaline, smooth, multiguttulate, multi-septate, break into several pieces, in fascicle, 192–208 × 1.5–2.0 μm. Paraphyses filiform, slightly enlarged at the apex, hyaline, branched at upper portion, 3.0–5.0 μm wide at apex and 2.0–2.5 μm wide blow, exceeding the asci by 20–35 μm.

Specimen examined. CHINA, Beijing, Yunmeng Moutain, 40°33.00"N, 116°40.80'E, alt. 800 m, on herbaceous stem of unidentified plant submerged in water, 10 July 2016, H.D. Zheng, Z.Q. Zeng, X.C. Wang, K. Chen & Y.B. Zhang 10660 (HMAS 275653).

Notes. This is the first report of *V. flavovirens* from China. The fungus was originally described from France and currently known in Denmark, Germany, Madeira, New Zealand, UK and USA (Korf 1974; Iturriaga 1995; Sandoval-Leiva et al. 2014). The Chinese collection agrees with the description of *V. flavovirens* by Iturriaga (1995). The ITS sequence of the Chinese specimen shared high similarity (99%) with those of North American and New Zealand materials, and the sequences of materials from different geographic regions formed a strongly supported terminal branch (Fig. 1).

Discussion

The three sexual genera in Vibrisseaceae are mainly differentiated by color of apothecia and structure of ectal excipulum. The excipular cells of *Vibrissea* are more or less angular to globose and lying at a high angle to the receptacle surface, while those of *Chlorovibrissea* and *Leucovibrissea* are rectangular and axes of cells are nearly parallel to the receptacle surface. *Chlorovibrissea* is different from *Leucovibrissea* in having greenish apothecia instead of the whitish ones. Differences between *Chlorovibrissea* and *Vibrissea* were found in ascal apex, which is round to somewhat truncate and with the apical ring placed subapically in the former genus, while that of the latter is acute with apical ring placed at the tip (Sandoval-Leiva et al. 2014). The ascal apex of *C. korfii* is somewhat conical and with apical ring placed apically, broader at tip and narrower downward (Fig. 2g), unlike that of other known *Chlorovibrissea* species. Further studies are needed to evaluate whether ascal apical apparatus is phylogenetically informative in Vibrisseaceae.

Chlorovibrissea was assumed to have a southern hemisphere distribution because species of the genus was never reported from north hemisphere (Kohn 1989; Sandoval-Leiva et al. 2014). The discovery of *C. korfii* from China expands the distribution of the genus to north hemispheres, which might break the assumption "the origin of the southern hemisphere vibrisseaceous fungi could be independent from the northern hemisphere representative" (Wang et al. 2006).

In the family Vibrisseaceae, sequence data of *Leucovibrissea* are not available. The two asexual genera Vibrisseaceae are *Phialocephala* and *Acephala*. Due to the heterogeneity of *Phialocephala*, only the type species, *P. dimorphospora*, and two closely related taxa were included in our phylogenetic analyses. *Vibrissea*, *Acephala* and *Phialocephala* clustered as a highly supported group (MPBP/NJBP = 100%/100%, Fig. 1), while *Chlorovibrissea* were distantly related (Fig. 1). The results coincided with those of the previous studies (Wang et al. 2006; Sandoval-Leiva et al. 2014), in which *Chlorovibrissea* and *Vibrissea* appeared as two separate clades. As to relationships among species of *Chlorovibrissea*, *C. albofusca* and *C. chilensis* were very closely related (MPBP/NJBP = 100%/100%), and *C. korfii* is associated with the rest species of the genus, which did not receive a reasonable support (MPBP = 81%). The interspecific relationships of *Vibrissea* were hardly demonstrated (Fig. 1) since very few species were sampled.

The two asexual genera are recognizable and associated each other with low supports (Fig. 1). The two existing species of the genus *Acephala* were sisters (Fig. 1, MPBP/NJBP = 99%/99%). *Acephala* was thought to be congeneric with *Phialocephala* by some authors, and differentiated only by the lack of observed sporulation in culture (Grünig et al. 2009; Münzenberger et al. 2009; Tanney et al. 2016). *Phialocephala* species are commonly isolated as dark-septate endophytes from coniferous tree roots or from decomposing wood (Menkis et al. 2004), and attributed to Vibrisseaceae mainly based on sequence data (Wang et al. 2006; Kirk et al. 2008). Connections of some *Phialocephala* species with *Mollisia* or mollisioid sexual states were reported recently (Grünig et al. 2009; Tanney et al. 2016). It seems that a lot of work needs to be done to establish the generic concepts.

In conclusion, Vibrisseaceae established based on morphology is quite possibly polyphyletic. Sequence data of *Leucovibrissea* are desirable to get a more comprehensive outline of the family. *Phialocephala* s.l. is heterogeneous. Its generic concept needs to be clarified. As more sequences of vibrisseaceous fungi are available, the circumscription of the family will become monophyletic.

Acknowledgements

This work was supported by the National Natural Science Foundation of China (nos. 31570018, 31300021). The authors would like to thank Dr. X.H Wang and Dr. S.H. Li for their invaluable help during the field work.

References

Baral H-O (2009) Iodine reaction in Ascomycetes: why is Lugol's solution superior to Melzer's reagent? http://www.gbif-mycology.de/HostedSites/Baral/IodineReaction.htm. [Accessed on 18 March 2011]

Day MJ, Hall JC, Currah RS (2012) Phialide arrangement and character evolution in the helotialean anamorph genera *Cadophora* and *Phialocephala*. Mycologia 104: 371–381. https://doi.org/10.3852/11-059

Grünig C, Duò A, Sieber T, Holdenrieder O (2008) Assignment of species rank to six reproductively isolated cryptic species of the *Phialocephala fortinii* s.l.-*Acephala applanata* species complex. Mycologia 100: 47–67. https://doi.org/10.1080/15572536.2008.11832498

Grünig CR, Queloz V, Duò A, Sieber TN (2009) Phylogeny of *Phaeomollisia piceae* gen. sp. nov.: a dark, septate, conifer-needle endophyte and its relationships to *Phialocephala* and *Acephala*. Mycological Research 113: 207–221. https://doi.org/10.1016/j.mycres.2008.10.005

Grünig CR, Sieber TN (2005) Molecular and phenotypic description of the widespread root symbiont *Acephala applanata* gen. et sp. nov., formerly known as Dark-Septate Endophyte Type 1. Mycologia 97: 628–640. https://doi.org/10.1080/15572536.2006.11832794

Hall TA (1999) BioEdit: a user-friendly biological sequence alignment editor and analysis program for Windows 95/98/NT. Nucleic Acids Symposium Series 41: 95–98.

He SC (1988) A new record genus and species of aquatic cup fungi from China. Acta Mycologica Sinica 7: 120–121.

Index Fungorum (2017) http://www.indexfungorum.org/names/Names.asp. [Accessed on 13 April 2017]

Iturriaga T (1995) A preliminary discomycete flora of Macaronesia: part 9, Vibrisseaceae. Mycotaxon 54: 1–17.

Johnston PR, Seifert KA, Stone JK, Rossman AY, Marvanová L (2014) Recommendations on generic names competing for use in Leotiomycetes (Ascomycota). IMA Fungus 5: 91–120. https://doi.org/10.5598/imafungus.2014.05.01.11

Kirk PM, Cannon PF, Minter DW, Stalpers JA (2008) Dictionary of the Fungi. 10th edition. CABI, Wallingford, 1–771.

Kohn LM (1989) *Chlorovibrissea* (Helotiales, Leotiaceae), a new genus of Austral Discomycetes. Memoirs of the New York Botanical Garden 49: 112–118.

Korf RP (1974) *Peziza flavovirens*, an older name for *Vibrissea pezizoides*. Mycotaxon 1: 134.

Korf RP (1990) Discomycete systematics today: a look at some unanswered questions in a group of unitunicate ascomycetes. Mycosystema 3: 19–27.

Menkis A, Allmer J, Vasiliauskas R, Lygis V, Stenlid J, Finlay R (2004) Ecology and molecular characterization of dark septate fungi from roots, living stems, coarse and fine woody debris. Mycological Research 108: 965–973. https://doi.org/10.1017/S0953756204000668

Münzenberger B, Bubner B, Wöllecke J, Sieber TN, Bauer R, Fladung M, Hüttl RF (2009) The ectomycorrhizal morphotype Pinirhiza sclerotia is formed by *Acephala macrosclerotiorum* sp. nov., a close relative of *Phialocephala fortinii*. Mycorrhiza 19: 481–492. https://doi.org/10.1007/s00572-009-0239-0

Page RDM (1996) Treeview: An application to display phylogenetic trees on personal computers. Comp Appl Biosci 12: 357–358.

Redhead SA, Norvell LL (2012) MycoBank, Index Fungorum, and Fungal Names recommended as official nomenclatural repositories for 2013. IMA Fungus 3(2): 44–45.

Sandoval-Leiva P, Carmaran CC, Park D, Romero AI, Johnston PR (2014) Vibrisseaceous fungi from the southern hemisphere, including *Chlorovibrissea chilensis* (Helotiales, incertaesedis) sp. nov. Mycologia 106: 1159–1167. https://doi.org/10.3852/14-009

Wang W, Mcghee D, Gibas CFC, Tsuneda A, Currah RS (2009) *Phialocephala urceolata*, sp. nov., from a commercial, water-soluble heparin solution. Mycologia 101: 136–141. https://doi.org/10.3852/08-066

Wang Z, Johnston PR, Takamatsu S, Spatafora JW, Hibbett DS (2006) Toward a phylogenetic classification of the Leotiomycetes based on rDNA data. Mycologia 98: 1065–1075. https://doi.org/10.1080/15572536.2006.11832634

White TJ, Bruns T, Lee S, Taylor J (1990) Amplification and direct sequencing of fungal ribosomal RNA genes for phylogenetics. In:Innis MA, Gelfand DH, Snisky JJ, White TJ (Eds) PCR Protocols: a guide to methods and applications. Academic Press, London, 315–322. https://doi.org/10.1016/B978-0-12-372180-8.50042-1

Zheng H-D, Zhuang W-Y (2014) *Hymenoscyphus albidoides* sp. nov. and *H. pseudoalbidus* from China. Mycol Prog 13: 625–638. https://doi.org/10.1007/s11557-013-0945-z

Zheng H-D, Zhuang W-Y (2016) Two new species of *Crocicreas* (Helotiaceae, Ascomycota) revealed by morphological and molecular data. Phytotaxa 272: 149–156. https://doi.org/10.11646/phytotaxa.272.2.6

Zhuang W, Yu Z, Zhang Y, Ye M (2002) Some new species and new records of discomycetes from China. IX. Mycotaxon 81: 27–34.

MycoKeys 26: 13–24 (2017)
doi: 10.3897/mycokeys.26.14591
http://mycokeys.pensoft.net

RESEARCH ARTICLE

A peer-reviewed open-access journal
MycoKeys
Launched to accelerate biodiversity research

Read quality-based trimming of the distal ends of public fungal DNA sequences is nowhere near satisfactory

R. Henrik Nilsson[1,2], Marisol Sánchez-García[3], Martin Ryberg[4], Kessy Abarenkov[5], Christian Wurzbacher[1,2], Erik Kristiansson[6]

1 *Department of Biological and Environmental Sciences, University of Gothenburg, Box 461, 405 30 Göteborg, Sweden* **2** *Gothenburg Global Biodiversity Centre, Box 461, SE-405 30 Göteborg, Sweden* **3** *Department of Biology, Clark University, 950 Main St., Worcester, MA 01610-1477, USA* **4** *Department of Organismal Biology, Uppsala University, Norbyv. 18D, 75236 Uppsala, Sweden* **5** *Natural History Museum, University of Tartu, Vanemuise 46, Tartu 51014, Estonia* **6** *Department of Mathematical Statistics, Chalmers University of Technology, Göteborg, Sweden*

Corresponding author: *R. Henrik Nilsson* (henrik.nilsson@bioenv.gu.se)

Academic editor: *I. Schmitt* | Received 19 June 2017 | Accepted 28 July 2017 | Published 14 August 2017

Citation: Nilsson RH, Sánchez-García M, Ryberg M, Abarenkov K, Wurzbacher C, Kristiansson E (2017) Read quality-based trimming of the distal ends of public fungal DNA sequences is nowhere near satisfactory. MycoKeys 26: 13–24. https://doi.org/10.3897/mycokeys.26.14591

Abstract

DNA sequences are increasingly used for taxonomic and functional assessment of environmental communities. In mycology, the nuclear ribosomal internal transcribed spacer (ITS) region is the most commonly chosen marker for such pursuits. Molecular identification is associated with many challenges, one of which is low read quality of the reference sequences used for inference of taxonomic and functional properties of the newly sequenced community (or single taxon). This study investigates whether public fungal ITS sequences are subjected to sufficient trimming in their distal (5' and 3') ends prior to deposition in the public repositories. We examined 86 species (and 10,584 sequences) across the fungal tree of life, and we found that on average 13.1% of the sequences were poorly trimmed in one or both of their 5' and 3' ends. Deposition of poorly trimmed entries was found to continue through 2016. Poorly trimmed reference sequences add noise and mask biological signal in sequence similarity searches and phylogenetic analyses, and we provide a set of recommendations on how to manage the sequence trimming problem.

Key words

Molecular identification, DNA barcoding, database curation, Sanger sequencing, high-throughput sequencing, molecular ecology

Copyright *R. Henrik Nilsson et al.* This is an open access article distributed under the terms of the Creative Commons Attribution License (CC BY 4.0), which permits unrestricted use, distribution, and reproduction in any medium, provided the original author and source are credited.

Introduction

Molecular (DNA-based) species identification is the process by which newly generated DNA sequences are examined for taxonomic affiliation and sometimes functional aspects by comparison to reference sequences of firmly established taxonomic origin. It is a powerful tool to identify organisms, particularly those with few or no discriminatory morphological characters and those with cryptic or inconspicuous life styles (Pečnikar and Buzan 2014). Fungi are one such group (Stajich et al. 2009). Molecular exploration of substrates such as soil, water, and even household dust from the built environment has revealed a spectacular diversity of hitherto unrecognized fungal lineages (Grossart et al. 2016, Nilsson et al. 2016, Abarenkov et al. 2016), and recent estimates put the number of extant fungal species at upwards of 6 million (Blackwell 2011, Taylor et al. 2014). The number of recognized, validly described species, in contrast, stands at ~135,000 (http://www.speciesfungorum.org, July 2017). Fruiting bodies or other tangible somatic structures are not known for any of the 40 previously unknown fungal lineages examined by Tedersoo et al. (2017), and at present DNA-based methods represent the only way to approach the taxonomic affiliation of these and other lineages.

Several factors combine to make molecular identification of fungi complicated. In addition to the lack of reference sequences for more than 99% of the estimated number of extant species of fungi, technical complications such as chimera formation and low read quality may introduce noise and bias to such efforts (Hyde et al. 2013, Kõljalg et al. 2013). To some extent, software tools are available to exercise some degree of control over these complications (e.g., Edgar et al. 2011, Bengtsson-Palme et al. 2013). Furthermore, many – perhaps even most – researchers seem to be aware of the need to approach existing as well as newly generated sequences in a critical way (e.g., Nilsson et al. 2012, Alm Rosenblad et al. 2016), which nevertheless does not appear to prevent substandard entries from being deposited in the databases of the International Nucleotide Sequence Database Collaboration (INSDC: GenBank, ENA, and DDBJ, Schoch et al. 2014, Cochrane et al. 2016). Such substandard INSDC entries may skew research efforts through, e.g., BLAST sequence similarity searches (Altschul et al. 1997) or inclusion in multiple sequence alignments and phylogenetic analyses.

One aspect of sequence reliability that remains largely unexplored is quality trimming of the distal (approximately 25 bases at the very 5' and 3') ends of Sanger sequences. Owing to the nature of the Sanger sequencing process, the very first bases are often hard to resolve due to the presence of un-incorporated nucleotides and leftover primers. Similarly, the signal-to-noise ratio typically drops with the length of the amplicon in that it becomes increasingly difficult to separate amplicons of near-identical lengths from each other on the electrophoresis gel. Thus, an important part of Sanger sequencing is to inspect the resulting chromatograms and remove any noisy distal sequence parts in the newly generated sequence data. This step is, however, sometimes overlooked. When working with INSDC data for fungal molecular identification and sequence analysis purposes, we regularly come across entries whose distal ends appear to be very poorly trimmed. They may feature extended homopolymer regions (e.g.,

AAAAAAAAA…) or stretches of seemingly random bases that are not found in other conspecific sequences (Nilsson et al. 2012). These potentially noisy sequence ends make it difficult to judge BLAST results: are the mismatches in the distal ends of sequences due to actual biological (nucleotide) differences, or is the reason for the mismatches simply low read quality owing to poor trimming of the reference sequences? There is no direct way of knowing, although clues can perhaps be gleaned from the BLAST alignment and comparison with other conspecific sequences. We fear that, in many cases, researchers will not ponder this question, but will rather assume (or will use automated sequence processing tools that assume) that the mismatches observed are of a biological nature. This will translate into compromised molecular identification, suboptimal assignment of taxonomic affiliations, and unsatisfactory use of sequence data.

The problem is of particular concern for the nuclear ribosomal internal transcribed spacer (ITS) region, the formal fungal barcode and the most popular genetic marker for assessing the taxonomic composition of fungal communities (Schoch et al. 2012, Lindahl et al. 2013). This marker is used by hundreds of studies annually, such that the ramifications of poorly trimmed reference sequences could taint the results of numerous studies each year (cf. Gilks et al. 2002). In an effort to assess the extent of poor sequence trimming in the public sequence repositories, we compared the ITS sequences from 86 fungal (draft) genomes with the public fungal ITS sequences from the same species in the INSDC. We found that in many cases, researchers do not seem to have applied stringent sequence trimming; indeed, in many cases, researchers do not appear to have inspected the chromatograms at all before depositing the sequence data in the INSDC. We conclude by offering a set of observations and recommendations to alleviate the sequence trimming problem in present and future molecular research efforts.

Materials and methods

Retrieval of reference ITS sequences from genomes

The ribosomal operon is regularly left out from genome sequencing efforts due to assembly difficulties (Schoch et al. 2014, Hibbett et al. 2016), such that there is no straightforward way to obtain the ITS region from all existing fungal genomes (as has been reported for other genes, Bai et al. (2015)). We therefore used BLAST in the NCBI Whole Genome Shotgun database (https://www.ncbi.nlm.nih.gov/genbank/wgs/) to identify fully assembled ribosomal regions, using the very conserved 5.8S gene of the ITS region as the BLAST seed. Of the 130 matches returned, 86 were found to represent full-length ITS regions of distinct species that were also represented by at least one reasonably full-length Sanger-derived ITS sequence in the INSDC. In addition to the full ITS region, we kept 50 bases of the upstream nuclear ribosomal small subunit (nSSU/18S) gene and 50 bases of the downstream nuclear ribosomal large subunit (nLSU/28S) gene in the genome-derived ITS sequences to guide the subsequent alignment step.

Retrieval of INSDC sequences

For each of the 86 species (spanning 3 fungal phyla and 29 orders, Suppl. material 1), we downloaded all reasonably full-length ITS sequences from the INSDC using the NCBI query phrase "Species name[ORGN] AND 5.8S[TITL] AND 200:900[SLEN]". We were specifically interested in sequences generated using the traditional ITS1/ITS1F and ITS4/ITS4B primer sets (cf. Tedersoo et al. 2015) since sequences of this coverage are frequently used in DNA barcoding and systematics efforts (Lindahl et al. 2013). Each set of conspecific sequences (the genome-derived sequence plus the conspecific INSDC sequences) was aligned separately in MAFFT 7.307 (Katoh and Standley 2013), and sequences found to contain more than 50 bases of SSU or more than 50 bases of LSU were excluded. Similarly, sequences found to lack more than 50 bases of the 5' end of the ITS1 region, or more than 50 bases of the 3' end of the ITS2 region, were discarded. Alignments were adjusted manually, as needed, following Hyde et al. (2013). Sequences found to be chimeric, taxonomically misidentified, or the subject of other severe technical complications were removed from the alignments prior to statistical analysis. Wherever we found evidence of significant taxonomic variation (e.g., cryptic species) in the alignments, we removed all sequences (alleles) that we deemed to come from a different cryptic species/allele compared to the genome-derived sequence in question. In this study we sought to compare sequence variation in the context of poor sequence trimming rather than in the context of major sequencing artifacts, cryptic species, or allelic divergence.

Multiple sequence alignment and analysis

We went through each position in each of the alignments, starting from the 50th-to-last base of the SSU to the 50th base of LSU, and noted the proportion of INSDC sequences that produced a different nucleotide base from that of the corresponding genome-derived ITS sequence. All three of DNA base mismatches, gaps, and DNA ambiguity symbols (Cornish-Bowden 1985) were counted as mismatches. For each sequence in the alignment, we calculated the dissimilarity (proportion of mismatches) as a function of its relative position. The dissimilarities of the 86 species were then combined using a weighted average with weights proportional to the total number of available sequences for each species. The standard errors were calculated based on the corresponding weighted sample standard deviation. To examine the average age (NCBI date of last modification) of the poorly trimmed sequences, all sequences with at least 5% average dissimilarity among the 5% of its first bases or 5% of its last bases were classified as "potentially poorly trimmed", and their date of NCBI modification was assessed. The association between year and proportion of "potentially poorly trimmed" sequences was examined using overdispersed Poisson rate regression. The relative number of "potentially poorly trimmed" sequences was used as the response variable and time (year) as covariate. All statistical analyses were done in R 3.2.1 (R Core Team 2017).

Results

Multiple sequence alignment

The 86 multiple sequence alignments, each covering at most 50 bases of the SSU, the full ITS region (minus at most 50 bases of the 5' end of ITS1 and/or 50 bases of the end of ITS2), and at most 50 bases of the LSU, are provided in Suppl. material 2. The average length of the alignments was 648 bases (SD: 90, min: 416, max: 941), and the average number of sequences was 123 (SD: 219, min: 1, max: 1586).

Read quality variation

The plotting of disagreements with respect to the genome-derived sequences revealed that insufficient trimming of sequence data seems to be a widespread problem (Figs 1–2). An average of 13.1% of the sequences (SD: 19.6%) in each alignment were classified as "potentially poor trimmed", i.e. they showed at least 5% dissimilarity compared to the corresponding genome sequence over the first or last 5% of the aligned bases. For the remaining (non-distal) bases, those values were down to 0.22% (SD: 0.90%). The dissimilarity was found to be 7.9% and 5.3% in the 5' and 3' ends, respectively (Fig. 2b–c). The proportion of potentially poorly trimmed sequences was consistently high over the years 1997-2016, with a weak but significantly increasing trend ($p=0.0291$, Fig. 3).

Discussion

We provide data to suggest that many public DNA sequences are poorly trimmed in their distal parts. The fact that poorly trimmed sequences continue to be deposited through 2016 furthermore suggests that this problem will not go away by itself over time. We hope that the present paper will serve as an eye-opener, both for researchers who risk using the poorly trimmed data for molecular identification and for researchers generating and depositing sequences in public sequence repositories. The way it is now, these sequences may confound sequence similarity searches by falsely suggesting that two sequences (biological entities) are less similar than what really is the case. This reduces the precision in taxonomic and functional assessment – whether manual or carried out through some software pipeline – of newly generated sequences. Other kinds of sequence analysis, such as phylogenetic analyses, will similarly be distorted by poorly trimmed sequences.

Fortunately, managing read quality in Sanger sequences is fairly straightforward. The chromatograms, indicating the relative signal strength for each of the four purines/pyrimidines C, T, A, and G for each position in the sequence, are a key resource in this pursuit. Brief guidelines for how chromatograms should be processed are available in Hyde et al. (2013) and through various textbooks, online tutorials, and troubleshooting guides (e.g., Kearse et al. 2012, Green and Sambrook 2012). Trying to squeeze out

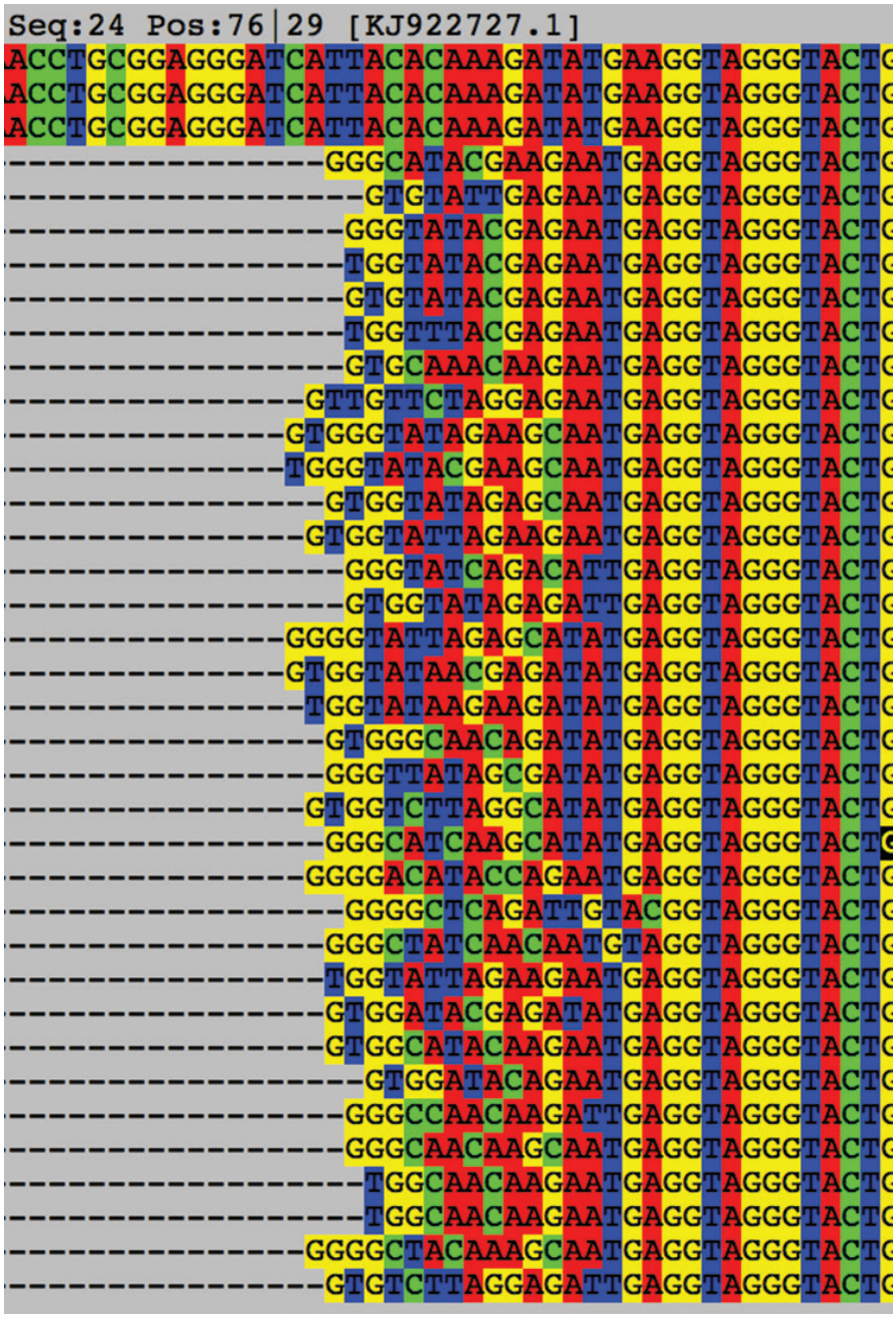

Figure 1. Example of poorly trimmed sequences (sequence four and on) from the species *Setosphaeria turcica*. The 5' end of the alignment is shown, and the poorly trimmed sequences cover the last ~5 bases of SSU and the immediate start of ITS1. The topmost sequence is genome-derived, and sequences two and three are regular Sanger sequences retrieved from the INSDC from other studies than the one with the poorly trimmed sequences (sequences four and on). SeaView v. 4 (Gouy et al. 2010) was used to visualize the alignment.

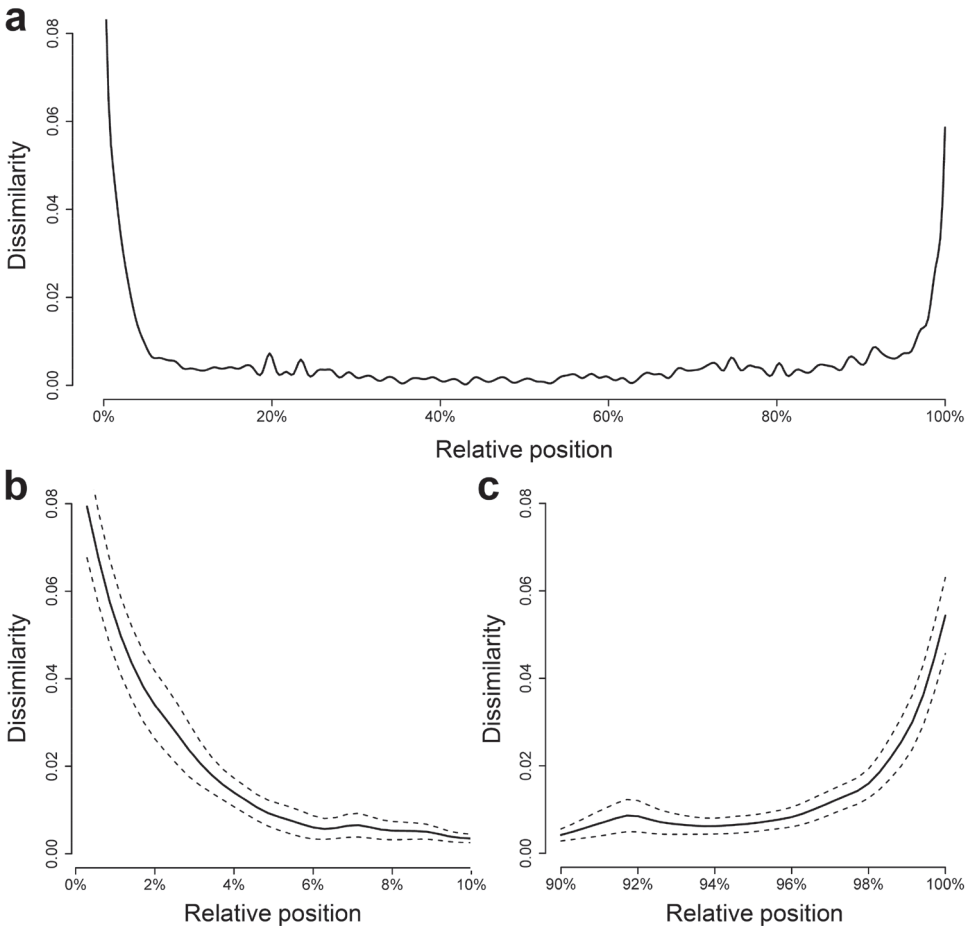

Figure 2. Public fungal ITS sequences are subjected to insufficient trimming in their distal ends. Panel a shows the dissimilarity (y-axis) as a function of the relative sequence position (x-axis). The plot is based on 10,584 sequences from 86 species. Panel b and c show zoom-ins of the 5' and 3' ends, respectively. Dashed lines indicate point-wise standard errors.

extra information from chromatograms by progressing too far in the 5' or 3' ends is not a good idea, and researchers should make it a habit to crop sequence ends aggressively. Generally speaking, habitually trying to salvage sequences with chromatograms of modest overall quality is not likely to be in the best interest of science. In most cases, it would appear to be better to re-process and re-sequence the material using other DNA extraction protocols, primers, or PCR conditions (cf. Larsson and Jacobsson 2004, Young et al. 2014, Lorenz et al. 2017). Finally, sequence similarity searches using BLAST may be used to get an idea of the technical quality of newly generated sequences (cf. Hyde et al. 2013), including at least cursory inspection of whether the distal ends of sequences are trimmed well enough. BLAST is, however, a somewhat blunt tool when it comes to assessing the read quality of sequence ends and we recommend it as a complement to,

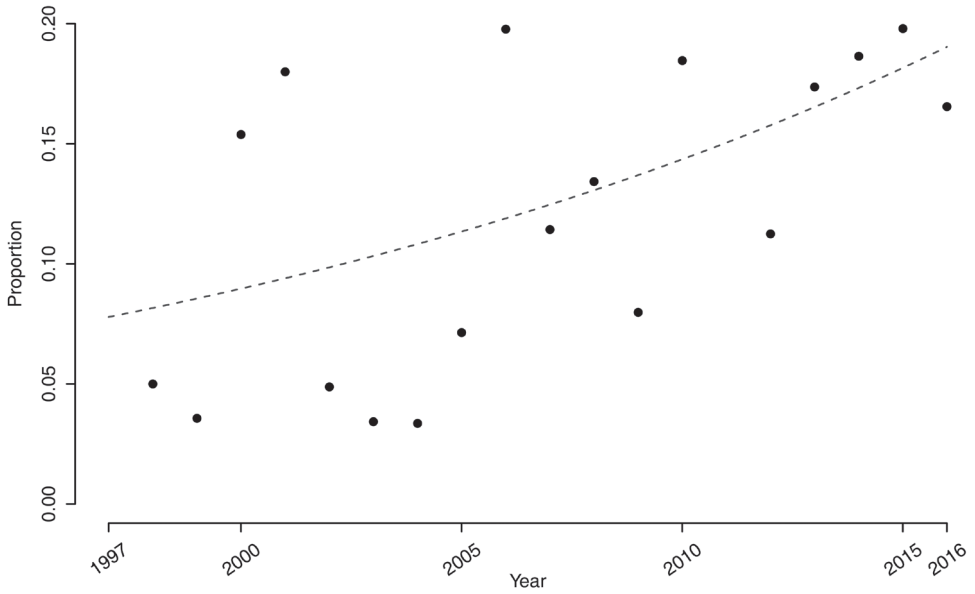

Figure 3. The proportion of poorly trimmed (y-axis) fungal ITS sequences submitted to the INSDC does not decrease over time (x-axis). The regression line (dashed), which was derived by overdispersed Poisson rate regression, shows a weak but significant increasing trend (yearly relative increase of 0.047, p=0.0291).

rather than as a replacement of, manual inspection of chromatograms. NCBI recently launched a unified system for multiple rRNA submission types, the Submission Portal (https://submit.ncbi.nlm.nih.gov/). This includes an ITS submission wizard specifically tailored to provide various verification steps that should decrease the likelihood of low quality submissions. This includes the use of ITSx (Bengtsson-Palme et al. 2013) to improve annotation, vector screening and automatic trimming, plus/minus mis-assembly checks, and trimming or removal of sequences with a high number of ambiguities. Hopefully, this will raise the awareness on part of sequence authors of the need to screen sequence data for quality issues prior to deposition.

In this study we show that incomplete (or lack of) trimming of sequence ends remains abundant in molecular mycology. Although this was expected based on our experience, this is the first study to provide at least an initial estimate of the magnitude of the problem. We used genome-derived ITS sequences from 86 fungal species from 29 different orders in our pursuit, such that we think that it is reasonable to extrapolate our findings to the fungal kingdom at large. Furthermore, we cannot think of any reason why this would be a uniquely fungus-specific problem, and we consider that our findings in fact may hold true for Sanger sequences from all genes and groups of organisms, possibly excluding groups and genes that only a few meticulous researchers have worked on. We would, however, like to stress that we provide estimates rather than hard facts. Our approach relied on genome-derived ITS sequences, and we quantified deviations from the genome sequences among conspecific ITS sequences in the INSDC as assessed through species names (Latin binomials). However, some degree

of deviation from the genome-derived sequences is expected, since intraspecific ITS variation may reach 3% or in some cases more (Schoch et al. 2012, Garnica et al. 2016). Similarly, the multicopy nature of the ITS region is a potential complication in that we may inadvertently have used a rare and perhaps deviant genome ITS copy and compared it to more common ITS copies (cf. Lindner et al. 2013). That said, such intraspecific or intragenomic variation is not known to be limited to the very start and end of the ITS region or other genetic markers and should not be able to produce the pattern seen in Figs 1 and 2a. In addition, we explicitly sought to avoid comparing sequences across different alleles and cryptic species by excluding sequences that did not match the respective genome-derived sequence closely.

In conclusion, we have shown beyond reasonable doubt that there is room for improvement in the way the mycological community – and to some degree the scientific community at large – trim their DNA sequences. The poor sequence trimming leaves a mark on all subsequent studies that make use of those sequences through BLAST searches or otherwise. Mycology faces enough challenges as it is without having to worry about the burden of poorly trimmed sequences (cf. Pautasso 2013), and we hope that this study will serve as a wake-up call when it comes to trimming of sequence entries in mycology and elsewhere.

Acknowledgements

RHN acknowledges financial support from the Swedish Research Council of Environment, Agricultural Sciences, and Spatial Planning (FORMAS, 215-2011-498) and MR from the same agency (FORMAS, 226-2014-1109). RHN, KA, and the UNITE community acknowledge support from the Alfred P. Sloan Foundation. EK acknowledges funding from FORMAS and Wallenberg. CW and RHN acknowledges funding from Stiftelsen Olle Engkvist, Stiftelsen Lars Hiertas Minne, Stiftelsen Birgit och Birger Wåhlströms minnesfond för den bohuslänska havs- och insjömiljön, and Kapten Carl Stenholms donationsfond. Conrad Schoch (NCBI) is gratefully acknowledged for valuable comments on the manuscript. CW acknowledges a Marie Skłodowska-Curie postdoctoral grant (CRYPTRANS).

References

Abarenkov K, Adams RI, Irinyi L et al. (2016) Annotating public fungal ITS sequences from the built environment according to the MIxS-Built Environment standard – a report from a May 23-24, 2016 workshop (Gothenburg, Sweden). MycoKeys 16: 1–15. https://doi.org/10.3897/mycokeys.16.10000

Alm Rosenblad M, Martin MP, Tedersoo L et al. (2016) Detection of signal recognition particle (SRP) RNAs in the nuclear ribosomal internal transcribed spacer 1 (ITS1) of three lineages of ectomycorrhizal fungi (Agaricomycetes, Basidiomycota). MycoKeys 13: 21–33. https://doi.org/10.3897/mycokeys.13.8579

Altschul SF, Madden TL, Schäffer AA, Zhang J, Zhang Z, Miller W, Lipman DJ (1997) Gapped BLAST and PSI-BLAST: a new generation of protein database search programs. Nucleic Acids Research 25(17): 3389–3402. https://doi.org/10.1093/nar/25.17.3389

Bai L, Xie T, Hu Q et al. (2015) Genome-wide comparison of ferritin family from Archaea, Bacteria, Eukarya, and Viruses: its distribution, characteristic motif, and phylogenetic relationship. The Science of Nature 102(9-10): 64. https://doi.org/10.1007/s00114-015-1314-3

Bengtsson-Palme J, Ryberg M, Hartmann M et al. (2013) Improved software detection and extraction of ITS1 and ITS2 from ribosomal ITS sequences of fungi and other eukaryotes for analysis of environmental sequencing data. Methods in Ecology and Evolution 4(10): 914–919. https://doi.org/10.1111/2041-210X.12073

Blackwell M (2011) The Fungi: 1, 2, 3… 5.1 million species? American Journal of Botany 98(3): 426–438. https://doi.org/10.3732/ajb.1000298

Cochrane G, Karsch-Mizrachi I, Takagi T, International Nucleotide Sequence Database Collaboration (2016) The International Nucleotide Sequence Database Collaboration. Nucleic Acids Research 44(D1): D48–D50. https://doi.org/10.1093/nar/gkv1323

Cornish-Bowden A (1985) Nomenclature for incompletely specified bases in nucleic acid sequences: recommendations 1984. Nucleic Acids Research 13(9): 3021–3030. https://doi.org/10.1093/nar/13.9.3021

Edgar RC, Haas BJ, Clemente JC, Quince C, Knight R (2011) UCHIME improves sensitivity and speed of chimera detection. Bioinformatics 27(16): 2194–2200. https://doi.org/10.1093/bioinformatics/btr381

Garnica S, Schön ME, Abarenkov K et al. (2016) Determining threshold values for barcoding fungi: lessons from *Cortinarius* (Basidiomycota), a highly diverse and widespread ectomycorrhizal genus. FEMS Microbiology Ecology 92(4): fiw045. https://doi.org/10.1093/femsec/fiw045

Gilks WR, Audit B, De Angelis D, Tsoka S, Ouzounis CA (2002) Modeling the percolation of annotation errors in a database of protein sequences. Bioinformatics 18(12): 1641–1649. https://doi.org/10.1093/bioinformatics/18.12.1641

Gouy M, Guindon S, Gascuel O (2010) SeaView version 4: a multiplatform graphical user interface for sequence alignment and phylogenetic tree building. Molecular Biology and Evolution 27(2): 221–224. https://doi.org/10.1093/molbev/msp259

Green MR, Sambrook J (2012) Molecular cloning: a laboratory manual. 4th ed, CSH Press, USA.

Grossart HP, Wurzbacher C, James TY, Kagami M (2016) Discovery of dark matter fungi in aquatic ecosystems demands a reappraisal of the phylogeny and ecology of zoosporic fungi. Fungal Ecology 19: 28–38. https://doi.org/10.1016/j.funeco.2015.06.004

Hibbett D, Abarenkov K, Kõljalg U et al. (2016) Sequence-based classification and identification of Fungi. Mycologia 108(6): 1049–1068. https://doi.org/10.3852/16-130

Hyde KD, Udayanga D, Manamgoda DS et al. (2013) Incorporating molecular data in fungal systematics: a guide for aspiring researchers. Current Research in Environmental and Applied Mycology 3(1): 1–32. https://doi.org/10.5943/cream/3/1/1

Katoh K, Standley DM (2013) MAFFT multiple sequence alignment software version 7: improvements in performance and usability. Molecular Biology and Evolution 30(4): 772–780. https://doi.org/10.1093/molbev/mst010

Kearse M, Moir R, Wilson A et al. (2012) Geneious Basic: an integrated and extendable desktop software platform for the organization and analysis of sequence data. Bioinformatics 28(12): 1647–1649. https://doi.org/10.1093/bioinformatics/bts199

Kõljalg U, Nilsson RH, Abarenkov K et al. (2013) Towards a unified paradigm for sequence-based identification of Fungi. Molecular Ecology 22(21): 5271–5277. https://doi.org/10.1111/mec.12481

Larsson E, Jacobsson S (2004) Controversy over *Hygrophorus cossus* settled using ITS sequence data from 200 year-old type material. Mycolological Research 108(7): 781–786. https://doi.org/10.1017/S0953756204000310

Lindahl BD, Nilsson RH, Tedersoo L et al. (2013) Fungal community analysis by high-throughput sequencing of amplified markers - a user's guide. New Phytologist 199(1): 288–299. https://doi.org/10.1111/nph.12243

Lindner DL, Carlsen T, Nilsson RH, Davey M, Schumacher T, Kauserud H (2013) Employing 454 amplicon pyrosequencing to reveal intragenomic divergence in the internal transcribed spacer (ITS) rDNA region in fungi. Ecology and Evolution 3(6): 1751–1764. https://doi.org/10.1002/ece3.586

Lorenz MG, Lustig M, Linow M (2017) Fungal-grade reagents and materials for molecular analysis. Methods in Molecular Biology 1508: 141–150. https://doi.org/10.1007/978-1-4939-6515-1_6

Nilsson RH, Tedersoo L, Abarenkov K et al. (2012) Five simple guidelines for establishing basic authenticity and reliability of newly generated fungal ITS sequences. MycoKeys 4: 37–63. https://doi.org/10.3897/mycokeys.4.3606

Nilsson RH, Wurzbacher C, Bahram M et al. (2016) Top 50 most wanted fungi. MycoKeys 12: 29–40. https://doi.org/10.3897/mycokeys.12.7553

Pautasso M (2013) Fungal under-representation is (indeed) diminishing in the life sciences. Fungal Ecology 6(5): 460–463. https://doi.org/10.1016/j.funeco.2013.03.001

Pearson WR, Lipman DJ (1988) Improved tools for biological sequence comparison. Proceedings of the National Academy of Sciences USA 85(8): 2444–2448.

Pečnikar ŽF, Buzan EV (2014) 20 years since the introduction of DNA barcoding: from theory to application. Journal of Applied Genetics 55(1): 43–52. https://doi.org/10.1007/s13353-013-0180-y

R Core Team (2017) R: A language and environment for statistical computing. R Foundation for Statistical Computing, Vienna, Austria. http://www.R-project.org/

Schoch CL, Robbertse B, Robert V et al. (2014) Finding needles in haystacks: linking scientific names, reference specimens and molecular data for Fungi. Database (Oxford) vol. and 10.1093/database/bau061. https://doi.org/10.1093/database/bau061

Schoch CL, Seifert KA, Huhndorf S et al. (2012) Nuclear ribosomal internal transcribed spacer (ITS) region as a universal DNA barcode marker for Fungi. Proceedings of the National Academy of Sciences USA 109(16): 6241–6246. https://doi.org/10.1073/pnas.1117018109

Stajich JE, Berbee ML, Blackwell M, Hibbett DS, James TY, Spatafora JW, Taylor JW (2009) The fungi. Current Biology 19(18): R840–855. https://doi.org/10.1016/j.cub.2009.07.004

Taylor DL, Hollingsworth TN, McFarland JW, Lennon NJ, Nusbaum C, Ruess RW (2014) A first comprehensive census of fungi in soil reveals both hyperdiversity and fine-scale niche partitioning. Ecological Monographs 84(1): 3–20. https://doi.org/10.1890/12-1693.1

Tedersoo L, Anslan S, Bahram M et al. (2015) Shotgun metagenomes and multiple primer pair-barcode combinations of amplicons reveal biases in metabarcoding analyses of fungi. MycoKeys 10:1–43. https://doi.org/10.3897/mycokeys.10.4852

Tedersoo L, Bahram M, Puusepp R, Nilsson RH, James TY (2017) Novel soil-inhabiting clades fill gaps in the fungal tree of life. Microbiome 5(1): 42. https://doi.org/10.1186/s40168-017-0259-5

Young JM, Rawlence NJ, Weyrich LS, Cooper A (2014) Limitations and recommendations for successful DNA extraction from forensic soil samples: a review. Science and Justice 54(3): 238–244. https://doi.org/10.1016/j.scijus.2014.02.006

Supplementary material 1

Details on the fungal genomes/contigs targeted

Authors: R. Henrik Nilsson, Marisol Sánchez-García, Martin Ryberg, Kessy Abarenkov, Christian Wurzbacher, Erik Kristiansson

Data type: Excel spreadsheet

Explanation note: List of the fungal genomes/contigs targeted, their URL, their taxonomic affiliation, and the number of sequences (with and without poor trimming) for each entry.

Copyright notice: This dataset is made available under the Open Database License (http://opendatacommons.org/licenses/odbl/1.0/). The Open Database License (ODbL) is a license agreement intended to allow users to freely share, modify, and use this Dataset while maintaining this same freedom for others, provided that the original source and author(s) are credited.

Link: https://doi.org/10.3897/mycokeys.26.14591.suppl1

Supplementary material 2

The 86 multiple sequence alignments used

Authors: R. Henrik Nilsson, Marisol Sánchez-García, Martin Ryberg, Kessy Abarenkov, Christian Wurzbacher, Erik Kristiansson

Data type: Text

Explanation note: The multiple sequence alignments used to infer the statistics of the study. They are provided in the FASTA format (Pearson and Lipman 1988). The genome-derived sequence is given as the topmost sequence in each alignment.

Copyright notice: This dataset is made available under the Open Database License (http://opendatacommons.org/licenses/odbl/1.0/). The Open Database License (ODbL) is a license agreement intended to allow users to freely share, modify, and use this Dataset while maintaining this same freedom for others, provided that the original source and author(s) are credited.

Link: https://doi.org/10.3897/mycokeys.26.14591.suppl2

MycoKeys 26: 25–60 (2017)
doi: 10.3897/mycokeys.26.14688
http://mycokeys.pensoft.net

RESEARCH ARTICLE

A peer-reviewed open-access journal
MycoKeys
Launched to accelerate biodiversity research

Two novel species of *Calonectria* isolated from soil in a natural forest in China

QianLi Liu[1], ShuaiFei Chen[1]

1 *China Eucalypt Research Center (CERC), Chinese Academy of Forestry (CAF), ZhanJiang 524022, GuangDong Province, China*

Corresponding author: *ShuaiFei Chen* (shuaifei.chen@gmail.com)

Academic editor: *G.Mugambi* | Received 24 June 2017 | Accepted 3 August 2017 | Published 22 August 2017

Citation: Liu QL, Chen SF (2017) Two novel species of *Calonectria* isolated from soil in a natural forest in China. MycoKeys 26: 25–60. https://doi.org/10.3897/mycokeys.26.14688

Abstract

Species of *Calonectria* include important pathogens of numerous agronomic and forestry crops worldwide, and they are commonly distributed in soils of tropical and subtropical regions of the world. Previous research results indicated that species diversity of *Calonectria* in China is relatively high. Most *Calonectria* spp. reported and described from China were obtained from diseased *Eucalyptus* tissues or soils in *Eucalyptus* plantations established in tropical and subtropical areas in southern China. Recently, a number of *Calonectria* isolates were isolated from soils in a natural forest in the temperate region of central China. These isolates were identified by DNA sequence comparisons for the translation elongation factor 1-alpha (*tef1*), histone H3 (*his3*), calmodulin (*cmdA*) and β-tubulin (*tub2*) gene regions, combined with morphological characteristics. Two novel species of *Calonectria* were identified and described, and are named here as *Calonectria lichi* and *Ca. montana*, which reside in the Prolate Group and Sphaero-Naviculate Group, respectively. This study revealed that more species of *Calonectria* may occur in natural forests in central China than previously suspected.

Key words

Cylindrocladium, pathogen, phylogeny, taxonomy

Introduction

Calonectria species include many notorious plant pathogens and are widely distributed in tropical and subtropical areas of the world (Crous 2002, Lombard et al. 2010d, Aiello et al. 2013, Vitale et al. 2013, Alfenas et al. 2015). These species can cause serious plant

Copyright *QianLi Liu, ShuaiFei Chen*. This is an open access article distributed under the terms of the Creative Commons Attribution License (CC BY 4.0), which permits unrestricted use, distribution, and reproduction in any medium, provided the original author and source are credited.

epidemics on a wide range of plant hosts (Peerally 1991, Schoch et al. 2001, Crous 2002), and result in considerable economic losses to agriculture and forestry. Example include shoot blight on *Pinus* spp. in South African nurseries (Crous et al. 1991), root rot on *Myrtus communis* in Tunisia (Lombard et al. 2011), and leaf blight on *Buxus sempervirens* in Iran (Mirabolfathy et al. 2013). In addition, members of the genus *Calonectria* are responsible for red crown rot of *Glycine max* (soybean) in Japan (Yamamoto et al. 2017), fruit rot of *Nephelium lappaceum* (rambutan) in Puerto Rico (Serrato-Diaz et al. 2013) and root rot of *Arbutus unedo* (strawberry) in Italy (Vitale et al. 2009). As an important fast-growing tree species, *Eucalyptus* plays a significant role in the global pulpwood supply. Previous research showed that Calonectria leaf blight (CLB), associated with several species of *Calonectria*, is considered to be one of the most prominent *Eucalyptus* leaf diseases that has occurred in numerous countries such as Brazil (Alfenas et al. 2015, Lombard et al. 2016), China (Zhou et al. 2008, Chen et al. 2011), Colombia (Rodas et al. 2005), India (Sharma et al. 1984) and Vietnam (Old et al. 1999). Other fungal diseases of *Eucalyptus* spp. caused by *Calonectria* species include damping-off, shoot blight, and root rot, which have been observed in Brazil (Ferreira 1989) and South Africa (Crous et al. 1991), and these diseases have received considerable attention.

Calonectria spp. are soil-borne fungi, they can form microsclerotia in soil and infected plant roots, stem and leaves as primary inoculum. After diseased tissues decompose or the plants are harvested, microsclerotia are released into the soil, which allows them to survive for extended periods even up to 15 years or more (Sobers and Littrell 1974, Crous 2002). Species of *Calonectria* are also rapidly dispersed via aerial dissemination and water movement, which leads to the transmission of *Calonectria* disease (Vitale et al. 2013). Based on previous studies, at least 145 *Calonectria* species have been identified using molecular data and have been described worldwide (Crous 2002, Crous et al. 2004, 2006, 2012, 2013, 2015, Lombard et al. 2010a, b, c, 2011, 2015, 2016, Chen et al. 2011, Xu et al. 2012, Alfenas et al. 2013a, b, 2015, Gehesquière et al. 2015). Sixty species were isolated from soil samples collected in subtropical or tropical regions (Crous 2002, Crous et al. 2004, Lombard et al. 2010a, b, c, 2015, 2016, Chen et al. 2011, Xu et al. 2012, Alfenas et al. 2015).

In China, *Calonectria* has a relatively high species diversity, and to date, 28 *Calonectria* species have been identified and described. Based on previous studies, *Calonectria* species have been reported in nine provinces and one Special Administrative Region (SAR), which with the exception of LiaoNing and ShanDong Provinces belong to temperate regions (Luan et al. 2006, Li et al. 2010). Most *Calonectria* have been isolated from agronomic crops or forestry plantations in subtropical and tropical regions, including FuJian, GuangDong, GuangXi, GuiZhou, HaiNan, JiangXi and YunNan Provinces, as well as Hong Kong SAR (Crous et al. 2004, Lombard et al. 2010a, 2015, Chen et al. 2011, Gai et al. 2012, Xu et al. 2012, Pei et al. 2015).

China has large areas of plantation and natural forests. To date 27 *Calonectria* species have been isolated from *Eucalyptus* tissues with CLB/leaf rot symptoms or from soils originating from *Eucalyptus* plantations in tropical or subtropical areas in FuJian, GuangDong, GuangXi and HaiNan Provinces (Crous et al. 2004, Lombard et

al. 2010a, 2015, Chen et al. 2011). However, little information is known about the species diversity of *Calonectria* in natural forests. In this study, a number of soil samples were collected from a natural forest in the temperate region of central China, and baited with alfalfa seeds for *Calonectria*. The aim of the current study was to identify these isolates using a combination of phylogenetic analyses and morphological characteristics and to gain a preliminary understanding of the species diversity of *Calonectria* in natural forests in China.

Materials and methods

Fungal isolates

In April 2016, 17 soil samples were collected from a natural forestry area in central China. The collected soils were baited with surface-disinfested (30 s in 75% ethanol and washed several times with sterile water) *Medicago sativa* (alfalfa) seeds using the method described by Crous (2002). After one week, sporulating conidiophores were produced on infected alfalfa tissue. Using a dissection microscope AxioCam Stemi 2000C (Carl Zeiss, Germany), conidial masses were selected and scattered onto 2 % malt extract agar (MEA) (20 g malt extract powder and 20 g agar powder per liter of water: malt extract powder was obtained from Beijing Shuangxuan microbial culture medium products factory, Beijing, China; the agar powder was obtained from Beijing Solarbio Science & Technology Co., Ltd., Beijing, China) using sterile needles. After incubation at 25 °C for one day, germinated spores were individually transferred onto fresh MEA under the dissection microscope and were incubated at 25 °C for one week.

Single conidial cultures were deposited in the Culture Collection of the China Eucalypt Research Centre (CERC), Chinese Academy of Forestry (CAF), ZhanJiang, GuangDong Province, China. Representative isolates were stored in the China General Microbiological Culture Collection Center (CGMCC), Beijing, China. The specimens (pure fungal cultures) were deposited in the Collection of Central South Forestry Fungi of China (CSFF), GuangDong Province, China.

DNA extraction, PCR and sequence reactions

Single conidial cultures grew on MEA for one week at 25 °C, after which actively growing mycelium was scraped using a sterilized scalpel and transferred into 2 mL Eppendorf tubes. Total genomic DNA was extracted following the protocols "Extraction method 5: grinding and CTAB" described by Van Burik et al. (1998). The extracted DNA was dissolved in 30 μL TE buffer (1 M Tris-HCl and 0.5 M EDTA, pH 8.0), and a Nano-Drop 2000 spectrometer (Thermo Fisher Scientific, Waltham, MA, USA) was used to quantify the concentration.

Based on previous research (Lombard et al. 2010d, Alfenas et al. 2015), partial gene regions including translation elongation factor 1-alpha (*tef1*), histone H3 (*his3*), calmodulin (*cmdA*) and β-tubulin (*tub2*), were used as successful DNA barcodes at species, being able to clearly distinguish between intra- and inter-specific divergence. The primer pairs EF1-728F/EF2, CYLH3F/CYLH3R, CAL-228F/CAL-2Rd and T1/CYLTUB1R were used to amplify the fragments of the respective *tef1*, *his3*, *cmdA* and *tub2* genes (Lombard et al. 2010d).

The PCR reaction mixture used to amplify the different loci consisted of TopTaq™ Master Mix 12.5 μL (Qiagen Inc., Hilden, Germany), forward primer 1 μL, 10 μM (Invitrogen, Shanghai, China), reverse primer 1 μL, 10 μM (Invitrogen, Shanghai, China), and RNase-Free H_2O 8.5 μL (Qiagen Inc., Hilden, Germany), and 2 μL (100 ng/μL) of the DNA samples was added as the template to each PCR reaction. The amplifications were performed in 25 μL reaction volumes on an MJ Mini Cycler (BIO-RAD, Hercules, CA, USA) under the conditions described by Groenewald et al. (2013). The amplification products were separated by 1.5% agarose gel electrophoresis and visualized with SYBR Safe DNA gel stain (Thermo Fisher Scientific Inc., USA).

Amplified fragments were sequenced in both directions using the same primer pairs used for amplification by the Beijing Genomics Institute, Guangzhou, China. Sequences were edited using MEGA v. 6.0.5 software (Tamura et al. 2013). All sequences of the isolates obtained in this study were submitted to GenBank (http://www.ncbi.nlm.nih.gov) (Table 1).

Phylogenetic analyses

The sequences generated from this study were added to other sequences of closely related *Calonectria* species downloaded from GenBank for phylogenetic analyses. All sequences used in this study were aligned using the online MAFFT v. 7 (http://mafft.cbrc.jp/alignment/server) with the alignment strategy FFT-NS-i (Slow; interactive refinement method). The aligned sequences were manually edited using MEGA v. 6.0.5 and were deposited in TreeBASE (http://treebase.org).

Phylogenetic analyses were conducted on individual *tef1*, *his3*, *cmdA* and *tub2* sequence datasets and on the combined datasets for the four gene regions, depending on the sequence availability. Two methods, maximum parsimony (MP) and maximum likelihood (ML) were used for phylogenetic analyses.

MP analyses were performed using PAUP v. 4.0 b10 (Swofford 2003), gaps were treated as a fifth character, and characters were unordered and of equal weight with 1000 random addition replicates. A partition homogeneity test (PHT) was conducted to determine whether data for the four genes could be combined. The most parsimonious trees were acquired using the heuristic search option with stepwise addition, tree bisection, and reconstruction branch swapping. MAXTREES was set to 5,000, and zero-length branches were collapsed. A bootstrap analysis (50% majority rule, 1,000 replicates) was carried out to determine statistical support for internal nodes in trees.

Table 1. The species of *Calonectria* used in this study.

Species	Isolate No.[†,‡]	Substrate	Sampling site	Collector	GenBank accession No.[§,|]				Reference
					tef1	*his3*	*cmdA*	*tub2*	
Calonectria acicola	**CBS 114813**	*Pinus radiata*	New Zealand	H. Pearson	GQ267292	DQ190693	GQ267360	DQ190591	Gadgil and Dick 2004
	CBS 114812	*P. radiata*	New Zealand	H. Pearson	GQ267291	DQ190692	GQ267359	DQ190590	Gadgil and Dick 2004
Ca. aconidialis	**CBS 136086**	Soil in *Eucalyptus* plantation	HaiNan, China	X. Mou & S.F. Chen	KJ462785	KJ463133	KJ463017	N/A[¶]	Lombard et al. 2015
Ca. arbusta	**CBS 136079**	Soil in *Eucalyptus* plantation	GuangXi, China	X. Zhou & G. Zhao	KJ462787	KJ463135	KJ463018	KJ462904	Lombard et al. 2015
Ca. asiatica	**CBS 114073**	Leaf litter	Thailand	N.L. Hywel-Jones	AY725705	AY725658	AY725741	AY725616	Crous et al. 2004
	CBS 112711	Leaf litter	Thailand	N.L. Hywel-Jones	AY725702	AY725655	AY725738	AY725613	Crous et al. 2004
Ca. australiensis	**CBS 112954**	*Ficus pleurocarpa*	Australia	C. Pearce & B. Paulu	GQ267293	DQ190699	GQ267363	DQ190596	Crous et al. 2006
Ca. brassicicola	**CBS 112841**	*Brassica* sp.	Indonesia	M.J. Wingfield	KX784689	N/A	KX784561	KX784619	Lombard et al. 2016
Ca. canadiana	**CBS 110817**	*Picea* sp.	Canada	S. Greifenhagen	GQ267297	AF348228	AY725743	AF348212	Lombard et al. 2010b
Ca. chinensis	**CBS 114827**	Soil	Hong Kong	E.C.Y. Liew	AY725710	AY725661	AY725747	AY725619	Lombard et al. 2010b
	CBS 112744	Soil	Hong Kong	E.C.Y. Liew	AY725709	AY725660	AY725746	AY725618	Lombard et al. 2010b
Ca. colhounii	**CBS 293.79**	*Camellia sinensis*	Indonesia	N/A	GQ267301	DQ190639	GQ267373	DQ190564	Lombard et al. 2010b
	CBS 114704	*Arachis pintoi*	Australia	D. Hutton	GQ267300	DQ190638	GQ267372	DQ190563	Lombard et al. 2010b
Ca. colombiensis	**CBS 112220**	*Eucalyptus grandis*	Colombia	M.J. Wingfield	AY725711	AY725662	AY725748	GQ267207	Lombard et al. 2010b
	CBS 112221	*E. grandis*	Colombia	M.J. Wingfield	AY725712	AY725663	AY725749	AY725620	Lombard et al. 2010b
Ca. crousiana	**CBS 127198**	*E. grandis*	FuJian, China	M.J. Wingfield	HQ285822	HQ285808	**MF527084**	HQ285794	Chen et al. 2011; This study
	CBS 127199	*E. grandis*	FuJian, China	M.J. Wingfield	HQ285823	HQ285809	**MF527085**	HQ285795	Chen et al. 2011; This study
Ca. curvispora	**CBS 116159**	Soil	Madagascar	P.W. Crous	GQ267302	AY725664	GQ267374	AF333394	Lombard et al. 2010b
Ca. eucalypti	**CBS 125275**	*E. grandis*	Sumatra Utara	M.J. Wingfield	GQ267338	GQ267267	GQ267430	GQ267218	Lombard et al. 2010b
	CBS 125276	*E. grandis*	Sumatra Utara	M.J. Wingfield	GQ267339	GQ267268	GQ267431	GQ267219	Lombard et al. 2010b
Ca. expansa	**CBS 136247**	Soil in *Eucalyptus* plantation	Guangxi, China	X. Zhou & G. Zhao	KJ462798	KJ463146	KJ463029	KJ462914	Lombard et al. 2015
	CBS 136078	Soil in *Eucalyptus* plantation	Guangdong, China	X. Zhou & G. Zhao	KJ462797	KJ463145	KJ463028	KJ462913	Lombard et al. 2015
Ca. fujianensis	**CBS 127201**	*E. grandis*	FuJian, China	M.J. Wingfield	HQ285820	HQ285806	**MF527089**	HQ285792	Chen et al. 2011; This study
	CBS 127200	*E. grandis*	FuJian, China	M.J. Wingfield	HQ285819	HQ285805	**MF527088**	HQ285791	Chen et al. 2011; This study

Species	Isolate No.[†,‡]	Substrate	Sampling site	Collector	GenBank accession No.[§,|]				Reference
					tef1	*his3*	*cmdA*	*tub2*	
Ca. guangxiensis	**CBS 136092**	Soil in *Eucalyptus* plantation	Guangxi, China	X. Mou & R. Chang	KJ462803	KJ463151	KJ463034	KJ462919	Lombard et al. 2015
	CBS 136094	Soil in *Eucalyptus* plantation	Guangxi, China	X. Mou & R. Chang	KJ462804	N/A	KJ463035	KJ462920	Lombard et al. 2015
Ca. hainanensis	**CBS 136248**	Soil in *Eucalyptus* plantation	Hainan, China	X. Mou & S.F. Chen	KJ462805	KJ463152	KJ463036	N/A	Lombard et al. 2015
Ca. hongkongensis	**CBS 114828**	Soil	Hong Kong	E.C.Y. Liew	AY725717	AY725667	AY725755	AY725622	Lombard et al. 2010b
	CBS 114711	Soil	Hong Kong	M.J. Wingfield	AY725716	AY725666	AY725754	AY725621	Lombard et al. 2010b
Ca. ilicicola	**CBS 190.50**	*Solanum tuberosum*	Indonesia	K.B. Boedijn & J. Reitsma	AY725726	AY725676	AY725764	AY725631	Lombard et al. 2010b
	CBS 112215	*A. hypogaea*	U.S.A.	Beute	AY725726	AY725684	AY725765	AY725639	Crous et al. 2004
Ca. indonesiae	**CBS 112823**	*Syzygium aromaticum*	Indonesia	M.J. Wingfield	AY725718	AY725668	AY725756	AY725623	Lombard et al. 2010b
	CBS 112840	*S. aromaticum*	Indonesia	M.J. Wingfield	AY725720	AY725670	AY725758	AY725625	Lombard et al. 2010b
C. indonesiana	**CBS 112936**	Soil	Indonesia	M.J. Wingfield	KX784701	N/A	KX784573	KX784631	Lombard et al. 2016
Ca. indusiata	CBS 144.36	N/A	N/A	N/A	GQ267332	GQ267262	GQ267453	GQ267239	Lombard et al. 2010b
	CBS 114684	*Rhododendron* sp.	U.S.A.	N.E. El-Gholl	GQ267333	DQ190653	GQ267454	AF232862	Lombard et al. 2010b
Ca. kyotensis	CBS 170.77	*Idesia polycarpa*	New Zealand	N/A	GQ267308	GQ267249	GQ267380	GQ267209	Lombard et al. 2010b
	CBS 413.67	*Paphiopedilum callosum*	Celle, Germany	W. Gerlach	GQ267307	GQ267248	GQ267379	GQ267208	Lombard et al. 2010b
Ca. lateralis	**CBS 136629**	Soil in *Eucalyptus* plantation	Guangxi,China	X. Zhou & G. Zhao	KJ462840	KJ463186	KJ463070	KJ462955	Lombard et al. 2015
Ca. lichi	**CERC 8866**	Soil	Central China	S.F. Chen	**MF527039**	**MF527055**	**MF527071**	**MF527097**	This study
	CERC 8841	Soil	Central China	S.F. Chen	**MF527036**	**MF527052**	**MF527068**	**MF527094**	This study
	CERC 8848	Soil	Central China	S.F. Chen	**MF527037**	**MF527053**	**MF527069**	**MF527095**	This study
	CERC 8850	Soil	Central China	S.F. Chen	**MF527038**	**MF527054**	**MF527070**	**MF527096**	This study
	CERC 8871	Soil	Central China	S.F. Chen	**MF527040**	**MF527056**	**MF527072**	**MF527098**	This study
	CERC 8890	Soil	Central China	S.F. Chen	**MF527041**	**MF527057**	**MF527073**	**MF527099**	This study
	CERC 8900	Soil	Central China	S.F. Chen	**MF527042**	**MF527058**	**MF527074**	**MF527100**	This study
	CERC 8906	Soil	Central China	S.F. Chen	**MF527043**	**MF527059**	**MF527075**	**MF527101**	This study
	CERC 8928	Soil	Central China	S.F. Chen	**MF527044**	**MF527060**	**MF527076**	**MF527102**	This study
Ca. macroconidialis	**CBS 114880**	*E. grandis*	South Africa	P.W. Crous	GQ267313	DQ190655	GQ267393	AF232855	Lombard et al. 2010b
Ca. magnispora	**CBS 136249**	Soil in *Eucalyptus* plantation	Guangxi, China	X. Mou & R. Chang	KJ462841	KJ463187	KJ463071	KJ462956	Lombard et al. 2015
Ca. malesiana	**CBS 112752**	Soil	Indonesia	M.J. Wingfield	AY725722	AY725672	AY725760	AY725627	Lombard et al. 2010b
	CBS 112710	Debris	Thailand	N.L. Hywel-Jones	AY725721	AY725671	AY725759	AY725626	Lombard et al. 2010b

Species	Isolate No.[†,‡]	Substrate	Sampling site	Collector	GenBank accession No.[§,|]				Reference
					tef1	*his3*	*cmdA*	*tub2*	
Ca. microconidialis	**CBS 136638**	*E. urophylla* × *E. grandis* clone seedling leaf	Guangdong, China	G. Zhao	KJ462845	KJ463191	KJ463075	KJ462960	Lombard et al. 2015
	CBS 136633	*E. urophylla* × *E. grandis* clone seedling leaf	Guangdong, China	G. Zhao	KJ462842	KJ463188	KJ463072	KJ462957	Lombard et al. 2015
Ca. montana	**CERC 8952**	Soil	Central China	S.F. Chen	**MF527049**	**MF527065**	**MF527081**	**MF527107**	This study
	CERC 8930	Soil	Central China	S.F. Chen	**MF527045**	**MF527061**	**MF527077**	**MF527103**	This study
	CERC 8932	Soil	Central China	S.F. Chen	**MF527046**	**MF527062**	**MF527078**	**MF527104**	This study
	CERC 8936	Soil	Central China	S.F. Chen	**MF527047**	**MF527063**	**MF527079**	**MF527105**	This study
	CERC 8938	Soil	Central China	S.F. Chen	**MF527048**	**MF527064**	**MF527080**	**MF527106**	This study
	CERC 8957	Soil	Central China	S.F. Chen	**MF527050**	**MF527066**	**MF527082**	**MF527108**	This study
	CERC 8966	Soil	Central China	S.F. Chen	**MF527051**	**MF527067**	**MF527083**	**MF527109**	This study
Ca. monticola	**CPC 28835**	Soil	Thailand	P.W. Crous	KT964773	N/A	KT964771	KT964769	Crous et al. 2015
	CPC 28836	Soil	Thailand	P.W. Crous	KT964774	N/A	KT964772	KT964770	Crous et al. 2015
Ca. multiseptata	**CBS 112682**	*Eucalyptus* sp.	Indonesia	M.J. Wingfield	FJ918535	DQ190659	GQ267397	DQ190573	Lombard et al. 2010b
Ca. nymphaeae	**CBS 131802**	*Nymphaea tetragona*	Guiyang, Guizhou	S.Y. Qin	KC555273	N/A	N/A	JN984864	Xu et al. 2012
	HGUP 100004	*N. tetragona*	Guiyang, Guizhou	Y. Wang	KC555274	N/A	N/A	JN984865	Xu et al. 2012
Ca. pacifica	**CBS 109063**	*Araucaria heterophylla*	Hawaii, USA	M. Aragaki	AY725724	GQ267255	AY725762	GQ267213	Lombard et al. 2010b
	CBS 114038	*Ipomoea aquatica*	New Zealand	C.F. Hill	GQ267320	AY725675	GQ267402	AY725630	Lombard et al. 2010b
Ca. paracolhounii	**CBS 114679**	N/A	USA	A.Y. Rossman	KX784714	N/A	KX784582	KX784644	Lombard et al. 2016
	CBS 114705	*Annona reticulata*	Australia	D. Hutton	KX784715	N/A	N/A	KX784645	Lombard et al. 2016
Ca. parakyotensis	**CBS 136085**	Soil in *Eucalyptus* plantation	Guangdong, China	X. Mou & R. Chang	KJ462851	KJ463197	KJ463081	N/A	Lombard et al. 2015
	CBS 136095	Soil in *Eucalyptus* plantation	Guangxi, China	X. Mou & R. Chang	KJ462852	KJ463198	KJ463082	N/A	Lombard et al. 2015
Ca. parva	**CBS 110798**	*Eucalyptus grandis* roots	South Africa	P.W. Crous	KX784716	N/A	KX784583	KX784646	Lombard et al. 2016
Ca. pauciramosa	**CMW 5683**	*E. grandis*	South Africa	P.W. Crous	FJ918565	FJ918531	GQ267405	FJ918514	Lombard et al. 2010b
	CMW 30823	*E. grandis*	South Africa	P.W. Crous	FJ918566	FJ918532	GQ267404	FJ918515	Lombard et al. 2010b
Ca. penicilloides	**CBS 174.55**	*Prunus* sp.	Japan	Tubaki	GQ267322	GQ267257	GQ267406	AF333414	Lombard et al. 2010b
Ca. pluriramosa	**CBS 136976**	Soil in *Eucalyptus* plantation	Guangxi, China	X. Zhou & G. Zhao	KJ462882	KJ463228	KJ463112	KJ462995	Lombard et al. 2015
Ca. pseudokyotensis	**CBS 137332**	Soil in *Eucalyptus* plantation	Guangxi,China	X. Zhou & G. Zhao	KJ462881	KJ463227	KJ463111	KJ462994	Lombard et al. 2015

Species	Isolate No.[†,‡]	Substrate	Sampling site	Collector	GenBank accession No.[§,|]				Reference
					tef1	*his3*	*cmdA*	*tub2*	
Ca. pseudocolhounii	**CBS 127195**	*E. dunnii*	FuJian, China	M.J. Wingfield	HQ285816	HQ285802	**MF527091**	HQ285788	Chen et al. 2011; This study
	CBS 127196	*E. dunnii*	FuJian, China	M.J. Wingfield	HQ285817	HQ285803	**MF527092**	HQ285789	Chen et al. 2011; This study
Ca. pseudoreteaudii	**CBS 123694**	*E. urophylla* × *E. grandis* cutting	Guangdong, China	M.J. Wingfield	FJ918541	FJ918519	GQ267411	FJ918504	Lombard et al. 2010b
	CBS 123696	*E. urophylla* × *E. grandis* cutting	Guangdong, China	M.J. Wingfield	FJ918542	FJ918520	GQ267410	FJ918505	Lombard et al. 2010b
Ca. queenslandica	**CBS 112146**	*E. urophylla*	Australia	B. Brown	FJ918543	FJ918521	GQ267415	AF389835	Lombard et al. 2010b
	CBS 112155	*E. pellita*	Australia	K.M. Old	FJ918544	DQ190667	GQ267416	AF389834	Lombard et al. 2010b
Ca. reteaudii	**CBS 112144**	*E. camaldulensis*	Vietnam	M.J. Dudzinski	FJ918537	DQ190661	GQ267417	AF389833	Lombard et al. 2010b
	CBS 112143	*E. camaldulensis*	Vietnam	M.J. Dudzinski	FJ918536	DQ190660	GQ267418	GQ240642	Lombard et al. 2010b
Ca. sphaeropendunculata	**CBS 136081**	Soil in *Eucalyptus* plantation	Guangxi, China	X. Zhou & G. Zhao	KJ462890	KJ463236	KJ463120	KJ463003	Lombard et al. 2015
Ca. sumatrensis	**CBS 112829**	Soil	Indonesia	M.J. Wingfield	AY725733	AY725696	AY725771	AY725649	Lombard et al. 2010b
	CBS 112934	Soil	Indonesia	M.J. Wingfield	AY725735	AY725698	AY725773	AY725651	Lombard et al. 2010b
Ca. syzygiicola	**CBS 112831**	Soil	Indonesia	M.J. Wingfield	KX784736	N/A	N/A	KX784663	Lombard et al. 2016
Ca. terrae-reginae	**CBS 112151**	*E. urophylla*	Australia	C. Hanwood	FJ918545	FJ918522	GQ267451	FJ918506	Lombard et al. 2010b
	CBS 112634	*Xanthorrhoea australis*	Australia	T. Baigent	FJ918546	DQ190668	GQ267452	FJ918507	Lombard et al. 2010b
Ca. turangicola	**CBS 136077**	Soil in *Eucalyptus* plantation	Guangxi, China	X. Zhou & G. Zhao	KJ462900	KJ463246	N/A	KJ463013	Lombard et al. 2015
	CBS 136093	Soil in *Eucalyptus* plantation	Guangxi, China	X. Mou & R. Chang	KJ462901	KJ463247	KJ463130	KJ463014	Lombard et al. 2015

[†] CBS: Westerdijk Fungal Biodiversity Institute, Utrecht, The Netherlands; CERC: China Eucalypt Research Centre, Zhanjiang, GuangDong Province, China; CMW: culture collection of the Forestry and Agricultural Biotechnology Institute (FABI), University of Pretoria, Pretoria, South Africa; CPC: Pedro Crous working collection housed at CBS; HGUP: Plant Pathology Herbarium of Gui Zhou University, GuiYang 550025, China.

[‡] Isolates represent ex-type and indicated in bold.

[§] *tef1*: translation elongation factor 1-alpha; *his3*: histone H3; *cmdA*: calmodulin; *tub2*: β-tubulin.

[|] GenBank accession no. indicated in bold were generated in this study

[¶] "N/A" represents information that are not available.

The tree length (TL), consistency index (CI), retention index (RI) and homoplasy index (HI) were used to assess phylogenetic trees (Hillis and Huelsenbeck 1992).

ML analyses were performed using PHYML v. 3.0 (Guindon and Gascuel 2003), and the best evolutionary model was obtained using JMODELTEST v. 2.1.5 (Posada 2008). In PHYML, the maximum number of retained trees was set to 1,000, and nodal support was determined by non-parametric bootstrapping with 1,000 replicates.

Based on the morphological characteristics, datasets were separated into two groups: the Prolate Group and the Sphaero-Naviculate Group (Lombard et al. 2010b), and therefore phylogenetic analyses were performed with two separate sequence datasets. *Calonectria hongkongensis* (CBS 114711 and CBS 114828) and *Ca. pauciramosa* (CMW 5683 and CMW 30823) represented the outgroup taxa for the Prolate Group and Sphaero-Naviculate Group, respectively. The phylogenetic trees were viewed using MEGA v. 6.0.5 for both MP and ML analyses.

Sexual compatibility

Based on multi-gene phylogenetic analyses, isolates of each identified *Calonectria* species were crossed with each other in all possible combinations. Crosses were performed on minimal salt agar (MSA; Guerber and Correll 2001) on the surface of the medium using three sterile toothpicks. Isolates crossed with themselves were regarded as controls. These crosses were used to determine whether the identified species had a heterothallic or a homothallic mating system. The cultures were incubated at 25 °C for six weeks. When isolate combinations produced extruding viable ascospores, crosses were considered successful.

Morphology

To determine the morphological characteristics of the asexual morphs, representative isolates identified by DNA sequence comparisons were selected. Agar plugs from the periphery of actively growing single conidial cultures were transferred onto synthetic nutrient-poor agar (SNA; Nirenburg 1981) and incubated at 25 °C for one week (there were five replicates per isolate). Asexual structures that emerged on the surface of the SNA medium were mounted in one drop of 80% lactic acid on glass slides and examined under an Axio Imager A1 microscope (Carl Zeiss Ltd., Munchen, Germany) and an AxioCam ERc 5S digital camera with Zeiss Axio Vision Rel. 4.8 software (Carl Zeiss Ltd., Munchen, Germany). Sexual morphs were studied by transferring perithecia obtained from the sexual compatibility tests into a tissue-freezing medium (Leica Biosystems, Nussloch, Germany) and were hand-sectioned using an HM550 Cryostat Microtome (Microm International GmbH, Thermo Fisher Scientific, Wall-

dorf, Germany) at –20 °C. The 10-µm sections were mounted in 80% lactic acid and 3% KOH.

Fifty measurements were made for each morphological structure of the isolates selected as the holotype specimen, 30 measurements were made for the isolates selected as the paratype specimen. Minimum, maximum and average (mean) values were determined and presented as follows: (minimum–) (average – standard deviation) – (average + standard deviation) (–maximum).

The optimal growth temperature of the *Calonectria* species was determined by transferring the representative isolates to fresh 9 mm MEA Petri dishes, which were incubated under temperatures ranging from 5 to 35 °C at 5 °C intervals in the dark (there were five replicates per isolate). Colony colors were determined by inoculating the isolates on fresh MEA at 25 °C in the dark, after seven days incubation, a comparison was performed using the colour charts of Rayner (1970).

Results

Fungal isolates

A total of 40 isolates with the typical morphological of *Calonectria* species were obtained from the infected alfalfa tissue cultivated in the soil samples. Based on preliminary phylogenetic analysis of the *tef1* gene region (data not shown), 16 isolates from all soil samples were selected for further study (Table 1).

Phylogenetic analyses

Sequences for the 78 ex-type and other strains of 48 *Calonectria* species closely related to isolates obtained in this study were downloaded from GenBank (Table 1). For the 16 isolates collected in this study, nine resided in the Prolate Group, and seven were clustered in the Sphaero-Naviculate Group. Phylogenetic analyses of individual *tef1*, *his3*, *cmdA* and *tub2* and the combined sequence datasets were conducted using both MP and ML method. For both the Prolate and Sphaero-Naviculate Groups, although the related position of some *Calonectira* species were slightly different between the MP and ML trees, the overall topologies were similar, and the ML trees were exhibited.

For the Prolate and Sphaero-Naviculate Groups, the PHT comparing the combined *tef1*, *his3*, *cmdA* and *tub2* gene datasets generated P values of 0.141 and 0.333, respectively, which indicated that no significant difference existed between these datasets. These datasets were consequently combined and subjected to phylogenetic analyses. For each of the two groups, the sequence alignments of *tef1*, *his3*, *cmdA*, *tub2* and the combination of the four genes were deposited in TreeBASE (TreeBASE No. 21357). The number of parsimony informative characters, the statistical values for the

Table 2. Statistics resulting from phylogenetic analyses.

Dataset	Phylogenetic group	No. of taxa	No. of bp[†]	Maximum parsimony						
				PIC[‡]	No. of trees	Tree length	CI[§]	RI[|]	RC[¶]	HI[#]
tef1	Prolate	45	515	210	8	448	0.7054	0.8847	0.6240	0.2946
his3	Prolate	38	449	140	6	340	0.6941	0.9176	0.6369	0.3059
cmdA	Prolate	42	476	152	792	245	0.7591	0.9295	0.7056	0.2408
tub2	Prolate	45	579	204	18	350	0.8085	0.9395	0.7597	0.1914
tef1/*his3*/*cmdA*/*tub2*	Prolate	45	2019	706	1	1484	0.6880	0.8940	0.6150	0.3120
tef1	Sphaero-Naviculate	51	522	159	33	330	0.7030	0.9056	0.6367	0.2969
his3	Sphaero-Naviculate	47	455	138	11	386	0.6632	0.9110	0.6042	0.3367
cmdA	Sphaero-Naviculate	49	473	138	48	228	0.7763	0.9406	0.7302	0.2236
tub2	Sphaero-Naviculate	47	534	174	4	401	0.7107	0.9216	0.6550	0.2892
tef1/*his3*/*cmdA*/*tub2*	Sphaero-Naviculate	51	1984	609	1350	1535	0.6190	0.8790	0.6047	0.3810

Dataset	Phylogenetic group	Maximum likelihood							
		Subst. model[††]	NST[‡‡]	Rate matrix					Rates
tef1	Prolate	TIM2+G	6	1.6588	2.3553	1.6588	1.0000	4.4652	Gamma
his3	Prolate	GTR+G	6	1.8190	7.5654	4.6281	1.4320	15.6259	Gamma
cmdA	Prolate	HKY+G	2						Gamma
tub2	Prolate	TPM3uf+G	6	1.5151	4.2112	1.0000	1.5151	4.2112	Gamma
tef1/*his3*/*cmdA*/*tub2*	Prolate	TIM2+I+G	6	1.3725	3.6221	1.3725	1.0000	5.1226	Gamma
tef1	Sphaero-Naviculate	GTR+G	6	2.3612	2.5155	0.6227	0.7074	5.0226	Gamma
his3	Sphaero-Naviculate	HKY+I+G	2						Gamma
cmdA	Sphaero-Naviculate	TrN+G	6	1.0000	3.8308	1.0000	1.0000	6.4755	Gamma
tub2	Sphaero-Naviculate	TPM3uf+G	6	1.5714	4.6055	1.0000	1.5714	4.6055	Gamma
tef1/*his3*/*cmdA*/*tub2*	Sphaero-Naviculate	GTR+I+G	6	1.6318	3.8130	1.0888	1.1609	5.2579	Gamma

[†] bp = base pairs.

[‡] PIC = number of parsimony informative characters.

[§] CI = consistency index.

[|] RI = retention index.

[¶] RC = rescaled consistency index.

[#] HI = homoplasy index.

[††] Subst. model = best fit substitution model.

[‡‡] NST = number of substitution rate categories.

phylogenetic trees of the MP analyses, and the parameters for the best-fit substitution models of ML analyses are shown in Table 2.

Phylogenetic analyses of each of the individual and combined sequence datasets indicated that in the Prolate Group, the nine isolates resided in the *Ca. colhounii* species complex and were closely related to *Ca. colhounii*, *Ca. eucalypti*, *Ca. fujianensis*, *Ca. nymphaeae*, *Ca. paracolhounii* and *Ca. pseudocolhounii*. In the *his3* and *cmdA* phylogenetic trees, the nine isolates and *Ca. fujianensis* were clustered in the same clade (Suppl. materials 2, 3), while in the trees based on the *tef1* and *tub2* sequences, the nine isolates formed an independent clade (Supplementary Figures 1, 4). Based on the phylogenetic analyses of the combined sequences of the four genes, the nine isolates formed a new, strongly defined phylogenetic clade that was distinct from other *Calonectria* species and was supported by high bootstrap values (ML = 94%, MP = 93%) (Figure 1). Fixed unique single nucleotide polymorphisms (SNPs) were identified in the new phylogenetic clades of the nine isolates and their phylogenetically closed *Calonectria* species (Table 3). The total number of SNP differences between the new clade and the other closely related species varied between 10–34 for all four gene regions combined (Table 4). The results of these phylogenetic and SNP analyses indicate that the nine isolates in the Prolate Group represent a distinct, undescribed species.

Phylogenetic analyses of each of the individual and combined datasets indicated that in the Sphaero-Naviculate Group, the seven isolates were clustered in the *Ca. kyotensis* species complex and were closely related to *Ca. canadiana*. In the *tef1* phylogenetic trees, the seven isolates were grouped in the same clade with *Ca. canadiana* (Suppl. material 5). In the phylogenetic trees based on the *his3*, *cmdA* and *tub2* sequences, the seven isolates formed an independent clade distinct from *Ca. canadiana* and other species in the *Ca. kyotensis* species complex (Suppl. materials 6, 7 and 8). Based on the combined sequences of the four genes, the seven isolates formed a strongly defined phylogenetic clade that was distinct from *Ca. canadiana* and was supported by high bootstrap values (ML = 100%, MP = 100%) (Figure 2). The seven isolates obtained in this study were distinguished from *Ca. canadiana* using SNP analyses for each of the *tef1*, *his3*, *cmdA* and *tub2* gene region sequences (Tables 5). The total number of SNP differences between the seven isolates and *Ca. canadiana* for all four genes was 51 (Table 6). The results indicate that the seven isolates in the Sphaero-Navivulate Group represent a novel species.

Sexual compatibility

After a six-week mating test on MSA, all 16 isolates and the crosses of isolates of each identified species failed to yield sexual structures, indicating that they were either self-sterile (heterothallic) or had retained the ability to recombine to produce fertile progeny.

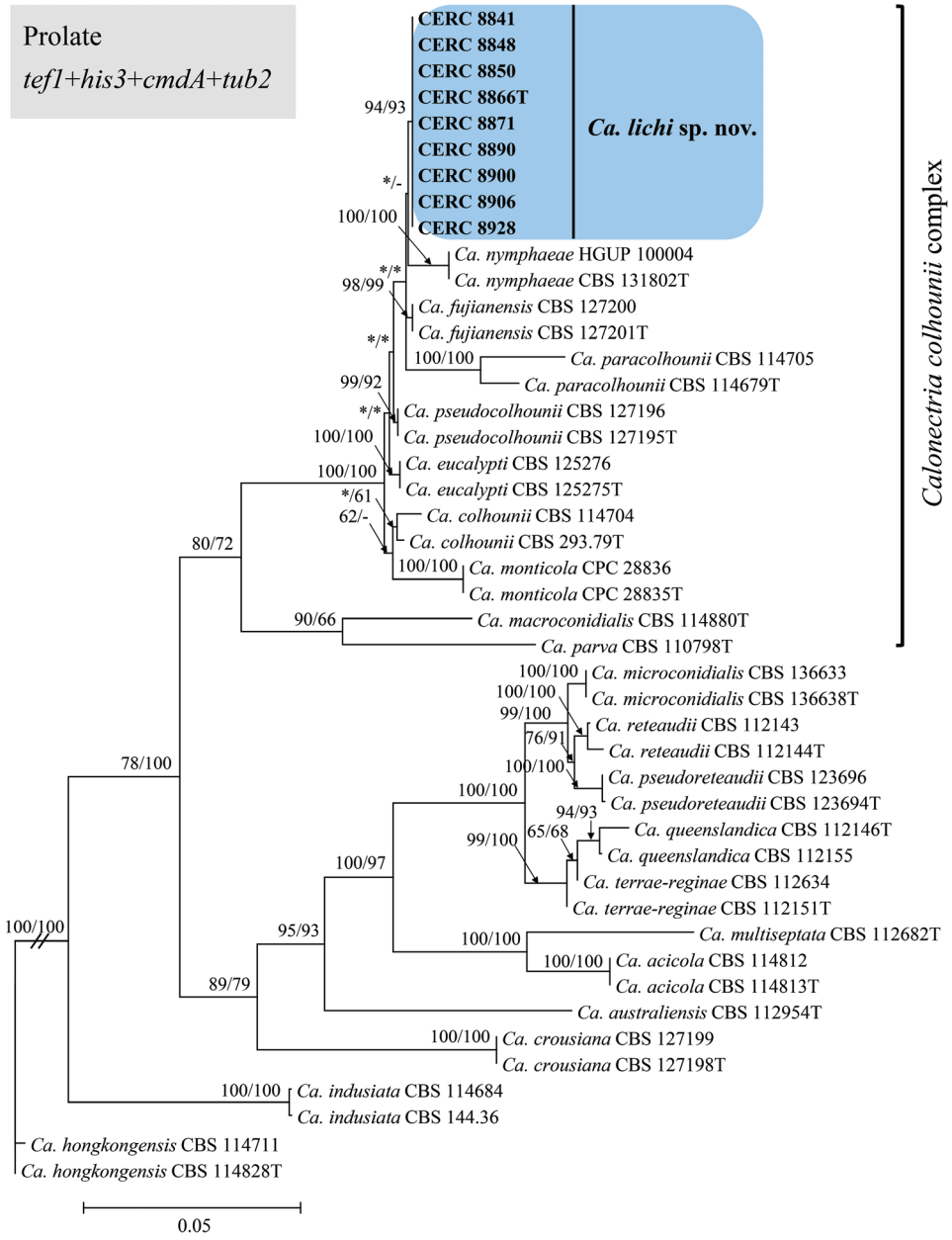

Figure 1. Phylogenetic tree of *Calonectria* species in the Prolate group based on maximum likelihood (ML) analysis of combined DNA dataset of *tef1*, *his3*, *cmdA* and *tub2* gene sequences. ML and MP (maximum parsimony) bootstrap values (ML/MP) are shown above branches, with bootstrap values below 60 % marked with an *, and absent analysis values are marked with -. Isolates representing ex-type material are marked with "T", isolates highlighted in bold were sequenced in this study and novel species were covered in blue. The tree was rooted to *Ca. hongkongensis* (CBS 114711 and CBS 114828).

Table 3. Single nucleotide polymorphism comparisons in four gene regions between *Calonectria lichi* and the phylogenetically closest related species.

Species	Isolate no.	*tef1*†																	
		28‡	81	89	90	91	92	93	100	120	121	124	184	185	186	243	418	425	432
Ca. lichi	**CERC 8866**§	A	**A**|	–	–	–	–	–	C	T	T	A	–	–	–	A	C	–	A
	CERC 8841	A	**A**	–	–	–	–	–	C	T	T	A	–	–	–	A	C	–	A
	CERC 8848	A	**A**	–	–	–	–	–	C	T	T	A	–	–	–	A	C	–	A
	CERC 8850	A	**A**	–	–	–	–	–	C	T	T	A	–	–	–	A	C	–	A
	CERC 8871	A	**A**	–	–	–	–	–	C	T	T	A	–	–	–	A	C	–	A
	CERC 8890	A	**A**	–	–	–	–	–	C	T	T	A	–	–	–	A	C	–	A
	CERC 8900	A	**A**	–	–	–	–	–	C	T	T	A	–	–	–	A	C	–	A
	CERC 8906	A	**A**	–	–	–	–	–	C	T	T	A	–	–	–	A	C	–	A
	CERC 8928	A	**A**	–	–	–	–	–	C	T	T	A	–	–	–	A	C	–	A
Ca. colhounii	**CBS 293.79**	**C**	T	**A**	**C**	**A**	**A**	**C**	C	**–**	–	A	–	–	–	**G**	C	–	A
	CBS 114704	**C**	T	**A**	**C**	**A**	**A**	**C**	C	**–**	–	A	–	–	–	**G**	C	–	A
Ca. eucalypti	**CBS 125275**	A	T	–	–	–	–	–	C	T	–	A	–	–	–	A	C	–	A
	CBS 125276	A	T	–	–	–	–	–	C	T	–	A	–	–	–	A	C	–	A
Ca. fujianensis	**CBS 127201**	A	T	–	–	–	–	–	C	T	–	G	**A**	**A**	**A**	A	C	–	A
	CBS 127200	A	T	–	–	–	–	–	C	T	–	G	**A**	**A**	**A**	A	C	–	A
Ca. nymphaeae	**CBS 131802**	A	T	–	–	–	–	–	C	T	–	G	–	–	–	A	C	–	A
	HGUP 100004	A	T	–	–	–	–	–	C	T	–	G	–	–	–	A	C	–	A
Ca. paracolhounii	**CBS 114679**	A	T	–	–	–	–	–	**T**	T	T	A	–	–	–	A	**G**	**C**	**C**
Ca. pseudocolhounii	**CBS 127195**	A	T	–	–	–	–	–	C	T	–	A	–	–	–	A	C	–	A
	CBS 127196	A	T	–	–	–	–	–	C	T	–	A	–	–	–	A	C	–	A

Table 3. Continue.

Species	Isolate no.	*tef1*																
		433	435	436	437	438	441	443	444	446	447	448	450	452	453	457	473	483
Ca. lichi	**CERC 8866**[§]	T	T	C	T	C	T	T	A	C	T	A	C	T	T	T	G	–
	CERC 8841	T	T	C	T	C	T	T	A	C	T	A	C	T	T	T	G	–
	CERC 8848	T	T	C	T	C	T	T	A	C	T	A	C	T	T	T	G	–
	CERC 8850	T	T	C	T	C	T	T	A	C	T	A	C	T	T	T	G	–
	CERC 8871	T	T	C	T	C	T	T	A	C	T	A	C	T	T	T	G	–
	CERC 8890	T	T	C	T	C	T	T	A	C	T	A	C	T	T	T	G	–
	CERC 8900	T	T	C	T	C	T	T	A	C	T	A	C	T	T	T	G	–
	CERC 8906	T	T	C	T	C	T	T	A	C	T	A	C	T	T	T	G	–
	CERC 8928	T	T	C	T	C	T	T	A	C	T	A	C	T	T	T	G	–
Ca. colhounii	**CBS 293.79**	T	T	C	C	C	**C**	T	A	C	T	A	C	C	T	C	G	C
	CBS 114704	T	T	C	C	C	**C**	T	A	C	T	A	C	C	T	C	G	C
Ca. eucalypti	**CBS 125275**	T	T	C	T	C	T	T	A	C	T	A	C	T	T	T	G	C
	CBS 125276	T	T	C	T	C	T	T	A	C	T	A	C	T	T	T	G	C
Ca. fujianensis	**CBS 127201**	T	T	C	T	C	T	T	A	C	T	A	C	T	T	T	G	–
	CBS 127200	T	T	C	T	C	T	T	A	C	T	A	C	T	T	T	G	–
Ca. nymphaeae	**CBS 131802**	T	T	C	T	C	T	T	A	C	T	A	C	–	T	T	–	N/A[¶]
	HGUP 100004	T	T	C	T	C	T	T	A	C	T	A	C	–	T	T	–	N/A
Ca. paracolhounii	**CBS 114679**	**A**	**G**	**–**	**–**	**T**	T	**C**	**T**	**G**	**G**	**G**	**T**	G	**G**	N/A	N/A	N/A
Ca. pseudocolhounii	**CBS 127195**	T	T	C	T	C	T	T	A	C	T	A	C	T	T	T	G	–
	CBS 127196	T	T	C	T	C	T	T	A	C	T	A	C	T	T	T	G	–

Table 3. Continue.

Species	Isolate no.	*His3*							*cmdA*														
		45	234	272	293	344	353	368	169	204	205	210	238	244	266	293	325	334	411	429	432	474
Ca. lichi	**CERC 8866**[§]	A	T	A	C	C	C	A	G	A	C	C	G	G	G	A	G	G	C	C	C	T
	CERC 8841	A	T	A	C	C	C	A	G	A	C	C	G	G	G	A	G	G	C	C	C	T
	CERC 8848	A	T	A	C	C	C	A	G	A	C	C	G	G	G	A	G	G	C	C	C	T
	CERC 8850	A	T	A	C	C	C	A	G	A	C	C	G	G	G	A	G	G	C	C	C	T
	CERC 8871	A	T	A	C	C	C	A	G	A	C	C	G	G	G	A	G	G	C	C	C	T
	CERC 8890	A	T	A	C	C	C	A	G	A	C	C	G	G	G	A	G	G	C	C	C	T
	CERC 8900	A	T	A	C	C	C	A	G	A	C	C	G	G	G	A	G	G	C	C	C	T
	CERC 8906	A	T	A	C	C	C	A	G	A	C	C	G	G	G	A	G	G	C	C	C	T
	CERC 8928	A	T	A	C	C	C	A	G	A	C	C	G	G	G	A	G	G	C	C	C	T
Ca. colhounii	**CBS 293.79**	A	T	A	T	C	T	C	G	A	C	C	G	G	G	A	G	G	C	T	C	C
	CBS 114704	A	T	A	T	C	T	C	G	A	C	C	G	G	G	A	G	G	C	T	C	C
Ca. eucalypti	**CBS 125275**	–	T	T	T	T	T	C	G	A	C	C	G	G	G	A	G	G	C	C	T	C
	CBS 125276	–	T	T	T	T	T	C	G	A	C	C	G	G	G	A	G	G	C	C	T	C
Ca. fujianensis	**CBS 127201**	A	T	A	C	C	C	A	G	A	C	C	G	G	G	A	G	G	C	C	C	T
	CBS 127200	A	T	A	C	C	C	A	G	A	C	C	G	G	G	A	G	G	C	C	C	T
Ca. nymphaeae	**CBS 131802**	N/A	N/A	N/A	N/A	N/A	N/A	N/A	N/A	N/A	N/A	N/A	N/A	N/A	N/A	N/A	N/A	N/A	N/A	N/A	N/A	N/A
	HGUP 100004	N/A	N/A	N/A	N/A	N/A	N/A	N/A	N/A	N/A	N/A	N/A	N/A	N/A	N/A	N/A	N/A	N/A	N/A	N/A	N/A	N/A
Ca. paracolhounii	**CBS 114679**	N/A	N/A	N/A	N/A	N/A	N/A	N/A	T	T	G	A	C	C	A	T	C	A	G	C	C	N/A
Ca. pseudocolhounii	**CBS 127195**	A	C	A	T	C	T	C	G	A	C	C	G	G	G	A	G	G	C	C	T	T
	CBS 127196	A	C	A	T	C	T	C	G	A	C	C	G	G	G	A	G	G	C	C	T	T

Table 3. Continue.

Species	Isolate no.	*tub2*																	
		24	28	33	68	98	103	427	442	446	455	534	535	536	537	541	547	550	551
Ca. lichi	**CERC 8866**[§]	C	G	C	C	A	C	C	C	T	A	G	T	G	C	T	C	T	C
	CERC 8841	C	G	C	C	A	C	C	C	T	A	G	T	G	C	T	C	T	C
	CERC 8848	C	G	C	C	A	C	C	C	T	A	G	T	G	C	T	C	T	C
	CERC 8850	C	G	C	C	A	C	C	C	T	A	G	T	G	C	T	C	T	C
	CERC 8871	C	G	C	C	A	C	C	C	T	A	G	T	G	C	T	C	T	C
	CERC 8890	C	G	C	C	A	C	C	C	T	A	G	T	G	C	T	C	T	C
	CERC 8900	C	G	C	C	A	C	C	C	T	A	G	T	G	C	T	C	T	C
	CERC 8906	C	G	C	C	A	C	C	C	T	A	G	T	G	C	T	C	T	C
	CERC 8928	C	G	C	C	A	C	C	C	T	A	G	T	G	C	T	C	T	C
Ca. colhounii	**CBS 293.79**	N/A	N/A	N/A	C	C	C	C	C	T	A	G	T	G	C	T	C	T	C
	CBS 114704	N/A	N/A	N/A	C	C	C	C	C	T	A	G	T	G	C	T	C	T	C
Ca. eucalypti	**CBS 125275**	T	A	T	C	C	C	C	C	**C**	**G**	G	T	G	C	T	C	T	C
	CBS 125276	T	A	T	C	C	C	C	C	**C**	**G**	G	T	G	C	T	C	T	C
Ca. fujianensis	**CBS 127201**	C	A	C	C	C	**T**	C	C	T	A	G	T	G	C	T	C	T	C
	CBS 127200	C	A	C	C	C	**T**	C	C	T	A	G	T	G	C	T	C	T	C
Ca. nymphaeae	**CBS 131802**	C	A	C	C	A	C	C	C	T	A	–	–	–	–	–	**T**	**C**	**G**
	HGUP 100004	C	A	C	C	A	C	C	C	T	A	–	–	–	–	–	**T**	**C**	**G**
Ca. paracolhounii	**CBS 114679**	N/A	N/A	N/A	**A**	C	C	C	**G**	T	A	G	T	G	C	T	C	T	C
Ca. pseudocolhounii	**CBS 127195**	T	A	T	C	C	C	**T**	C	T	A	G	T	G	C	T	C	T	C
	CBS 127196	T	A	T	C	C	C	**T**	C	T	A	G	T	G	C	T	C	T	C

[†] Polymorphic nucleotides occurring only in all of the isolates are shown, not alleles that partially occur in individuals per phylogenetic group.

[‡] Numerical positions of the nucleotides in the DNA sequence alignments are indicated.

[§] Ex-type isolates are indicated in bold.

[|] Fixed polymorphisms for each group are shaded and in bold, those fixed but shared between two or more groups are only shaded.

[¶] "N/A" represents sequences that are not available.

Table 4. Number of unique alleles found in *Calonectria lichi* and the phylogenetically closest related species in total and in the four gene regions.

	Ca. colhounii	***Ca. eucalypti***	***Ca. fujianensis***	***Ca. nymphaeae***	***Ca. paracolhounii***	***Ca. pseudocolhounii***
Ca. lichi	22(16/3/2/1)[†]	19(4/6/2/7)	10(6/0/0/4)	14(5/NA[‡]/NA/9)	34(19/NA/11/4)	13(3/4/1/5)
Ca. colhounii		19(12/3/2/2)	24(18/3/2/1)	24(15/NA/NA/9)	42(28/NA/12/2)	18(13/1/3/1)
Ca. eucalypti			22(6/6/2/8)	18(4/NA/NA/14)	45(26/NA/12/7)	11(1/4/1/5)
Ca. fujianensis				16(5/NA/NA/11)	37(23/NA/11/3)	15(5/4/1/5)
Ca. nymphaeae					32(20/NA/NA/12)	16(4/NA/NA/12)
Ca. paracolhounii						36(20/NA/12/4)

[†] The order of the four genes: total (*tef1*, *his3*, *cmdA* and *tub2*).

[‡] "NA" represents sequences that are not available.

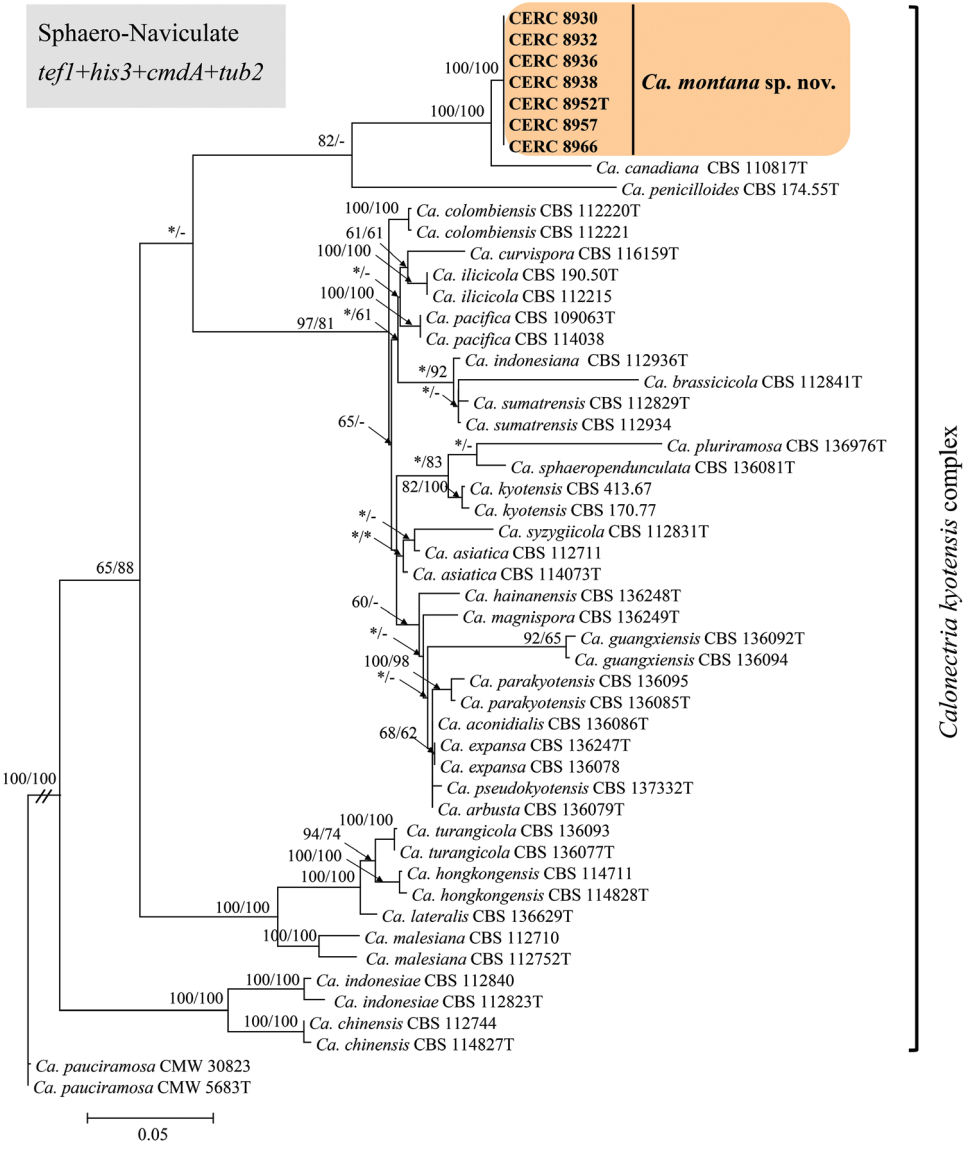

Figure 2. Phylogenetic tree of *Calonectria* species in the Sphaero-Naviculate group based on maximum likelihood (ML) analysis of combined DNA dataset of *tef1*, *his3*, *cmdA* and *tub2* gene sequences. ML and MP (maximum parsimony) bootstrap values (ML/MP) are shown above branches, with bootstrap values below 60 % marked with an *, and absent analysis values are marked with -. Isolates representing ex-type material are marked with "T", isolates highlighted in bold were sequenced in this study and novel species were covered in orange. The tree was rooted to *Ca. pauciramosa* (CMW 5683 and CMW 30823).

Table 5. Single nucleotide polymorphism comparisons in four gene regions between *Calonectria montana* and *Ca. canadiana.*

Species	Isolate no.	*tef1*[†]		*his3*																		
		50[‡]	497	28	29	34	47	49	50	58	64	92	110	123	138	157	159	177	180	188	196
Ca. montana	**CERC 8952**[§]	C	–	C	C	C	–	G	C	G	C	C	C	C	C	–	C	G	A	T	G
	CERC 8930	C	–	C	C	C	–	G	C	G	C	C	C	C	C	–	C	G	A	T	G
	CERC 8932	C	–	C	C	C	–	G	C	G	C	C	C	C	C	–	C	G	A	T	G
	CERC 8936	C	–	C	C	C	–	G	C	G	C	C	C	C	C	–	C	G	A	T	G
	CERC 8938	C	–	C	C	C	–	G	C	G	C	C	C	C	C	–	C	G	A	T	G
	CERC 8957	C	–	C	C	C	–	G	C	G	C	C	C	C	C	–	C	G	A	T	G
	CERC 8966	C	–	C	C	C	–	G	C	G	C	C	C	C	C	–	C	G	A	T	G
Ca. canadiana	**CBS 110817**	–	T	G	G	T	A	T	G	A	T	T	G	T	A	A	A	C	T	A	T

Species	Isolate no.	*his3*																				
		199	202	205	212	213	220	227	229	257	300	321	336	339	372	378	397	400	403	418	421
Ca. montana	**CERC 8952**	C	C	C	C	T	C	C	C	C	C	C	C	T	C	–	C	C	C	T	C
	CERC 8930	C	C	C	C	T	C	C	C	C	C	C	C	T	C	–	C	C	C	T	C
	CERC 8932	C	C	C	C	T	C	C	C	C	C	C	C	T	C	–	C	C	C	T	C
	CERC 8936	C	C	C	C	T	C	C	C	C	C	C	C	T	C	–	C	C	C	T	C
	CERC 8938	C	C	C	C	T	C	C	C	C	C	C	C	T	C	–	C	C	C	T	C
	CERC 8957	C	C	C	C	T	C	C	C	C	C	C	C	T	C	–	C	C	C	T	C
	CERC 8966	C	C	C	C	T	C	C	C	C	C	C	C	T	C	–	C	C	C	T	C
Ca. canadiana	**CBS 110817**	T	A	T	G	G	A	G	T	G	G	A	A	C	G	G	T	T	–	G	A

Species	Isolate no.	*cmdA*	*tub2*									
		470	3	4	7	10	174	181	336	403	439	502
Ca. montana	**CERC 8952**	T	G	T	C	T	C	T	C	C	T	C
	CERC 8930	T	G	T	C	T	C	T	C	C	T	C
	CERC 8932	T	G	T	C	T	C	T	C	C	T	C
	CERC 8936	T	G	T	C	T	C	T	C	C	T	C
	CERC 8938	T	G	T	C	T	C	T	C	C	T	C
	CERC 8957	T	G	T	C	T	C	T	C	C	T	C
	CERC 8966	T	G	T	C	T	C	T	C	C	T	C
Ca. canadiana	**CBS 110817**	C	A	C	G	C	T	C	T	A	C	T

[†] Polymorphic nucleotides occurring only in all of the isolates are shown, not alleles that partially occur in individuals per phylogenetic group.

[‡] Numerical positions of the nucleotides in the DNA sequence alignments are indicated.

[§] Ex-type isolates are indicated in bold.

Table 6. Number of unique alleles found in *Calonectria montana* and *Ca. canadiana* in total and in the four gene regions.

	Ca. canadiana
Ca. montana	51(2/38/1/10)†

† The order of the four genes: total (*tef1*, *his3*, *cmdA* and *tub2*).

Taxonomy

Based on DNA sequence comparisons, the 16 isolates collected in this study presented two strongly defined phylogenetic clades in both the Prolate Group and the Sphaero-Naviculate Group. Morphological differences were observed between each phylogenetic clade and its phylogenetically closed species, especially with respect to the size of the macroconidia (Table 7). Based on the phylogenetic analyses, as well as morphological characteristics, the fungi isolated from the soil in this study represent two novel species of *Calonectria*, they are described as follows:

Calonectria lichi **Q.L. Liu & S.F. Chen, sp. nov.**
MycoBank MB821348
Figure 3

Etymology. *lichi*, which is *Calonectria* in Chinese.

Diagnosis. *Calonectria lichi* differs from the phylogenetically closely related species *Ca. colhounii*, *Ca. eucalypti*, *Ca. fujianensis*, *Ca. nymphaeae*, *Ca. paracolhounii* and *Ca. pseudocolhounii* with respect to the macroconidia dimensions.

Type. CHINA. From soil under a natural forest in central China, 07 April 2016, ShuaiFei Chen, CSFF 2019 – holotype, CERC 8866 = CGMCC 3.18733 – ex-type culture.

Description. Sexual morph unknown. Macroconidiophores consisting of a stipe, a suite of penicillate arranged fertile branches, a stipe extension, and a terminal vesicle; stipe septate, hyaline, smooth, (39.5–)78.5–160.5(–206.5) × (4.5–)5.5–7.5(–8.5) µm; stipe extension septate, straight to flexuous, (124–)139.5–187.5(–218) µm long, 2.5–5 µm wide at the apical septum, terminating in a clavate vesicle, (3.5–)4–5(–5.5) µm diam, lateral stipe extensions (90° to main axis) absent. Conidiogenous apparatus (44–)56–92(–108.5) µm long, (35–)52–82.5(–94) µm wide; primary branches aseptate to 1–septate, (12–)16.5–33.5(–46.5) × (4–)4.5–6.5(–9) µm; secondary branches aseptate, (7–)9.5–16(–21) × (3–)3.5–5(–6) µm; tertiary branches aseptate, (7.5–)9–12.5(–14.5) × (3–)3.5–4.5(–6) µm; additional branches (–5), aseptate, (5.5–)8.5–12.5(–14) × (2.5–)3.5–4.5(–5.5) µm; each terminal branch producing 2–4 phialides; phialides doliiform to reniform, hyaline, aseptate, (6–)8–12(–14.5) × (2.5–)3–4(–5) µm, apex with minute periclinal thickening and inconspicuous collarette. Macroconidia cylindrical, rounded at both ends, straight, (53–)60.5–70.5(–79) × (5–)5.5–6.5(–7) µm (av. = 65.7 × 6 µm), 3–septate, lacking a visible abscission scar,

Table 7. Morphological comparisons of *Calonectria lichi*, *Ca. montana* and their phylogenetically closely related species.

Speices	Macroconidia (L × W)[†,‡]	Macroconidia average (L × W)[†,‡]	Macroconidia septation	Vesicle (Min. – Max.)[†,§]	Vesicle shape	Reference
Ca. lichi[|]	(53–)60.5–70.5(–79) × (5–)5.5–6.5(–7)[¶]	65.7 × 6	3	(3.5–)4–5(–5.5)	clavate	This study
Ca. colhounii	(45–)60–70(–80) × (4–)5(–6)	65 × 5	(1–)3	3–4	clavate	Crous 2002
Ca. eucalypti	(66–)69–75(–80) × (5–)6	72 × 6	3	4–6	broadly clavate	Lombard et al. 2010b
Ca. fujianensis	(48–)50–55(–60) × (2.5–)3.5–4.5(–5)	52.5 × 4	(1–)3	(3–)3.5–4.5(–5)	clavate	Chen et al. 2011
Ca. nymphaeae	55–63 × 5.3–6.3	61 × 5.9	3–4	3–5	clavate	Xu et al. 2012
Ca. paracolhounii	(37–)39–43(–45) × 4–5	41 × 5	3	3–5	narrowly clavate	Lombard et al. 2016
Ca. pseudocolhounii	(49–)55–65(–74) × (3.5–)4–5(–5.5)	60 × 4.5	(1–)3	(3.5–)4–5(–6)	clavate	Chen et al. 2011
Ca. montana	(37.5–)40.5–45.5(–51.5) × 4–5(–5.5)	43.2 × 4.6	1	(4–)7–11(–12.5)	sphaeropedunculate	This study
Ca. canadiana	(38–)48–55(–65) × 4(–5)	50 × 4	1	6–10	pyriform to sphaeropedunculate	Kang et al. 2001; Lechat et al. 2010

[†] All measurements are in µm.

[‡] L × W = length × width.

[§] Min.–Max. = minimum–maximum.

[|] Species indicated in bold are described in this study.

[¶] Measurements are presented in the format [(minimum–) (average – standard deviation) – (average + standard deviation) (–maximum)].

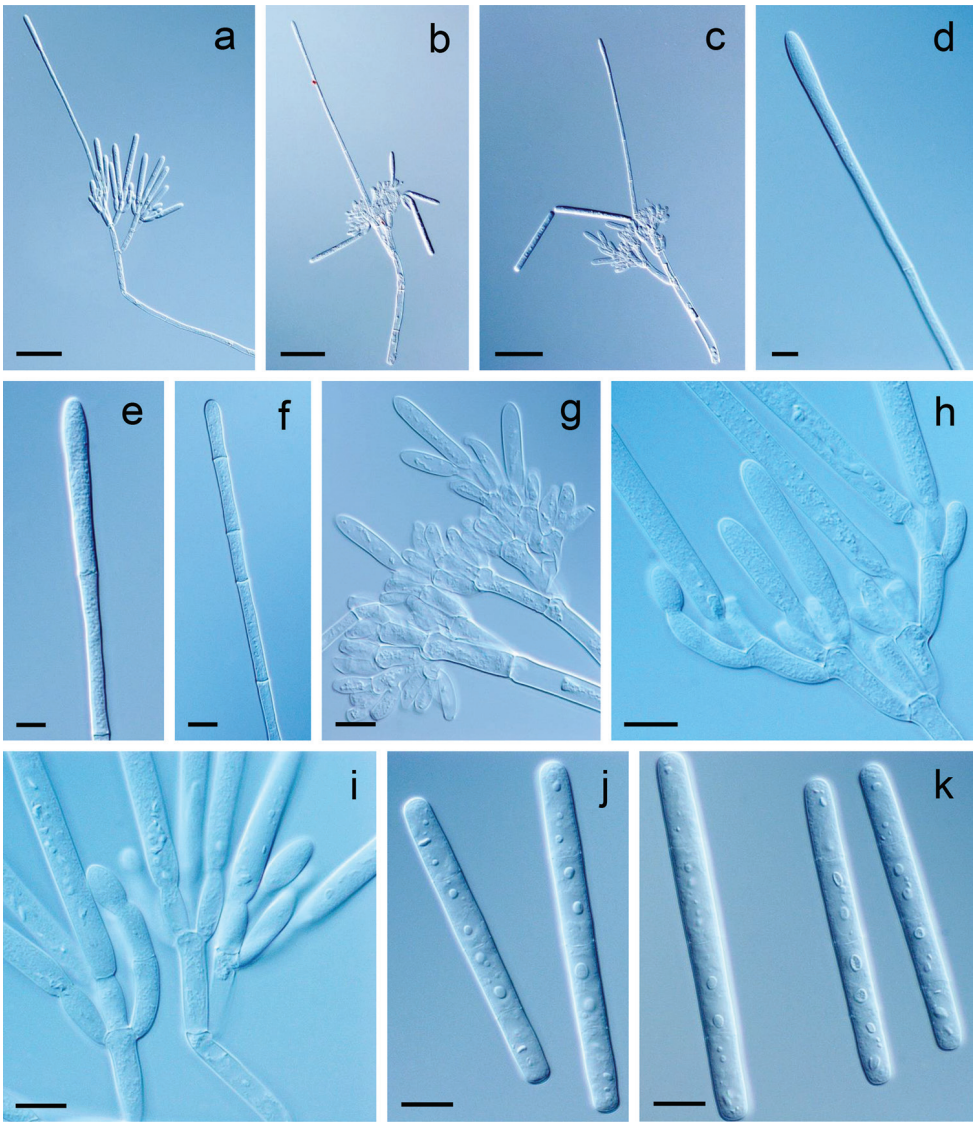

Figure 3. *Calonectria lichi*. **a–c** Macroconidiophore **d–f** Clavate vesicles **g–i** Conidiogenous apparatus with conidiophore branches and doliiform to reniform phialides **j–k** Macroconidia Scale bars: **a–c** = 50 µm; **d–f** = 5 µm; **g–k** = 10 µm.

held in parallel cylindrical clusters by colorless slime. Megaconidia and microconidia not observed.

Culture characteristics. Colonies forming abundant white aerial mycelium on MEA at 25 °C after seven days, with feathery, irregular margins at the edges, moderate sporulation. Surface with white to buff outer margins, and salmon (13'd) inner region, becoming ochreous (44) towards the center, reverse sienna (8) to umber (9) with abundant chlamydospores throughout the medium, forming microsclerotia. Optimal

growth temperature at 25 °C, no growth at 5 °C and 35 °C, after seven days, colonies at 10 °C, 15 °C, 20 °C, 25 °C and 30 °C reached 21.9 mm, 30.8 mm, 41.5 mm, 54.4 mm and 37.2 mm, respectively.

Substratum. Soil in a natural forest.

Distribution. Central China.

Other specimens examined. CHINA. From soil in a natural forest in central China, 07 April 2016, ShuaiFei Chen, CSFF 2020, culture CERC 8850 = CGMCC 3.18732; CHINA. From soil under a natural forest in central China, 07 April 2016, ShuaiFei Chen, CSFF 2021, culture CERC 8890 = CGMCC 3.18734; CHINA. From soil in a natural forest in central China, 07 April 2016, ShuaiFei Chen, culture CERC 8841, CERC 8848, CERC 8871, CERC 8900, CERC 8906 and CERC 8928.

Notes. *Calonectria lichi* is a new species in the *Ca. colhounii* complex and is closely related to *Ca. colhounii*, *Ca. eucalypti*, *Ca. fujianensis*, *Ca. nymphaeae*, *Ca. paracolhounii* and *Ca. pseudocolhounii* (Crous 2002, Lombard et al. 2010b, 2016, Chen et al. 2011, Xu et al. 2012, Crous et al. 2015). The macroconidia of *Ca. lichi* (av. 65.7 × 6.0 µm) are longer and wider than those of *Ca. colhounii* (av. 65 × 5 µm), *Ca. fujianensis* (av. 52.5 × 4 µm), *Ca. nymphaeae* (av. 61 × 5.9 µm), *Ca. paracolhounii* (av. 41 × 5 µm) and *Ca. pseudocolhounii* (av. 60 ×4.5 µm), but narrower than those of *Ca. eucalypti* (av. 72 × 6µm).

Calonectria montana **Q.L. Liu & S.F. Chen, sp. nov.**
MycoBank MB821349
Figure 4

Etymology. *montis*, meaning mountain in Latin, referring to the location where this fungus was collected.

Diagnosis. *Calonectria montana* can be distinguished from the phylogenetically closely related species *Ca. canadiana* by the size of macroconidia.

Type. CHINA. From soil under a natural forest in central China, 07 April 2016, ShuaiFei Chen, holotype CSFF 2022, ex-type culture CERC 8952 = CGMCC 3.18735.

Description. Sexual morph unknown. Macroconidiophores consisting of a stipe, a suite of penicillate arranged fertile branches, a stipe extension, and a terminal vesicle; stipe septate, hyaline, smooth, (30–)52–91(–123.5) × (4–)5.5–8(–9.5) µm; stipe extension septate, straight to flexuous (76.5–)107–168(–211.5) µm long, (2.5–)3–4.5(–5.5) µm wide at the apical septum, terminating in a pyriform to sphaeropedunculate vesicle, (4–)7–11(–12.5) µm diam, lateral stipe extensions (90° to main axis) absent. Conidiogenous apparatus (40–)49–87.5(–102.5) µm long, (44–)62–91(–104) µm wide; primary branches aseptate to 1–septate, (14.5–)19.5–34(–55.5) × (4–)4.5–6(–7) µm; secondary branches aseptate, (11–)13.5–23(–33) × (3–)4–5(–6) µm; tertiary branches aseptate, (9–)11–15(–16.5) × (3.5–)3.5–4.5(–5) µm; each terminal branch producing 2–6 phialides; phialides doliiform to reniform, hyaline, aseptate, (8–)10.5–

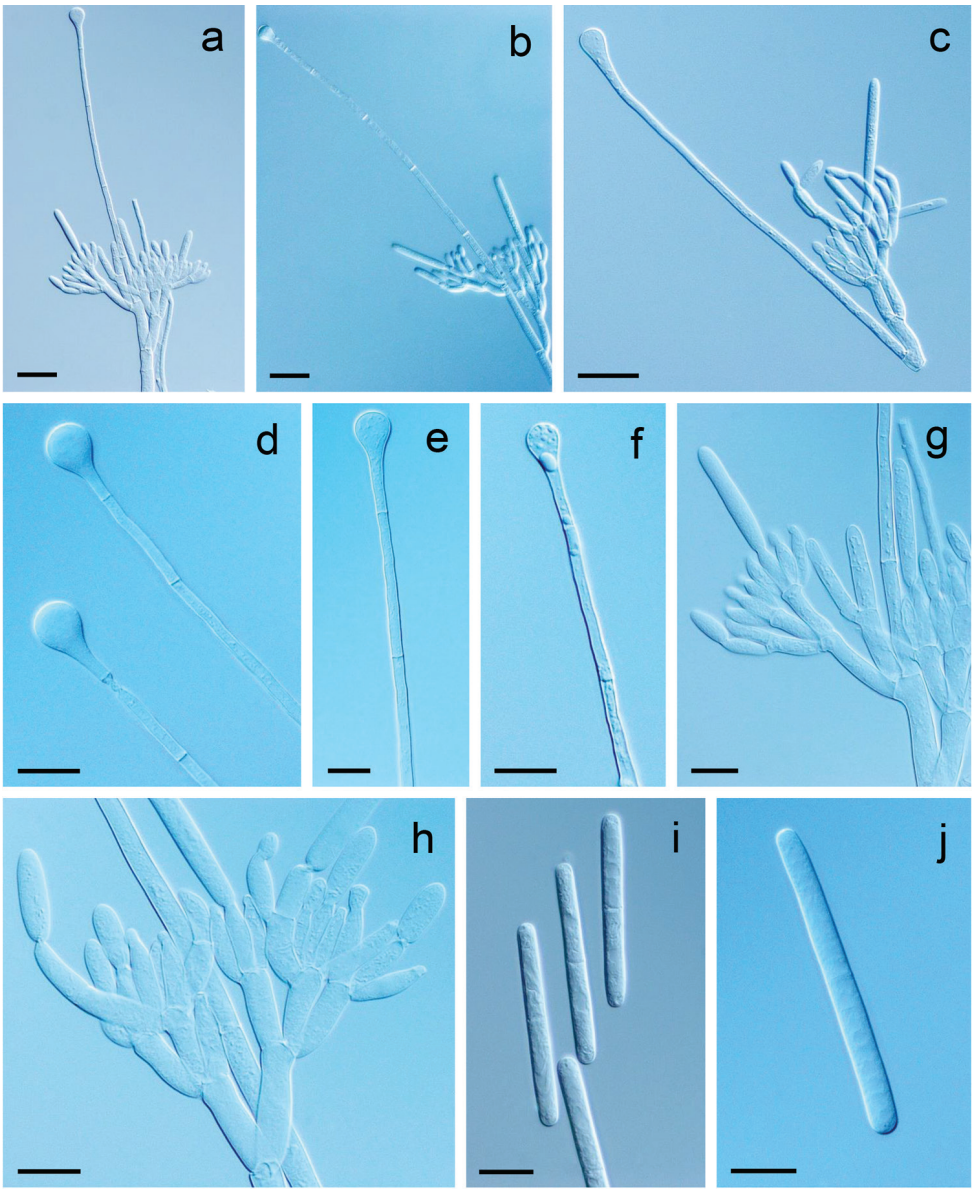

Figure 4. *Calonectria montana*. **a–c** Macroconidiophores **d–f** Sphaeropedunculate vesicles **g–h** Conidiogenous apparatus with conidiophore branches and doliiform to reniform phialides **i–j** Macroconidia Scale bars: **a–c** = 20 µm; **d–j** = 10 µm.

12.5(–15.5) × (2.5–)3.5–4.5(–5) µm, apex with minute periclinal thickening and inconspicuous collarette. Macroconidia cylindrical, rounded at both ends, straight, (37.5–)40.5–45.5(–51.5) × 4–5(–5.5) µm (av. = 43.2 × 4.6 µm), 1–septate, lacking a visible abscission scar, held in parallel cylindrical clusters by colorless slime. Megaconidia and microconidia not observed.

Culture characteristics. Colonies forming abundant buff and wooly aerial mycelium on MEA at 25 °C after seven days, with feathery, irregular margins at the edges, sporulation moderate and more concentrated in the colony centre. Surface with buff to sienna (8) outer margins, reverse sienna (8) to umber (9), and chesnut (9'm) inner region, abundant chlamydospores throughout the medium, forming microsclerotia. Optimal growth temperature at 30 °C, no growth at 5 °C and 35 °C, after seven days, colonies at 10 °C, 15 °C, 20 °C, 25 °C and 30 °C reached 22.9 mm, 31.5 mm, 51.1 mm, 61.9 mm and 77.2 mm, respectively, this is a high-temperature species.

Substratum. Soil under the natural forest.

Distribution. Central China.

Other specimens examined. CHINA. From soil in a natural forest in central China, 07 April 2016, ShuaiFei Chen, CSFF 2023, culture CERC 8957 = CGMCC 3.18736; From soil in a natural forest in central China, 07 April 2016, ShuaiFei Chen, CSFF 2024, culture CERC 8966 = CGMCC 3.18737; From soil in a natural forest in central China, 07 April 2016, ShuaiFei Chen, culture CERC 8930, CERC 8932, CERC 8936 and CERC 8938.

Notes. *Calonectria montana* is a new addition to the *Ca. kyotensis* complex and is phylogenetically closely related to *Ca. canadiana* (Crous 2002, Crous et al. 2004, Lombard et al. 2015, 2016). The macroconidia of *Ca. montana* (av. 43.2 × 4.6 μm) are shorter and wider than those of *Ca. canadiana* (av. 50 × 4 μm).

Discussion

This study identified two novel species of *Calonectria* from soil in a natural forest in the temperate region of central China. The identification of the fungi was supported by DNA sequence comparisons and morphological features. The two species were named *Calonectria lichi* and *Ca. montana*.

Calonectria lichi is a new addition to the *Ca. colhounii* complex that belongs to the Prolate Group. Based on phylogenetic analyses of four gene sequences, *Ca. lichi* formed a distinct and well-supported phylogenetic clade closely related to *Ca. fujianensis*, *Ca. nymphaeae* and *Ca. paracolhounii*, but it can be distinguished from these species by its larger macroconidia. To date, 10 species in the *Ca. colhounii* complex have been identified and described. Other than *Ca. lichi* described in this study, the other species include *Ca. colhounii*, *Ca. eucalypti*, *Ca. fujianensis*, *Ca. macroconidialis*, *Ca. monticola*, *Ca. nymphaeae*, *Ca. paracolhounii*, *Ca. parva* and *Ca. pseudocolhounii* (Crous 2002, Lombard et al. 2010b, 2016, Chen et al. 2011, Xu et al. 2012, Crous et al. 2015). Of these species, *Ca. colhounii*, *Ca. eucalypti*, *Ca. fujianensis*, *Ca. nymphaeae* and *Ca. pseudocolhounii* have been shown to be homothallic and always produce bright yellow perithecia (Crous 2002, Lombard et al. 2010b, Chen et al. 2011, Xu et al. 2012). In China, four species in the *Ca. colhounii* complex have been reported: except for *Ca. lichi*, which was isolated from a natural forest in the temperate zone in central China, the other species, including *Ca. fujianensis*, *Ca. pseudocolhounii* and *Ca. nym-*

phaeae, were previously isolated from tropical or subtropical regions in southern China (Chen et al. 2011, Xu et al. 2012).

Calonectria montana adds a new species to the *Ca. kyotensis* complex that belongs to the Sphaero-Naviculate Group. Phylogenetic analyses showed that *Ca. montana*, which formed an independent clade with a high bootstrap value, is closely related to *Ca. canadiana.* Morphological differences were observed between *Ca. montana* and *Ca. canadiana*, especially with respect to the size of the macroconidia and the shape of the vesicles (Kang et al. 2001, Crous 2002). Species in the *Ca. kyotensis* complex are characterized by having sphaeropedunculate vesicles with lateral stipe extensions on a conidiogenous apparatus (Crous et al. 2004, Lombard et al. 2010b, 2015, 2016). No lateral stipe extensions were produced by *Ca. montana*, indicating that this species is different from other species in the *Ca. kyotensis* complex. In this study, *Ca. montana* was isolated from soil in central China, 14 species residing in the *Ca. kyotensis* complex were previously reported in China, and all of them were isolated from soil in southern China (Crous et al. 2004, Lombard et al. 2015). The results from this study suggest that more species in *Ca. kyotensis* complex have yet to be discovered from China.

Species of *Calonectria* are important plant pathogens that can cause devastating diseases on various plant hosts worldwide, especially on horticultural, agronomic and forestry crops (Polizzi et al. 2001, 2009, Crous 2002, Saracchi et al. 2008, Chen et al. 2011, Pan et al. 2012). In China, *Calonectria* species have been reported as pathogens of various important agronomic and forestry crops. In agriculture, the *Fabaceae* and *Arecaceae* plant families are susceptible to infection by *Calonectria* species, including *Ca. ilicicola*, which causes black rot (CBR) of *Arachis hypogaea* (peanut) and *Medicago sativa* (Gai et al. 2012, Pan et al. 2012, Pei et al. 2015), *Ca. ilicicola* causes red crown rot of *Glycine max* (soybean) (Guan et al. 2010), and *Ca. colhounii* and *Ca. pteridis* cause leaf spot on *Phoenix canariensis* and *Serenoa repens*, respectively (Luo et al. 2009, Yang et al. 2014). In forestry, leaf blight caused by *Calonectria* species is considered as one of the most serious threats to *Eucalyptus* plantations and nurseries in southern China (Zhou et al. 2008, Lombard et al. 2010a, Chen et al. 2011). The leaf inoculations showed that all tested *Calonectria* species were pathogenic to the tested *Eucalyptus* clones, including the clones that are widely planted in southern China (Chen et al. 2011, Li et al. 2014a, b). These research results suggest that species of *Calonectria* need to be monitored carefully, both in agronomic crops and forests.

Accurate diagnosis of plant diseases and identification of their casual agents provide the foundation for developing effective disease management strategies (Booth et al. 2000, Crous 2002, Old et al. 2003, Vitale et al. 2013, Wingfield et al. 2015). Based on previous research results, the majority of *Calonectria* species identified and described in China were isolated from diseased plant tissues or soil under forestry plantations in subtropical and tropical regions (Crous et al. 2004, Lombard et al. 2010a, 2015, Chen et al. 2011). In this study, two novel *Calonectria* species were described, and they were isolated from soil in a natural forest in the temperate zone. The results from this study suggest that more extensive surveys need to be conducted to collect *Calonectria* in more geographic regions with different climate zones, which will help to clarify the species diversity of *Calonectria* in China.

Acknowledgments

This study was supported by the Fundamental Research Funds for the Central Non-Profit Research Institution of CAF (Project No. CAFYBB2014MA018) and the National Natural Science Foundation of China (NSFC) (Project numbers: 31622019 and 31400546). We thank LetPub (www.letpub.com) for linguistic assistance during the preparation of this manuscript.

References

Aiello D, Cirvilleri G, Polizzi G, Vitale A (2013) Effects of fungicide treatments for the control of epidemic and exotic *Calonectria* diseases in Italy. Plant Disease 97: 37–43. https://doi.org/10.1094/PDIS-03-12-0266-RE

Alfenas RF, Pereira OL, Jorge VL, Crous PW, Alfenas AC (2013a) A new species of *Calonectria* causing leaf blight and cutting rot of three forest tree species in Brazil. Tropical Plant Pathology 38: 513–521. https://doi.org/10.1590/S1982-56762013000600007

Alfenas RF, Pereira OL, Ferreira MA, Jorge VL, Crous PW, Alfenas AC (2013b) *Calonectria metrosideri*, a highly aggressive pathogen causing leaf blight, root rot, and wilt of *Metrosideros* spp. in Brazil. Forest Pathology 43: 257–265. https://doi.org/10.1111/efp.12035

Alfenas RF, Lombard L, Pereira OL, Alfenas AC, Crous PW (2015) Diversity and potential impact of *Calonectria* species in *Eucalyptus* plantations in Brazil. Studies in Mycology 80: 89–130. https://doi.org/10.1016/j.simyco.2014.11.002

Booth TH, Jovanovic T, Old KM, Dudzinski MJ (2000) Climatic mapping to identify high-risk areas for *Cylindrocladium quinqueseptatum* leaf blight on eucalypts in mainland South East Asia and around the world. Environmental Pollution 108: 365–372. https://doi.org/10.1016/S0269-7491(99)00215-8

Chen SF, Lombard L, Roux J, Xie YJ, Wingfield MJ, Zhou XD (2011) Novel species of *Calonectria* associated with *Eucalyptus* leaf blight in Southeast China. Persoonia 26: 1–12. https://doi.org/10.3767/003158511X555236

Crous PW, Phillips AJL, Wingfield MJ (1991) The genera *Cylindrocladium* and *Cylindrocladiella* in South Africa, with special reference to forest nurseries. South African Forestry Journal 157: 69–85. https://doi.org/10.1080/00382167.1991.9629103

Crous PW (2002) Taxonomy and pathology of *Cylindrocladium* (*Calonectria*) and allied genera. APS Press, St. Paul, Minnesota, USA.

Crous PW, Groenewald JZ, Risède JM, Simoneau P, Hywel-Jones NL (2004) *Calonectria* species and their *Cylindrocladium* anamorphs: species with sphaeropedunculate vesicles. Studies in Mycology 50: 415–430.

Crous PW, Groenewald JZ, Risède JM, Simoneau P, Hyde KD (2006) *Calonectria* species and their *Cylindrocladium* anamorphs: species with clavate vesicles. Studies in Mycology 55: 213–226. https://doi.org/10.3114/sim.55.1.213

Crous PW, Shivas RG, Wingfield MJ, Summerell BA, Rossman AY, et al (2012) Fungal Planet description sheets: 128–153. Persoonia 29: 146–201. https://doi.org/10.3767/003158512X661589

Crous PW, Wingfield MJ, Guarro J, Cheewangkoon R, Van der Bank M, et al (2013) Fungal Planet description sheets: 154–213. Persoonia 31: 188–296. https://doi.org/10.3767/003158513X675925

Crous PW, Wingfield MJ, Le Roux JJ, Richardson DM, Strasberg D, et al (2015) Fungal Planet description sheets: 371–399. Persoonia 35: 264–327. https://doi.org/10.3767/003158515X690269

Ferreira FA (1989) Patologia florestal. Principais doenças florestais no Brasil. Viçosa, Sociedade de Investigaçoes Florestais, Viçosa, MG, Brazil. 570 pp.

Gadgil PD, Dick MA (2004) Fungi silvicolae novazelandae: 5. New Zealand Journal of Forestry Science 34: 316–323.

Gai Y, Deng Q, Pan R, Chen X, Deng M (2012) First Report of Cylindrocladium Black Rot of Peanut Caused by *Cylindrocladium parasiticum* (Teleomorph *Calonectria ilicicola*) in Jiangxi Province, China. Plant Disease 96: 586. https://doi.org/10.1094/PDIS-11-11-1010

Gehesquière B, Crouch JA, Marra RE, Van Poucke K, Rys F, et al (2015) Characterization and taxonomic reassessment of the box blight pathogen *Calonectria pseudonaviculata*, introducing *Calonectria henricotiae* sp. nov. Plant Pathology 65: 37–52. https://doi.org/10.1111/ppa.12401

Groenewald JZ, Nakashima C, Nishikawa J, Shin HD, Park JH, Jama AN, Groenewald M, Braun U, Crous PW (2013) Species concepts in *Cercospora*: spotting the weeds among the roses. Studies in Mycology 75: 115–170. https://doi.org/10.3114/sim0012

Guan M, Pan R, Gao X, Xu D, Deng Q, Deng M (2010) First report of red crown rot caused by *Cylindrocladium parasiticum* on soybean in Guangdong, southern China. Plant Disease 94: 485. https://doi.org/10.1094/PDIS-94-4-0485B

Guerber JC, Correll JC (2001) Characterization of *Glomerella acutata*, the teleomorph of *Colletotrichum acutatum*. Mycologia 93: 216–229. https://doi.org/10.2307/3761619

Guindon S, Gascuel O (2003) A simple, Fast, and Accurate Algorithm to Estimate Large Phylogenies by Maximum Likelihood. Systematic biology 52: 696–704. https://doi.org/10.1080/10635150390235520

Hillis DM, Huelsenbeck JP (1992) Signal, noise and reliability in molecular phylogenetic analyses. Journal of Heredity 83: 189–195. https://doi.org/10.1093/oxfordjournals.jhered.a111190

Kang J, Crous PW, Schoch CL (2001) Species concepts in the *Cylindrocladium floridanum* and *Cy. Spathiphylli* complexes (Hypocreaceae) based on multi-allelic sequence data, sexual compatibility and morphology. Systematic and Applied Microbiology 24: 206–217. https://doi.org/10.1078/0723-2020-00026

Lechat C, Crous PW, Groenewald JZ (2010) The enigma of *Calonectria* species occurring on leaves of *Ilex aquifolium* in Europe. IMA fungus 1: 101–108. https://doi.org/10.5598/imafungus.2010.01.02.01

Li N, Zhao X, Liu AX, Liu H (2010) Brown spot disease of tree peony caused by *Cylindrocladium canadense* in China. Journal of General Plant Pathology 76: 295–298. https://doi.org/10.1007/s10327-010-0245-2

Li GQ, Chen SF, Wu ZH, Zhou XD, Xie YJ (2014a) Preliminary Analyses on Diversity and Pathogenicity of *Calonectria* spp. on *Eucalyptus* in China. Chinese Journal of Tropical Crops 35: 1183–1191. [In Chinese]

Li GQ, Li JQ, Liu FF, Li TH, Chen SF (2014b) Preliminary Analyses on Pathogenicity of Twelve *Calonectria* spp. on Ten *Eucalyptus* Clones in China. Eucalypt Science & Technology 31: 1–7. https://doi.org/10.13987/j.cnki.askj.2014.04.001 [In Chinese]

Lombard L, Zhou XD, Crous PW, Wingfield BD, Wingfield MJ (2010a) *Calonectria* species associated with cutting rot of *Eucalyptus*. Persoonia 24: 1–11. https://doi.org/10.3767/003158510X486568

Lombard L, Crous PW, Wingfield BD, Wingfield MJ (2010b) Phylogeny and systematics of the genus *Calonectria*. Studies in Mycology 66: 31–69. https://doi.org/10.3114/sim.2010.66.03

Lombard L, Crous PW, Wingfield BD, Wingfield MJ (2010c) Multigene phylogeny and mating tests reveal three cryptic species related to *Calonectria pauciramosa*. Studies in Mycology 66: 15–30. https://doi.org/10.3114/sim.2010.66.02

Lombard L, Crous PW, Wingfield BD, Wingfield MJ (2010d) Species concepts in *Calonectria* (*Cylindrocladium*). Studies in Mycology 66: 1–14. https://doi.org/10.3114/sim.2010.66.01

Lombard L, Polizzi G, Guarnaccia V, Vitale A, Crous PW (2011) *Calonectria* spp. causing leaf spot, crown and root rot of ornamental plants in Tunisia. Persoonia 27: 73–79. https://doi.org/10.3767/003158511X615086

Lombard L, Chen SF, Mou X, Zhou XD, Crous PW, Wingfield MJ (2015) New species, hyperdiversity and potential importance of *Calonectria* spp. from *Eucalyptus* in South China. Studies in Mycology 80: 151–188. https://doi.org/10.1016/j.simyco.2014.11.003

Lombard L, Wingfield MJ, Alfenas AC, Crous PW (2016) The forgotten *Calonectria* collection: pouring old wine into new bags. Studies in Mycology 85: 159–198. https://doi.org/10.1016/j.simyco.2016.11.004

Luan YS, Feng L, An LJ (2006) First Report of Blueberry Leaf Spot Caused by *Cylindrocladium colhounii* in China. Plant Disease 90: 1553. http://dx.doi.org/10.1094/PD901553A

Luo JS, Wang MS, Lin XX, Zhang YY (2009) Pathogenic identification of *Phoenix canariensis* leaf spot disease. Chinese journal of tropical crops 30: 104–107. [In Chinese]

Mirabolfathy M, Ahangaran Y, Lombard L, Crous PW (2013) Leaf blight of *Buxus sempervirens* in northern forests of Iran caused by *Calonectria pseudonaviculata*. Studies in Mycology 85: 159–198. http://dx.doi.org/10.1094/PDIS-03-13-0237-PDN

Nirenburg HI (1981) A simplified method for identifying *Fusarium* spp. occurring on wheat. Canadian Journal of Botany 59: 1599–1609. https://doi.org/10.1139/b81-217

Old KM, Pham QT, Dudzinski MJ, Gibbs RJ (1999) *Eucalyptus* pathology in Vietnam. In: Proceedings of the workshop on eucalypt diseases, ACIAR, Ho Chi Minh City, Vietnam. CSIRO Forestry and Forest Products, Canberra and Forest Science Institute of Vietnam, Hanoi, 5.

Old KM, Wingfield MJ, Yuan ZQ (2003) A manual of diseases of eucalypts in South-East Asia. Centre for International Forestry Research, Indonesia.

Pan R, Deng Q, Xu D, Ji C, Deng M, Chen W (2012) First Report of Peanut *Cylindrocladium* Black Rot Caused by *Cylindrocladium parasiticum* in Fujian Province, Eastern China. Plant Disease 99: 890. http://dx.doi.org/10.1094/PDIS11110982

Peerally A (1991) The classification and phytopathology of *Cylindrocladium* species. Mycotaxon 40: 323–366.

Pei WH, Cao JF, Yang MY, Zhao ZJ, Xue SM (2015) First report of black rot of *Medicago sativa* caused by *Cylindrocladium parasiticum* (teleomorph *Calonectria ilicicola*) in Yunnan Province, China. Plant Disease 99: 890. http://dx.doi.org/10.1094/PDIS11141171PDN

Polizzi G, Catara V (2001) First report of leaf spot caused by *Cylindrocladium pauciramosum* on *Acacia retinodes*, *Arbutus unedo*, *Feijoa sellowiana* and *Dodonaea viscosa* in southern Italy. Plant Disease 85: 803. https://doi.org/10.1094/PDIS.2001.85.7.803C

Polizzi G, Vitale A, Aiello D, Castello I, Guarnaccia V, Parlavecchio G (2009) First record of crown and root rot caused by *Cylindrocladium pauciramosum* on brush cherry in Italy. Plant Disease 93: 547. http://dx.doi.org/10.1094/PDIS9350547A

Posada D (2008) jModelTest: phylogenetic model averaging. Molecular biology and Evolution 25: 1253–1256. https://doi.org/10.1093/molbev/msn083

Rayner RW (1970) A mycological colour chart. Commonwealth Mycological Institute and British Mycological Society. Kew, Surrey, UK.

Rodas CA, Lombard L, Gryzenhoinf M, Slippers B, Wingfield MJ (2005) *Cylindrocladium* blight of *Eucalyptus grandis* in Colombia. Australasian Plant Pathology 34: 143–149. https://doi.org/10.1071/AP05012

Saracchi M, Rocchi F, Pizzatti C, Cortesi P (2008) Box blight, a new disease of *Buxus* in Italy caused by *Cylindrocladium buxicola*. Journal of plant pathology 90: 581–584.

Schoch CL, Crous PW, Wingfield BD, Wingfield MJ (2001) Phylogeny of *Calonectria* based on comparisons of β-tubulin DNA sequences. Mycological Research 105: 1045–1052. https://doi.org/10.1016/S0953-7562(08)61966-8

Serrato-Diaz LM, Latoni-Brailowsky EI, Rivera-Vargas LI, Goenaga R, Crous PW, French-Monar RD (2013) First Report of *Calonectria hongkongensis* Causing Fruit Rot of Rambutan (*Nephelium lappaceum*). Plant Disease 97: 1117. http://dx.doi.org/10.1094/PDIS01-130008PDN

Sharma JK, Mohanan C, Florence EJ (1984) Nursery diseases of *Eucalyptus* in Keralal. Forest Pathology 14: 77–89. http: //doi.org/10.1111/j.14390329.1984.tb00156.x

Sobers EK, Littrell RH (1974) Pathogenicity of three species of *Cylindrocladium* to select hosts. Plant Disease Reporter 58: 1017–1019.

Swofford DL (2003) PAUP*. Phylogenetic Analysis Using Parsimony (*and other methods). V. 4.0b10. Sinauer Associates, Sunderland, Massachusetts, USA.

Tamura K, Stecher G, Peterson D, Filipski A, Sudhir Kumar (2013) MEGA6: Molecular evolutionary genetics analysis v. 6.0. Molecular Biology and Evolution 30: 2725–2729. https://doi.org/10.1093/molbev/mst197

Van Burik JAH, Schreckhise RW, White TC, Bowden RA, Myerson D (1998) Comparison of six extraction techniques for isolation of DNA from filamentous fungi. Medical Mycology 36: 299–303. https://doi.org/10.1111/j.1365-280X.1998.00161.x

Vitale A, Aiello D, Castello I, Dimartino MA, Parlavecchio G, Polizzi G (2009) Severe outbreak of crown rot and root rot caused by *Cylindrocladium pauciramosum* on strawberry tree in Italy. Plant Disease 93: 842. http://dx.doi.org/10.1094/PDIS9380842B

Vitale A, Crous PW, Lombard L, Polizzi G (2013) *Calonectria* diseases on ornamental plants in Europe and the Mediterranean basin: an overview. Journal of Plant Pathology 95: 463–476. http: //doi .org/10.4454/JPP.V95I3.007

Wingfield MJ, Brockerhoff EG, Wingfield BD, Slippers B (2015) Planted forest health: the need for a global strategy. Science 349: 832–836. https://doi.org/10.1126/science.aac6674

Xu JJ, Qin SY, Hao YY, Ren J, Tan P, Bahkali AH, Hyde KD, Wang Y (2012) A new species of *Calonectria* causing leaf disease of water lily in China. Mycotaxon 122: 177–185. https://doi.org/10.5248/122.177

Yamamoto R, Nakagawa A, Shimada S, Komatsu S, Kanematsu S (2017) Histopathology of red crown rot of soybean. Journal of General Plant Pathology 83: 23–32. https://doi.org/10.1007/s10327-016-0694-3

Yang W, Zheng L, Wang C, Xie CP (2014) The First Report of *Calonectria pteridis* causing a Leaf Spot Disease on *Serenoa repens* in China. Plant Disease 98: 854–855. https://doi.org/10.1094/PDIS11131167PDN

Zhou XD, Xie YJ, Chen SF, Wingfield MJ (2008) Diseases of eucalypt plantations in China: challenges and opportunities. Fungal Diversity 32: 1–7.

Supplementary material 1

Phylogenetic tree of *Calonectria* species in the Prolate group based on maximum likelihood (ML) analysis of *tef1* gene sequences

Authors: QianLi Liu, ShuaiFei Chen

Data type: molecular data

Explanation note: ML and MP (maximum parsimony) bootstrap values (ML/MP) are shown above branches, with bootstrap values below 60 % marked with an *, and absent analysis values are marked with -. Isolates representing ex-type material are marked with "T", isolates highlighted in bold were sequenced in this study and novel species were covered in blue. The tree was rooted to *Ca. hongkongensis* (CBS 114711 and CBS 114828).

Copyright notice: This dataset is made available under the Open Database License (http://opendatacommons.org/licenses/odbl/1.0/). The Open Database License (ODbL) is a license agreement intended to allow users to freely share, modify, and use this Dataset while maintaining this same freedom for others, provided that the original source and author(s) are credited.

Link: https://doi.org/10.3897/mycokeys.26.14688.suppl1

Supplementary material 2

Phylogenetic tree of *Calonectria* species in the Prolate group based on maximum likelihood (ML) analysis of *his3* gene sequences

Authors: QianLi Liu, ShuaiFei Chen

Data type: molecular data

Explanation note: ML and MP (maximum parsimony) bootstrap values (ML/MP) are shown above branches, with bootstrap values below 60 % marked with an *, and absent analysis values are marked with -. Isolates representing ex-type material are marked with "T", isolates highlighted in bold were sequenced in this study and novel species were covered in blue. The tree was rooted to *Ca. hongkongensis* (CBS 114711 and CBS 114828).

Copyright notice: This dataset is made available under the Open Database License (http://opendatacommons.org/licenses/odbl/1.0/). The Open Database License (ODbL) is a license agreement intended to allow users to freely share, modify, and use this Dataset while maintaining this same freedom for others, provided that the original source and author(s) are credited.

Link: https://doi.org/10.3897/mycokeys.26.14688.suppl2

Supplementary material 3

Phylogenetic tree of *Calonectria* species in the Prolate group based on maximum likelihood (ML) analysis of *cmdA* gene sequences

Authors: QianLi Liu, ShuaiFei Chen

Data type: molecular data

Explanation note: ML and MP (maximum parsimony) bootstrap values (ML/MP) are shown above branches, with bootstrap values below 60 % marked with an *, and absent analysis values are marked with -. Isolates representing ex-type material are marked with "T", isolates highlighted in bold were sequenced in this study and novel species were covered in blue. The tree was rooted to *Ca. hongkongensis* (CBS 114711 and CBS 114828).

Copyright notice: This dataset is made available under the Open Database License (http://opendatacommons.org/licenses/odbl/1.0/). The Open Database License (ODbL) is a license agreement intended to allow users to freely share, modify, and use this Dataset while maintaining this same freedom for others, provided that the original source and author(s) are credited.

Link: https://doi.org/10.3897/mycokeys.26.14688.suppl3

Supplementary material 4

Phylogenetic tree of *Calonectria* species in the Prolate group based on maximum likelihood (ML) analysis of *tub2* gene sequences

Authors: QianLi Liu, ShuaiFei Chen

Data type: molecular data

Explanation note: ML and MP (maximum parsimony) bootstrap values (ML/MP) are shown above branches, with bootstrap values below 60 % marked with an *, and absent analysis values are marked with -. Isolates representing ex-type material are marked with "T", isolates highlighted in bold were sequenced in this study and novel species were covered in blue. The tree was rooted to *Ca. hongkongensis* (CBS 114711 and CBS 114828).

Copyright notice: This dataset is made available under the Open Database License (http://opendatacommons.org/licenses/odbl/1.0/). The Open Database License (ODbL) is a license agreement intended to allow users to freely share, modify, and use this Dataset while maintaining this same freedom for others, provided that the original source and author(s) are credited.

Link: https://doi.org/10.3897/mycokeys.26.14688.suppl4

Supplementary material 5

Phylogenetic tree of *Calonectria* species in the Sphaero-Naviculate group based on maximum likelihood (ML) analysis of *tef1* gene sequences

Authors: QianLi Liu, ShuaiFei Chen

Data type: molecular data

Explanation note: ML and MP (maximum parsimony) bootstrap values (ML/MP) are shown above branches, with bootstrap values below 60 % marked with an *, and absent analysis values are marked with -. Isolates representing ex-type material are marked with "T", isolates highlighted in bold were sequenced in this study and novel species were covered in orange. The tree was rooted to *Ca. pauciramosa* (CMW 5683 and CMW 30823).

Copyright notice: This dataset is made available under the Open Database License (http://opendatacommons.org/licenses/odbl/1.0/). The Open Database License (ODbL) is a license agreement intended to allow users to freely share, modify, and use this Dataset while maintaining this same freedom for others, provided that the original source and author(s) are credited.

Link: https://doi.org/10.3897/mycokeys.26.14688.suppl5

Supplementary material 6

Phylogenetic tree of *Calonectria* species in the Sphaero-Naviculate group based on maximum likelihood (ML) analysis of *his3* gene sequences

Authors: QianLi Liu, ShuaiFei Chen

Data type: molecular data

Explanation note: ML and MP (maximum parsimony) bootstrap values (ML/MP) are shown above branches, with bootstrap values below 60 % marked with an *, and absent analysis values are marked with -. Isolates representing ex-type material are marked with "T", isolates highlighted in bold were sequenced in this study and novel species were covered in orange. The tree was rooted to *Ca. pauciramosa* (CMW 5683 and CMW 30823).

Copyright notice: This dataset is made available under the Open Database License (http://opendatacommons.org/licenses/odbl/1.0/). The Open Database License (ODbL) is a license agreement intended to allow users to freely share, modify, and use this Dataset while maintaining this same freedom for others, provided that the original source and author(s) are credited.

Link: https://doi.org/10.3897/mycokeys.26.14688.suppl6

Supplementary material 7

Phylogenetic tree of *Calonectria* species in the Sphaero-Naviculate group based on maximum likelihood (ML) analysis of *cmdA* gene sequences

Authors: QianLi Liu, ShuaiFei Chen

Data type: molecular data

Explanation note: ML and MP (maximum parsimony) bootstrap values (ML/MP) are shown above branches, with bootstrap values below 60 % marked with an *, and absent analysis values are marked with -. Isolates representing ex-type material are marked with "T", isolates highlighted in bold were sequenced in this study and novel species were covered in orange. The tree was rooted to *Ca. pauciramosa* (CMW 5683 and CMW 30823).

Copyright notice: This dataset is made available under the Open Database License (http://opendatacommons.org/licenses/odbl/1.0/). The Open Database License (ODbL) is a license agreement intended to allow users to freely share, modify, and use this Dataset while maintaining this same freedom for others, provided that the original source and author(s) are credited.

Link: https://doi.org/10.3897/mycokeys.26.14688.suppl7

Supplementary material 8

Phylogenetic tree of *Calonectria* species in the Sphaero-Naviculate group based on maximum likelihood (ML) analysis of *tub2* gene sequences

Authors: QianLi Liu, ShuaiFei Chen

Data type: molecular data

Explanation note: ML and MP (maximum parsimony) bootstrap values (ML/MP) are shown above branches, with bootstrap values below 60 % marked with an *, and absent analysis values are marked with -. Isolates representing ex-type material are marked with "T", isolates highlighted in bold were sequenced in this study and novel species were covered in orange. The tree was rooted to *Ca. pauciramosa* (CMW 5683 and CMW 30823).

Copyright notice: This dataset is made available under the Open Database License (http://opendatacommons.org/licenses/odbl/1.0/). The Open Database License (ODbL) is a license agreement intended to allow users to freely share, modify, and use this Dataset while maintaining this same freedom for others, provided that the original source and author(s) are credited.

Link: https://doi.org/10.3897/mycokeys.26.14688.suppl8

MycoKeys 26: 61–75 (2017)
doi: 10.3897/mycokeys.26.14919
http://mycokeys.pensoft.net

RESEARCH ARTICLE

A peer-reviewed open-access journal
MycoKeys
Launched to accelerate biodiversity research

Two new green-spored species of *Trichoderma* (Sordariomycetes, Ascomycota) and their phylogenetic positions

Zhao-Xiang Zhu[1], Hao-Xiang Xu[1], Wen-Ying Zhuang[2], Yu Li[1]

1 *Engineering Research Center of Chinese Ministry of Education for Edible and Medicinal Fungi, Jilin Agricultural University, Changchun 130118, China* **2** *State Key Laboratory of Mycology, Institute of Microbiology, Chinese Academy of Sciences, Beijing 100101, China*

Corresponding author: *Yu Li* (fungi966@126.com)

Academic editor: *T. Lumbsch* | Received 8 July 2017 | Accepted 21 August 2017 | Published 15 September 2017

Citation: Zhu Z-X, Xu H-X, Zhuang W-Y, Li Y (2017) Two new green-spored species of *Trichoderma* (Sordariomycetes, Ascomycota) and their phylogenetic positions. MycoKeys 26: 61–75. https://doi.org/10.3897/mycokeys.26.14919

Abstract

Two new species of *Trichoderma* are described based on the collections producing ascomata or asexual morphs on woody substrates, and named as *Trichoderma fujianense* and *T. zonatum*. *Trichoderma fujianense* produces gliocladium to verticillium-like conidiophores, slender to lageniform phialides, green and ellipsoidal to cylindrical conidia. *Trichoderma zonatum* is characterized by pulvinate, pale yellow to light brown stromata with densely disposed dark green to black ostioles, monomorphic ascospores, simple trichoderma-like conidiophores, green, (sub)globose to pyriform conidia. Their phylogenetic positions were investigated inferred from sequence analyses of the combined RNA polymerase II subunit b and translation elongation factor 1-α genes. The results indicate that *T. fujianense*, along with *T. aureoviride* and *T. candidum*, represents an independent lineage with high statistical support. *Trichoderma zonatum* belongs to the Chlorosporum clade and is associated with but clearly separated from *T. rosulatum* and *T. costaricense*. Morphological distinctions and sequence divergences between the new species and their close relatives were discussed.

Key words

Hypocreales, morphology, phylogeny, taxonomy

Introduction

Trichoderma Pers. (Ascomycota, Sordariomycetes, Hypocreales, teleomorph *Hypocrea* Fr.) species are frequently found on dead wood and bark, on other fungi, in soil and

Copyright *Zhao-Xiang Zhu et al.* This is an open access article distributed under the terms of the Creative Commons Attribution License (CC BY 4.0), which permits unrestricted use, distribution, and reproduction in any medium, provided the original author and source are credited.

living within healthy plant roots, stems and leaves (Mukherjee et al. 2013). Species of the genus belong to one of the most useful groups of microbes to have had an immense impact on human welfare. Some species are widely used as effective biocontrol agents for several soil-borne plant pathogens (Harman et al. 2004, Hasan et al. 2012, Liu et al. 2012), producers of enzymes, antibiotics and heterologous proteins for food, feed, textile and biofuel industries (cellulases, hemicellulases) (Samuels 1996, Almeida et al. 2007, Cheng et al. 2012, Lopes et al. 2012, Mukherjee et al. 2013). Many members are treated as agents for improving seed germination and nutrient use efficiency, breaking of seed dormancy, as well as source of transgenes and herbicides, and are long known to improve plant growth through the production of phytohormones and certain secondary metabolites (Harman et al. 2004, Shoresh et al. 2010), whereas others are causal agents of opportunistic infections of humans and animals (Samuels 1996, Kuhls et al. 1999, Kredics et al. 2003), and due to association of certain species with economically significant production losses in commercial mushroom farms (Samuels et al. 2002, Park et al. 2006, Kim et al. 2012a, 2012b).

The genus *Trichoderma* was established in 1794 including four species (Samuels 1996). In recent years, the number of *Trichoderma* species increases dramatically. Bissett et al. (2015) presented a list of 254 names of species and two names of varieties in *Trichoderma* with name or names against which they are to be protected, following the ICN (Melbourne Code, Art. 14.13). More recently, In a large-scale survey of *Trichoderma* from rotten wood and soil in China, Qin and Zhuang (2016a, b, c, d, e, 2017) published 27 new species based on the collections producing ascomata or asexual morphs on woody substrates; Chen and Zhuang (2016) described two new species based on soil samples from the Hubei and Tibet regions of China; Montoya et al. (2016) found three new taxa in the attine ant environment; Sun et al. (2016) described a new fungicolous *Trichoderma* species which was isolated from surface of the stroma of *Hypoxylon anthochroum*. Until now, 287 *Trichoderma* species have been described.

During our investigation of the diversity of *Trichoderma* species in China, two species were found to represent undescribed new taxa, on the basis of both morphological and cultural characters and DNA sequence analyses of partial nuc translation elongation factor 1-α encoding gene (*TEF*1-α) and the gene for nuc RNA polymerase II second largest subunit (*RPB*2). Differences between the new species and their close relatives are discussed, and a phylogenetic analysis is provided.

Materials and methods

Specimens and strains

Specimens were collected from Henan and Fujian provinces, China, and deposited in the Mycological Herbarium of Jilin Agricultural University (HMJAU). Strains were obtained either by single ascospore isolation from fresh stromata of sexual morphs or by direct isolation from asexual morphs on the substrates. Cultures are deposited in the China General Microbiological Culture Collection Center (CGMCC).

Morphological study

Dried stromata were rehydrated and longitudinal sections through ascomata were made with a freezing microtome (Leica CM1950) at a thickness of 5–10 μm. Agar media employed were cornmeal dextrose agar (CMD, Difco, Sparks, MD, USA, with dextrose 20 g/L), potato dextrose agar (PDA, Solarbio, Beijing, CHINA) and synthetic low nutrient agar (SNA, Nirenberg 1976, pH adjusted to 5.5). Colonies were incubated in 9 cm diam Petri dishes at 25 °C with alternating light/darkness (12/12 h) at 20 °C, 25 °C, 30 °C and 35 °C and measured daily until the dishes were covered with mycelium. The characteristics of asexual and sexual states were described following the methods of Jaklitsch (2009) and Zhu and Zhuang (2015). Photographs were taken using a Leica DFC450C digital camera (Tokyo, Japan) connected to a Zeiss Axioskop 2 Plus microscope (Göttingen, Germany) for anatomical structures and to a Zeiss Stemi 2000C stereomicroscope for gross morphology.

DNA extraction, amplification and sequencing

Genomic DNA was extracted from mycelium harvested from colonies on PDA after 1–2 wk with a NuClean Plant Genomic DNA Extraction Kit (CoWin Biosciences, Beijing, China) according to the manufacturer's protocol. Fragments of the nuc rDNA internal transcribed spacers (ITS1-5.8S-ITS2 = ITS), *TEF*1-α and *RPB*2 were amplified with the primer pairs ITS4 and ITS5 (White et al. 1990), EF1-728F (Carbone and Kohn 1999) and TEF1LLErev (Jaklitsch et al. 2005), fRPB2-5f and fRPB2-7cr (Liu et al. 1999), respectively. PCR products were purified with the PCR Product Purification Kit (Biocolor BioScience and Technology Co., Shanghai, China) and cycle-sequenced on an ABI 3730 XL DNA Sequencer (Applied Biosciences, Foster City, Calofornia) with the same primer in fragments amplification for ITS and primers reported by Jaklitsch (2009) for *TEF*1-α, and *RPB*2 at Beijing Tianyihuiyuan Bioscience and Technology, China. The strains and the NCBI GenBank accession numbers of DNA sequences used in this work are listed in Table 1.

Phylogenetic analyses

Sequences were assembled, aligned and manually adjusted when needed with BioEdit 7.0.5.3 (Hall 1999). NEXUS files were generated with Clustal X 1.83 (Thompson et al. 1997). To identify the phylogenetic positions of *Trichoderma fujianense* and *T. zonatum*, *RPB*2 and *TEF*1-α sequences were combined for the analyses. Thirty-three sequences representing 30 *Trichoderma* taxa were selected for analyses, with *Nectria eustromatica* and *N. berolinensis* selected as outgroup taxa. Alignments are deposited in TreeBASE accession number 21272.

Maximum parsimony (MP) analysis was performed with PAUP 4.0b10 (Swofford 2002) using 1000 replicates of heuristic search with random addition of sequences

Table 1. Materials including strain numbers and GenBank accessions of sequences used for phylogenetic analyses.

Name	Strain	GenBank accession number	
		RPB2	TEF1-α
Trichoderma aerugineum Jaklitsch	CBS 120541	FJ860516	FJ860608
T. aureoviride Rifai	C.P.K. 2848	FJ860523	FJ860615
T. ceramicum P. Chaverri & Samuels	CBS 114576	FJ860531	FJ860628
T. chlorosporum P. Chaverri & Samuels	G.J.S. 88-33	AY391903	AY391966
T. chromospermum P. Chaverri & Samuels	G.J.S. 94-68	AY391913	AY391974
T. costaricense (P. Chaverri & Samuels) P. Chaverri, Jaklitsch & Voglmayr	P.C. 21	AY391921	AY391980
T. cremeoides Jaklitsch & Voglmayr	S112	KJ665253	KJ665456
T. cremeum P. Chaverri & Samuels	G.J.S. 91-125	AF545511	AF534598
T. cuneisporum P. Chaverri & Samuels	G.J.S. 91-93	AF545512	AF534600
T. danicum (Jaklitsch) Jaklitsch & Voglmayr	CBS 121273	FJ860534	FJ860634
T. estonicum P. Chaverri & Samuels	G.J.S. 96-129	AF545514	AF534604
T. fujianense Z.X. Zhu, W.Y. Zhuang &Y. Li	HMJAU 34830	**MF374808***	**MF374811**
T. gelatinosum P. Chaverri & Samuels	G.J.S. 88-17	AF545516	AF534579
T. gliocladium Jaklitsch & Voglmayr	S81	KJ665271	KJ665502
T. helicum Bissett, C.P. Kubicek & Szakács	DAOM 230021	DQ087239	KJ871125
T. longipile Bissett	CBS 120953	FJ860542	FJ860643
T. nigrovirens P. Chaverri & Samuels	G.J.S. 99-64	AF545518	AF534582
T. parestonicum Jaklitsch	CBS 120636	FJ860565	FJ860667
T. phyllostachydis P. Chaverri & Samuels	G.J.S. 92-123	AF545513	AF534576
T. pseudocandidum Minnis, Samuels & P. Chaverri	P.C. 59	AY391899	AY391962
T. rosulatum Z.X. Zhu & W.Y. Zhuang	HMAS 252548	KF730005	KF729984
T. sinuosum P. Chaverri & Samuels	G.J.S. 90-88	AY391932	AY391990
T. spinulosum (Fuckel) Jaklitsch & Voglmayr	CBS 121280	FJ860589	FJ860699
T. stipitatum Z.X. Zhu & W.Y. Zhuang	HMAS 266613	KF730012	KF729991
T. strictipile Bissett	C.P.K. 1601	FJ860594	FJ860704
T. surrotundum P. Chaverri & Samuels	G.J.S. 88-73	AF545540	AF534594
T. thailandicum P. Chaverri & Samuels	G.J.S. 97-61	AY391957	AY392005
T. thelephoricola P. Chaverri & Samuels	CBS 120925	FJ860600	FJ860711
T. virescentiflavum (Speg.) Jaklitsch & Voglmayr	P.C. 278	AY391959	AY392007
T. zonatum Z.X. Zhu, W.Y. Zhuang &Y. Li	HMJAU 34820	**MF374806**	**MF374809**
	HMJAU 34825	**MF374807**	**MF374810**
Nectria eustromatica Jaklitsch & Voglmayr	CBS 121896	HM534886	HM534875
N. berolinensis (Sacc.) Cooke	CBS 127382	HM534883	HM534872

Note: *Numbers in bold indicate newly submitted sequences.

and subsequent TBR (tree bisection and reconnection) branch swapping. Analyses were performed with all characters treated as unordered and unweighted, gaps treated as missing data. Topological confidence of resulted trees was tested by maximum parsimony bootstrap proportion (MPBP) with 1000 replications, each with 10 replicates of random addition of taxa.

Bayesian Inference (BI) analysis was conducted via MrBayes 3.1.2 (Ronquist and Huelsenbeck 2003) using a Markov Chain Monte Carlo (MCMC) algorithm. Nucleotide substitution models were determined by MrModeltest 2.3 (Nylander 2004). GTR+I+G was estimated as the best-fit model for combined sequences. Four MCMC chains were run from random trees for 2 000 000 generations and sampled every 100 generations. The first 5000 trees were discarded as the burn-in phase of the analyses, and Bayesian inference posterior probability (BIPP) was determined from the remaining trees. Trees were visualized in TreeView 1.6.6 (Page 1996).

Results

Phylogenetic analyses

The partition homogeneity test (P = 0.01) of *RPB*2 and *TEF*1-α sequences indicated that the individual partitions were generally congruent (Cunningham 1997). Phylogenetic positions of the new species were determined by analyses of the combined *RPB*2 and *TEF*1-α dataset containing 33 taxa and 2396 characters, of which 1304 characters were constant, 366 variable characters were parsimony-uninformative and 726 were parsimony-informative. Five most-parsimonious trees with the same topology were generated (Figure 1) (tree length = 3178, CI = 0.4685, HI = 0.4572, RI = 0.5493 and RC = 0.2982).

Thirty-three sequences representing 30 green-spored *Trichoderma* species and two outgroup taxa *Nectria berolinensis* and *N. eustromatica* were used to construct the phylogenetic tree (Figure 1). All the green-spored species formed a monophyletic group (100 % MPBP/BIPP), which is basically consistent with the previous study by Jaklitsch (2009) and Zhu and Zhuang (2015).

In our phylogenetic tree, the five major clades, Chlorosporum, Spinulosum, Virescentiflavum, Ceramicum and Strictipile were basically well supported. The first four clades received 100%/100%, 98%/100%, 100%/100% and 100%/- (MPBP/BIPP) support in the tree, respectively, but the Strictipile clade was less strongly supported at 61% (MPBP) in the tree.

In the Chlorosporum clade (Figure 1), two samples of *Trichoderma zonatum* (HMJAU 34820 and 34825), sharing identical sequences, constituted a well-supported independent lineage (MPBP/BIPP = 100 %/100 %). Although *T. zonatum* is morphologically similar to *T. chromospermum*, they are not phylogenetically close and have relatively low sequence similarities in *RPB*2, *TEF*1-α and ITS.

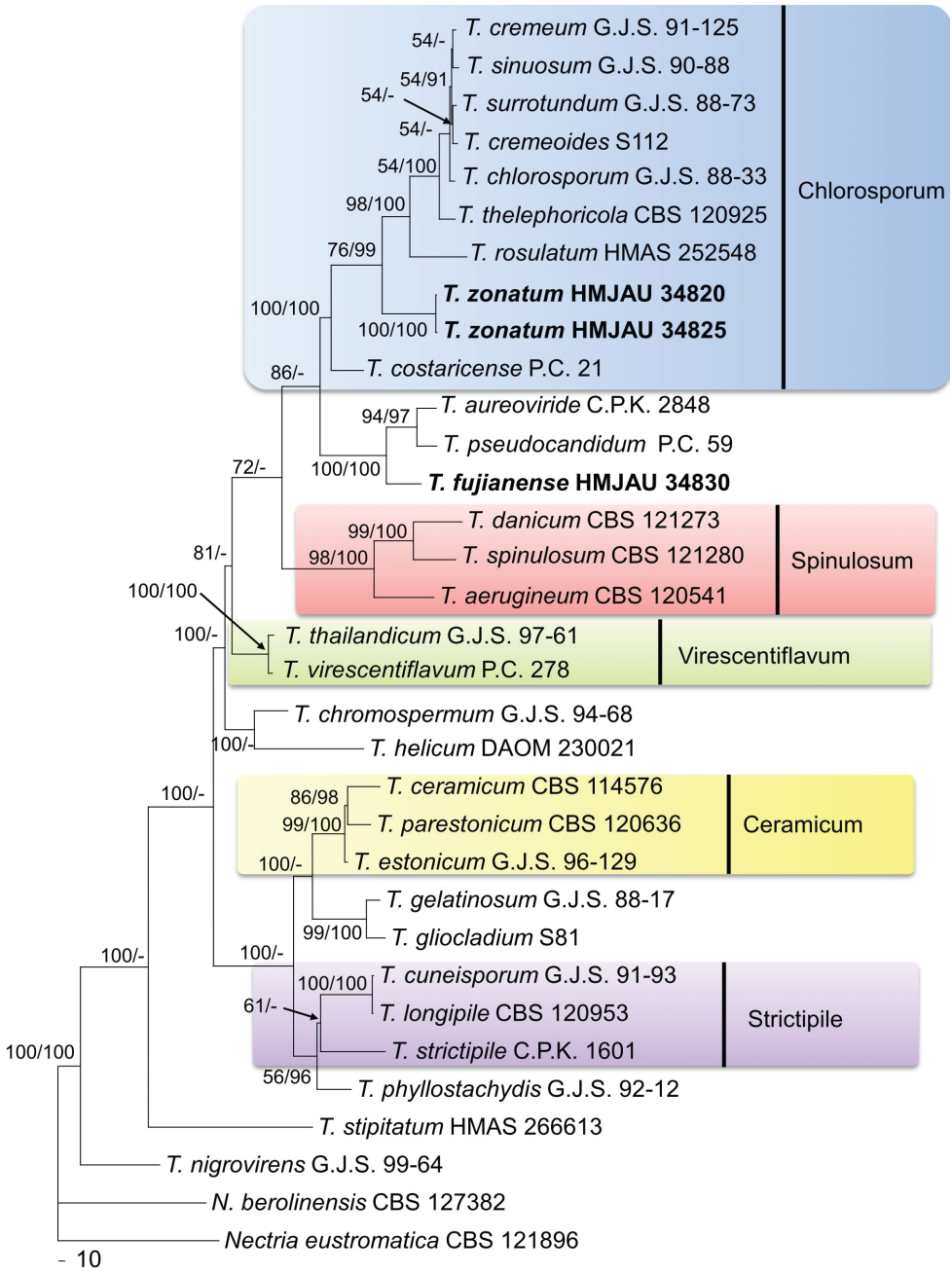

Figure 1. Maximum parsimony phylogram reconstructed from the combined squences of *RPB*2 and *TEF*1-α. MPBP above 50% (left) and BIPP above 90% (right) are indicated at the nodes.

Trichoderma aureoviride, *T. candidum* and *T. fujianense* form an independent lineage with high statistical support (MPBP/BIPP = 100%/100%), which still remains unnamed (Chaverri and Samuels 2003, Jaklitsch 2009).

Taxonomy

***Trichoderma fujianense* Z.X. Zhu, W.Y. Zhuang & Y. Li, sp. nov.**
MycoBank: MB821807
Figure 2

Diagnosis. Characterized by slender to lageniform, long phialides (14–23 × 2–3.5 µm), gliocladium to verticillium-like conidiophores, ellipsoidal to cylindrical conidia (4.5–5.5 × 2.5–3.5 µm).

Type. CHINA. Fujian: Quanzhou City, Qingyuan mountain. 24°56'51"N, 118°36'31"E, 150 m alt., on bark, 6 Aug 2015, Z.X. Zhu 230 (HMJAU 34830, holotype), Ex-type culture CGMCC 3.18757.

Description. Colony radius on CMD after 72 h 2.5–5 mm at 20 °C, 13–15 mm at 25 °C, 3.5–5 mm at 30 °C, no growth at 35 °C, mycelium covering the plate after 2 wk at 25°C. Colony circular, dense, finely zonate, becoming hairy to floccose by conidiophores, first whitish, turning light green. Aerial hyphae virtually absent. Autolytic excretions, pigment and coilings absent. Conidiation starting after 4 d in densely disposed gliocladium-like conidiophores, short-effuse, turning green after 1 wk.

Colony radius on PDA after 72 h 7.5–8.5 mm at 20 °C, 8.5–10 mm at 25 °C, 0.5–1 mm at 30 °C, no growth at 35 °C, mycelium covering the plate after 2 wk at 25 °C. Colony circular, compact with distinctly zonate, with commonly lobed or coarsely wavy margin, centre dense, green, margin relatively looser, whitish. Conidiation noted around the plug after 3–4 d, effuse, spreading from the centre over the entire colony surface. No distinct odor, no diffusing pigment observed.

Colony radius on SNA after 72 h 1.5–3 mm at 20 °C, 4–5 mm at 25 °C, 1–2 mm at 30 °C, no growth at 35 °C, mycelium covering the plate after 24 d at 25 °C. Colony hyaline, thin, irregular, not zonate, surface mycelium scant. Aerial hyphae inconspicuous, short. Conidiophores sparsely disposed, noted after 7 d, gliocladium to verticillium-like, with 1–3(–4) whorls arising from the main axis. Phialides arising in more or less narrow angles from cylindrical metulae, phialides slender to lageniform, somewhat curved, (10–)14–23(–28) × 2–3.5(–4) µm, l/w 4.8–7.2(–9.2), (1.5–)1.8–2.7(–3.2) µm wide at the base (n = 100). Conidia green, ellipsoidal to cylindrical, smooth, (4–)4.5–5.5(–6) × 2.5–3.5(–4) µm, l/w (1.2–)1.3–2.0 (n = 100). No distinct odor, no diffusing pigment observed.

Habitat and distribution. On the surface of rotten wood in humid forests of east China.

Etymology. The epithet "*fujian*", indicating occurrence of the fungus in Fujian province.

Teleomorph. Not known.

Remarks. Morphologically, the new species is most similar to *Trichoderma costaricense* in conidiophore character and phialide shape and size; while the latter fungus produces abundant chlamydospores on CMD, has relatively larger conidia (5.2–6.0 × 3.2–4.0 µm) and faster growth on PDA and SNA, and grows well and sporulates at 35 °C (Chaverri and Samuels 2003). Furthermore, sequence similarity

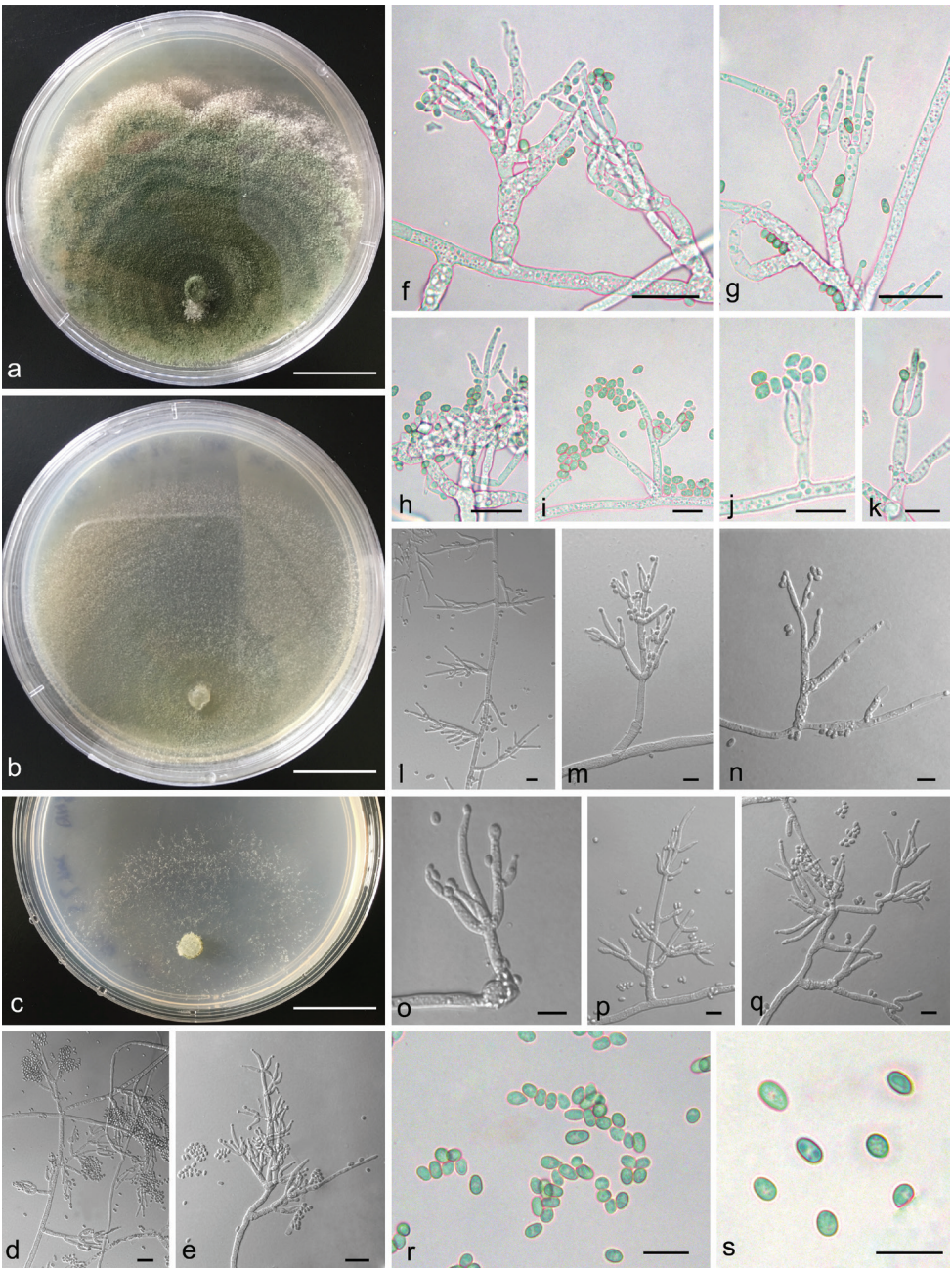

Figure 2. The new species *Trichoderma fujianense*, holotype (HMJAU 34830). **a–s** Asexual state **a–c** Cultures after 13 d at 25 °C (**a** PDA, **b** CMD, **c** SNA). **d–q** Conidiophores and phialides (SNA, 20 d) **r, s** Conidia (SNA, 20 d). Scales bars: 20 mm (**a–c**); 20 μm (**d–h**); 10 μm (**i–s**).

of ITS and *RPB*2 between these species was only 90.1% and 92.1%, with 60 bp and 68 bp differences among 606 bp and 864 bp, respectively. Among the species with green ascospores, *T. gelatinosum*, *T. nigrovirens*, *T. chromospermum* and *T. thelephoricola* also generated gliocladium to verticillium-like conidiophores, but they are not phylogenetically closely related.

The phylogenetic positions of the new taxa (Figure 1) demonstrated that *Trichoderma fujianense* is found to be closely related to *T. aureoviride* and *T. candidum*, and three of them form an independent lineage with high statistical support. However, *T. aureoviride* is distinctive by shorter conidia (3.8–4.0 × 3.0–3.3 µm, l/w 1.2–1.3); *T. candidum* differs by shorter phialides (7.3–)9.0–13.5(–16.5) µm, globose to subglobose and smaller conidia (3.2–3.5 × 3.0–3.2 µm, l/w (1.0–)1.1(–1.3) (Chaverri and Samuels 2003).

***Trichoderma zonatum* Z.X. Zhu, W.Y. Zhuang & Y. Li, sp. nov.**
MycoBank: MB821806
Figure 3

Diagnosis. Characterized by pulvinate, pale yellow to light brown stromata with densely disposed dark green to black ostioles, long asci (93–112 × 5.8–6.6 µm), monomorphic and subglobose ascospores (4.2–5 × 4–4.7 µm), simple trichoderma-like conidiophores, green, (sub)globose to pyriform conidia (2.8–3.8 × 2.3–2.8 µm).

Type. CHINA. Henan: Xinyang City, Jigong mountain. 31°49'2"N, 114°04'16"E, 1500 m alt., on bark, 16 Jul 2015, B. Zhang 220 (HMJAU 34820, holotype), Ex-type culture CGMCC 3.18758.

Description. Stromata generally solitary, scattered, gregarious, or aggregated in small groups, broadly attached, pulvinate to somewhat flattened, outline circular or with lobed margin, (0.5–)1.0–2.5(–3) mm diam (n = 20), (0.3–)0.5–0.8 mm high (n = 20). Surface flat, smooth, with slight perithecial protuberances, pale yellow to light brown, not changing colour in KOH, ostiolar openings obvious due to the green ascospores.

In section stroma cortical tissue of textura angularis, 13–28 µm thick, not changing colour in 3% KOH, cells yellow, thin-walled, 6–12(–17) × 5–10(–13) µm (n = 40); subcortical tissue of textura angularis, cells hyaline, thin-walled, 4–10 × 5–8 µm (n = 40); subperithecial tissue of textura epidermoidea, cells hyaline, thin-walled, 10–22 × 8–17 µm (n = 40); tissue at the base of textura intricata, hyphae hyaline, thin-walled, (2.5–)3.5–6(–8) µm (n = 40) wide. Perithecia subglobose or flask-shaped, crowded, 178–216 ×120–165 µm (n = 40); peridium yellow in lactic acid, not changing colour in 3% KOH, (8–)10–14(–17) µm thick at the sides, (12–)14–21(–27) µm at the base (n = 40). Ostioles conical or cylindrical, 51–70 µm high, 31–54 µm wide at the apex (n = 40). Asci cylindrical, 93–112 × 5.8–6.6(–7) µm, with a stipe (13–)18–23 µm long (n = 60). Part-ascospores green, turning brown in KOH, distinctly verrucose, cells monomorphic, subglobose, also slightly ovoid, 4.2–5 × 4–4.7 µm (n = 100), l/w 1.0–1.1.

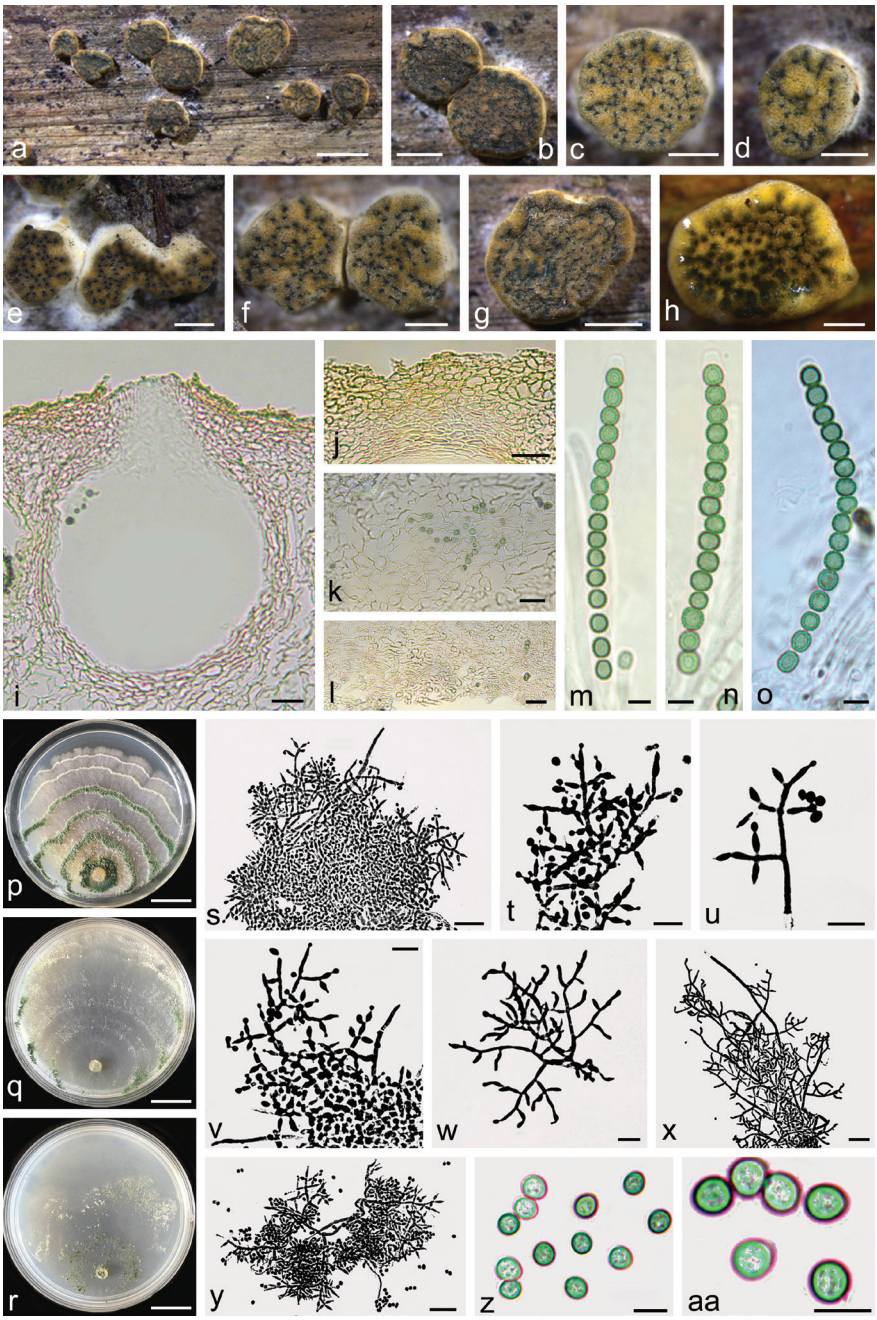

Figure 3. The new species *Trichoderma zonatum*, holotype (HMJAU 34820). **a–o** Sexual state. **a–g** Dry stromata on nature substrate **h** Mature stroma after rehydration **i** Perithecium in section **j** Cortical and subcortical tissue in section **k** Subperithecial tissue in section **l** Stroma base in section. **m–o** Ascus with part-ascospores. **p–aa** Asexual state. **p–r** Cultures after 7 d at 25 °C (**p** PDA, **q** CMD, **r** SNA). **s–y** Conidiophores and phialides (SNA, 7 d). **z, aa** Conidia (SNA, 7 d). Scales bars: 2 mm (**a**); 1 mm (**b, g**); 500 μm (**c–f, h**); 20 μm (**i–l, s, x, y**); 5 μm (**m–o, z, aa**); 20 mm (**p–r**); 10 μm (**t–w**).

On CMD colony radius after 72 h 30–43 mm at 20 °C, 32–46 mm at 25 °C, 17–34 mm at 30 °C, no growth at 35 °C. Colony hyaline, circular, loose, forming obvious zonate, covering the plate after 5–7 d at 25 °C. Aerial hyphae radially arranged. Conidiation at 25 °C noted after 3 d, first effuse, soon followed by formation of granules or pustules, particularly along the margin, spreading from the centre across the entire plate. No distinct odor, no diffusing pigment observed.

On PDA after 72 h 38–48 mm at 20 °C, 55–62 mm at 25 °C, 28–30 mm at 30 °C, no growth at 35 °C; mycelium covering the plate after 8 d at 25°C. Colony circular, conspicuously dense, becoming zonate with broad, slightly downy zones and narrow, well-defined, convex, white to green farinose zones. Aerial hyphae numerous, mostly short, becoming fertile from the centre. Conidiation at 25 °C starting after 2 d, green after 4 d, first simple, mostly on short aerial hyphae concentrated in the centre and in denser zones, later abundant in pustules. Autolytic activity lacking or inconspicuous, no coilings seen. No diffusing pigment, no distinct odour noted.

On SNA after 72 h 12–14 mm at 20 °C, 18–20 mm at 25 °C, 15–17 mm at 30 °C, no growth at 35 °C; mycelium covering the plate after 8–9 d at 25°C. Colony hyaline, thin, loose, irregularly lobed, not zonate. Aerial hyphae inconspicuous. Autolytic activity moderate. Conidiophores visible after 4 d, trichoderma-like, with 2–3(–4) whorls arising from the main axis. Phialides solitary or divergent in whorls of 2–3, mostly asymmetrically arranged, lageniform, (5–)7–11(–14) × 2–3(–4) µm, l/w 1.7–2.8(–4) (n = 60). Conidia green, (sub)globose to pyriform, smooth, (2.5–)2.8–3.8 × 2.3–2.8 µm, l/w (1.0–)1.1–1.3(–1.5) (n = 70). No chlamydospores formed. No distinct odor, no diffusing pigment observed.

Habitat and distribution. On the surface of rotten wood in humid forests of south central and east China.

Etymology. The specific epithet refers to the zonate colony on PDA.

Other specimens examined. CHINA. Fujian: Quanzhou City, Qingyuan mountain. 24°55'53"N, 118°36'31"E, 200 m alt., on bark, 6 Aug 2015, Z.X. Zhu 225, HMJAU 34825, Ex-type culture CGMCC 3.18759.

Remarks. Phylogenetic analyses based on *RPB2* and *TEF1*-α indicated that *Trichoderma zonatum* belongs to the Chlorosporum clade, previously consisting of eight species, *T. sinuosum*, *T. cremeum*, *T. surrotundum*, *T. chlorosporum*, *T. thelephoricola*, *T. rosulatum*, *T. cremeoides* and *T. costaricense*. Phylogenetically, *T. zonatum* is most related to *T. rosulatum* and *T. costaricense*, but *T. rosulatum* is clearly distinguishable by dimorphic ascospores, gliocladium-like conidiophores, production of abundant chlamydospores and rosulate colony on CMD (Zhu and Zhuang 2015); *T. costaricense* produces dimorphic and larger ascospores (5.5–6.0 × 5.2–5.7 µm), verticillium-like conidiophores and ellipsoidal to cylindrical conidia (Chaverri and Samuels 2003, Zhu and Zhuang 2015).

Species of the Chlorosporum clade usually produce pale yellow or pale green, semi-translucent stromata, globose to subglobose ascospores and gliocladium-like or verticillium-like conidiophores (Chaverri and Samuels 2003, Zhu and Zhuang 2015). *Trichoderma zonatum* is characterized by pulvinate, pale yellow to light brown stromata with densely disposed dark green to black ostioles, monomorphic ascospores, simple

trichoderma-like conidiophores, green, (sub)globose to pyriform conidia. Morphologically, stromata of *T. zonatum* are not typical of the Chlorosporum clade and differ from all other species by relatively larger and non-transparent. It is most similar to *T. chromospermum* in gross stromata morphology, while the latter fungus clearly differs by much shorter asci [(78–)85–90(–102) µm], gliocladium-like conidiophores and ellipsoidal to cylindrical conidia (Chaverri and Samuels 2003, Zhu and Zhuang 2015).

Discussion

Phylogenetic analyses of *Trichoderma* species with green spores based on sequences of *RPB*2 and *TEF*1-α were performed by Chaverri and Samuels (2003). In the more recent study by Zhu and Zhuang (2015) a phylogenetic tree with 45 species having green-spored was inferred from *RPB*2 and *TEF*1-α sequences. In our study analyses of the combined sequences of the same genes of 30 related *Trichoderma* species were carried out to ascertain the phylogenetic positions of our new species. The tree topology is basically consistent with previous researches (Chaverri and Samuels 2003, Jaklitsch 2009, Zhu and Zhuang 2015). The study of Chaverri and Samuels (2003) suggested that phenotypic characters, alone are usually not useful in understanding phylogenetic relationships in *Trichoderma*, because teleomorph characters, for example, the tissue structure of the stroma, the size and character of the perithecia, asci and ascospores, are generally highly conserved and anamorph characters tend to be morphologically divergent within monophyletic groups, clades or species complex. Based on the results of the present study, we conclude that similarity in teleomorphic characters is not indicative of close phylogenetic relationships, holomorphs must be studied in order to effectively determine both life cycles and species concepts.

Acknowledgments

The authors thank Dr. Bo Zhang for collecting specimens jointly for this study. This project was supported by Science and Technology Developing Plan of Jilin Province (20160520054JH), China Postdoctoral Science Foundation and University S & T Innovation Platform of Jilin Province for Economic Fungi (#2014B-1).

References

Almeida FB, Cerqueira FM, Silva RN, Ulhoa CJ, Lima AL (2007) Mycoparasitism studies of *Trichoderma harzianum* strains against *Rhizoctonia solani*: evaluation of coiling and hydrolytic enzyme production. Biotechnology letters 29: 1189–1193. https://doi.org/10.1007/s10529-007-9372-z

Bissett J, Gams W, Jaklitsch WM, Samuels GJ (2015) Accepted *Trichoderma* names in the year 2015. IMA Fungus 6: 263–295. https://doi.org/10.5598/imafungus.2015.06.02.02

Carbone I, Kohn LM (1999) A method for designing primer sets for speciation studies in filamentous ascomycetes. Mycologia 91: 553–556. https://doi.org/10.2307/3761358

Chaverri P, Samuels GJ (2003) *Hypocrea*/*Trichoderma* (Ascomycota, Hypocreales, Hypocreaceae): species with green ascospores. Studies in Mycology 48: 1–116.

Chen K, Zhuang WY (2016) *Trichoderma shennongjianum* and *Trichoderma tibetense*, two new soil-inhabiting species in the Strictipile clade. Mycoscience 57: 311–319. https://doi.org/10.1007/s00284-017-1282-2.

Cheng CH, Yang CA, Peng KC (2012) Antagonism of *Trichoderma harzianum* ETS 323 on *Botrytis cinerea* mycelium in culture conditions. Phytopathology 102: 1054–1063. https://doi.org/10.1094/Phyto-11-11-0315

Cunningham CW (1997) Can three incongruence tests predict when data should be combined? Molecular Biology and Evolution 14: 733–740. https://doi.org/10.1093/oxfordjournals.molbev.a025813

Hall TA (1999) BioEdit: a user-friendly biological sequence alignment editor and analysis program for Windows 95/98/NT. Nucleic Acids Symposium Series 41: 95–98.

Harman GE, Howell CR, Viterbo A, Chet I, Lorito M (2004) *Trichoderma* species–opportunistic, avirulent plant symbionts. Nature Reviews in Microbiology 2: 43–56. https://doi.org/10.1038/nrmicro797

Hasan MM, Rahman SM, Kim GH, Abdallah E, Oh DH (2012) Antagonistic potentiality of *Trichoderma harzianum* towards seed-borne fungal pathogens of winter wheat cv. Protiva in vitro and in vivo. Journal of Microbiology and Biotechnology 22: 585–591. https://doi.org/10.4014/jmb.1107.07063

Jaklitsch WM (2009) European species of *Hypocrea* I. The green-spored species. Studies in Mycology 63: 1–91. https://doi.org/10.3114/sim.2009.63.01

Jaklitsch WM, Komon M, Kubicek CP, Druzhinina IS (2005) *Hypocrea voglmayrii* sp. nov. from the Austrian Alps represents a new phylogenetic clade in *Hypocrea*/*Trichoderma*. Mycologia 97: 1365–1378. https://doi.org/10.3852/mycologia.97.6.1365

Kim CS, Shirouzu T, Nakagiri A, Sotome K, Nagasawa E, Maekawa N (2012a) *Trichoderma mienum* sp nov. isolated from mushroom farms in Japan. Antonie van Leeuwenhoek 102: 629–641. https://doi.org/10.1080/15572536.2006.11832743

Kim CS, Yu SH, Nakagiri A, Shirouzu T, Sotome K, Kim SC, Maekawa N (2012b) Re-evaluation of *Hypocrea pseudogelatinosa* and *H. pseudostraminea* isolated from shiitake mushroom (*Lentinula edodes*) cultivation in Korea and Japan. The Plant Pathology Journal 28: 341–356. https://doi.org/10.5423/PPJ.OA.05.2012.0068

Kredics L, Antal Z, Dóczi I, Manczinger L, Kevei F, Nagy E (2003) Clinical importance of the genus *Trichoderma*. Acta Microbiologica et Immunologica Hungarica 50: 105–117. https://doi.org/10.1556/AMicr.50.2003.2-3.1

Kuhls K, Lieckfeldt E, Börner T, Guého E (1999) Molecular re-identification of human pathogenic *Trichoderma* isolates as *Trichoderma longibrachiatum* and *Trichoderma citrinoviride*. Medical Mycology 37: 25–33. https://doi.org/10.1080/02681219980000041

Liu M, Liu J, Wang WM (2012) Isolation and functional analysis of Thmfs1, the first major facilitator superfamily transporter from the biocontrol fungus *Trichoderma harzianum*. Biotechnology Letters 34: 1857–1862. https://doi.org/10.1007/s10529-012-0972-x

Liu YJ, Whelen S, Hall BD (1999) Phylogenetic relationships among ascomycetes: evidence from an RNA polymerase II subunit. Molecular Biology and Evolution 16: 1799–1808. https://doi.org/10.1093/oxfordjournals.molbev.a026092

Lopes FAC, Steindorff AS, Geraldine AM, Brandao RS, Monteiro VN, Lobo M, Coelho ASG, Ulhoa CJ, SilvaRN (2012) Biochemical and metabolic profiles of *Trichoderma* strains isolated from common bean crops in the Brazilian Cerrado and potential antagonism against *Sclerotinia sclerotiorum*. Fungal Biology 116: 815–824. https://doi.org/10.1016/j.funbio.2012.04.015

Montoya QV, Meirelles LA, Chaverri P, Rodrigues A (2016) Unraveling *Trichoderma* species in the attine ant environment: description of three new taxa. Antonie Van Leeuwenhoek 109: 633–51. https://doi.org/10.1007/s10482-016-0666-9

Mukherjee PK, Horwitz BA, Singh US, Mukherjee M, Schmoll M (2013) *Trichoderma*: Biology and Applications. CABI, 327 pp. https://doi.org/10.1079/9781780642475.0000

Nylander JAA (2004) MrModeltest 2. Program distributed by the author. Evolutionary Biology Centre, Uppsala University.

Page RDM (1996) TreeView: an application to display phylogenetic trees on personal computers. Computer Applications in the Biosciences 12: 357–358.

Park MS, Bae KS, Yu SH (2006) Two new species of *Trichoderma* associated with green mold of oyster mushroom cultivation in Korea. Mycobiology 34: 111–113. https://doi.org/10.4489/MYCO.2006.34.3.111

Qin WT, Zhuang WY (2016a) Four new species of *Trichoderma* with hyaline ascospores from central China. Mycological Progress 15: 811–825. https://doi.org/10.1007/s11557-016-1211-y

Qin WT, Zhuang WY (2016b) Four new species of *Trichoderma* with hyaline ascospores in the Brevicompactum and Longibrachiatum clades. Mycosystema 35: 1317–1336. https://doi.org/10.13346/j.mycosystema.160158

Qin WT, Zhuang WY (2016c) Seven wood-inhabiting new species of the genus *Trichoderma* (Fungi, Ascomycota) in Viride clade. Scientific Reports 6: 27074. https://doi.org/10.1038/srep27074

Qin WT, Zhuang WY (2016d) Three *Trichoderma* species new to China. Mygosystema 35: 1008-1017. https://doi.org/10.13346/j.mycosystema.150230

Qin WT, Zhuang WY (2016e) Two new hyaline-ascospored species of *Trichoderma* and their phylogenetic positions. Mycologia 108: 205–214. https://doi.org/10.3852/15-144

Qin WT, Zhuang WY (2017) Seven new species of *Trichoderma* (Hypocreales) in the Harzianum and Strictipile clades. Phytotaxa 305: 121–139. https://doi.org/10.11646/phytotaxa.305.3.1

Ronquist F, Huelsenbeck JP (2003) MrBayes 3: Bayesian phylogenetic inference under mixed models. Bioinformatics 19: 1572–1574. https://doi.org/10.1093/bioinformatics/btg180

Samuels GJ (1996) *Trichoderma*: a review of biology and systematic of the genus. Mycological Research 100: 923–935. https://doi.org/10.1016/S0953-7562(96)80043-8

Samuels GJ, Dodd SL, Gams W, Castlebury LA, Petrini O (2002) *Trichoderma* species associated with the green mold epidemic of commercially grown *Agaricus bisporus*. Mycologia 94: 146–170. https://doi.org/10.1080/15572536.2003.11833257

Shoresh M, Harman GE, Mastouri F (2010) Induced systemic resistance and plant responses to fungal biocontrol agents. Annual Review of Phytopathology 48: 21–43. https://doi.org/10.1146/annurev-phyto-073009-114450

Sun JZ, Pei YF, Li E, Li W, Hyde KD, Yin WB, Liu XZ (2016) A new species of *Trichoderma hypoxylon* harbours abundant secondary metabolites. Scientific Reports 6: 37369. https://doi.org/10.1038/srep37369

Swofford DL (2002) PAUP 4.0b10: Phylogenetic analysis using parsimony. Sinauer Associates, Sunderland, MA, U.S.A.

Thompson JD, Gibson TJ, Plewniak F, Jeanmougin F, Higgins DG (1997) The Clustal X windows interface: flexible strategies for multiple sequence alignment aided by quality analysis tools. Nucleic Acids Research 25: 4876–4882. https://doi.org/10.1093/nar/25.24.4876

White TJ, Bruns T, Lee S, Taylor J (1990) Amplification and direct sequencing of fungal ribosomal RNA genes for phylogenetics. In: Innis MA, Gelfand DH, Sninsky JJ, White TJ (Eds) PCR Protocols: A Guide to Methods and Applications. Academic Press, New York, 315–322. https://doi.org/10.1016/b978-0-12-372180-8.50042-1

Zhu ZX, Zhuang WY (2015) *Trichoderma* (*Hypocrea*) species with green ascospores from China. Persoonia 34: 113–129. https://doi.org/10.3767/003158515X686732

MycoKeys 26: 77–83 (2017)
doi: 10.3897/mycokeys.26.14602
http://mycokeys.pensoft.net

SOFTWARE DESCRIPTION

A peer-reviewed open-access journal
MycoKeys
Launched to accelerate biodiversity research

A dynamic, web-based resource to identify rust fungi (Pucciniales) in southern Africa

Alistair R. McTaggart[1], Dean R. Beasley[2], Michael J. Wingfield[1], Alan R. Wood[3], Zakkie A. Pretorius[4], Andre Drenth[5], Roger G. Shivas[2,6], Jolanda Roux[1]

1 *Department of Plant and Soil Sciences, Forestry and Agricultural Biotechnology Institute (FABI), Faculty of Natural and Agricultural Sciences (NAS), University of Pretoria, Pretoria, South Africa* **2** *Plant Pathology Herbarium, Biosecurity Queensland, Department of Agriculture and Fisheries, Dutton Park, Queensland, Australia* **3** *ARC-Plant Protection Research Institute, Stellenbosch 7599, South Africa* **4** *Department of Plant Sciences, University of the Free State, Bloemfontein, South Africa* **5** *Queensland Alliance for Agriculture and Food Innovation, The University of Queensland, Ecosciences Precinct, Brisbane, Queensland, Australia* **6** *Centre for Crop Health, Institute for Agriculture and the Environment, University of Southern Queensland, Toowoomba, Queensland, Australia*

Corresponding author: *Alistair R. McTaggart* (alistair.mctaggart@gmail.com)

Academic editor: *D. Begerow* | Received 19 June 2016 | Accepted 27 August 2017 | Published 15 September 2017

Citation: McTaggart AR, Beasley DR, Wingfield MJ, Wood AR, Pretorius ZA, Drenth A, Shivas RG, Roux J (2017) A dynamic, web-based resource to identify rust fungi (Pucciniales) in southern Africa. MycoKeys 26: 77–83. https://doi.org/10.3897/mycokeys.26.14602

Abstract

Rust fungi (Pucciniales) are some of the most important plant pathogens that cause diseases of agricultural and tree crops. There are approximately 8,000 described species worldwide. The rust fungi of South Africa were extensively studied by Ethel M. Doidge (1887 – 1965), who listed 468 species. Many nomenclatural and taxonomic changes, together with the discovery of new species and incursions of exotic species, have subsequently outdated Doidge's monograph. To address this problem, we have developed an interactive Lucid key for the identification of 50 species of rust fungi in 17 genera from countries in southern Africa. The key is dynamic and may be updated in real-time. The Lucid key provides a platform to progressively provide descriptions and images for all rust fungi in southern Africa. Plant pathologists and mycologists are invited to participate in the development of this resource.

Keywords

cybertaxonomy, key, Lucid, morphology, *Puccinia porri*, rust fungi, taxonomy, Uredinales

Copyright *Alistair R. McTaggart et al.* This is an open access article distributed under the terms of the Creative Commons Attribution License (CC BY 4.0), which permits unrestricted use, distribution, and reproduction in any medium, provided the original author and source are credited.

Introduction

Rust fungi (Pucciniomycotina, Pucciniales) are highly specialized obligate plant pathogens. They cause some of the most important diseases of plants used for agriculture and forestry, as well as for natural ecosystems globally. There are approximately 550 species of rust recorded from southern Africa (Berndt 2008b). Some introduced taxa have severely impacted agriculture, forestry and endangered native plants, including *Austropuccinia psidii* (Roux et al. 2016), *Melampsora medusae* (Trench et al. 1988), *Puccinia graminis* (Pretorius et al. 2015; Visser et al. 2011), and *Uromycladium acaciae* (Little and Payn 2016). Rust fungi have also been intentionally introduced to South Africa as biological control agents, such as *Uromycladium tepperianum*, to control the weedy and exotic *Acacia saligna* (Wood and Morris 2007).

Doidge (1950) listed the rust fungi in southern Africa, and included information on host, location and specimens examined (available at: http://www.westerdijkinstitute.nl/BioloMICSNews.aspx?Rec=5637). This work covered 468 species, of which 128 were either described or re-combined in a series of earlier papers (Doidge 1926; 1928; 1939; 1941; 1948a; b). Doidge (1950) remains an essential reference for the identification of rust fungi in southern Africa, including Angola, Botswana, Lesotho, Malawi, Mozambique, Namibia, South Africa, Swaziland, Tanzania, Zambia and Zimbabwe.

Subsequent to Doidge (1950), there have been 43 new species described, 48 new introductions recorded, and 18 name changes in 27 scientific papers that treat rust fungi in South Africa. Most of these changes and additions were summarized by Berndt (2008b), who studied the biodiversity of rust fungi in southern Africa and estimated the potential species richness in relation to the diversity of plant species. Berndt (2008b) also published a species list that updated new reports, species descriptions and taxonomy of all rust fungi in Botswana, Namibia and South Africa.

Lists of species have two weaknesses for identification of taxa. Firstly, a list is outdated after any taxonomic change or new discovery. For example, since Berndt (2008b) compiled the latest list of rust fungi for southern Africa, at least four new species were described (Berndt 2008a; Maier et al. 2015; Martin et al. 2017; Wood et al. 2014), several new species reported (Berndt 2009; McTaggart et al. 2015b; Mostert et al. 2008; Mostert et al. 2010; Roux et al. 2013) and names changed (Beenken and Wood 2015; Berndt 2008a). Secondly, lists often do not provide information on morphology or how to identify taxa. Rust fungi are generally host specific and morphologically distinct, which helps identify species from a list. However, identification of a species from a list of names may be problematic in cases where either (i) the host identity is uncertain, (ii) there are more than one species of rust on one host, (iii) two hosts are required for the completion of the lifecycle (heteroecious rusts), or (iv) good quality drawings or images are not provided. To complicate matters, rust fungi, which have up to five stages in their life cycles, were often classified in anamorphic genera, e.g. *Aecidium* and *Uredo*, if their teliospores were not known.

Accurate identification of plant pathogenic fungi and the discovery of cryptic species has been advanced by molecular data (Crous et al. 2015). However, rust fungi are obligate pathogens and challenging for molecular work. Possibly for this reason, there

are few reference sequences of rust fungi publically available. For example, of the 4,000 described species of *Puccinia*, approximately 200 (0.05%) of these have either an ITS or LSU sequence on GenBank (Marin-Felix et al. 2017). Molecular identification from a barcode marker is more common for well-studied species of rust fungi.

A web-based resource to identify rust fungi by host and morphology in southern Africa is introduced in the present study. The resource is based around a Lucid key, freely available to all users. The key is dynamic, and can be updated according to taxonomic changes or the discovery of new taxa. The scientific community is invited to contribute specimens and images to the development of this key.

Methods

Taxon selection and identification

The first 50 species of rust that accompany the release of this key were collected from the Gauteng, KwaZulu-Natal, Limpopo and Mpumalanga provinces in South Africa, and from Botswana and Swaziland. Specimens were usually collected during field surveys of forestry plantations as well as in adjacent native or farmed vegetation. These 50 species are commonly encountered or important pathogens of trees in natural and planted forests, including *Austropuccinia psidii*, *Phakopsora myrtacearum*, *Ravenelia macowaniana*, *Uromyces aloës* and *Uromycladium acaciae*. Specimens were identified on the basis of their host and morphology of spores. In some cases molecular barcodes were used for identification. This is described below for the identification of *Puccinia porri*, and was published for identifications made in prior studies (Maier et al. 2015; McTaggart et al. 2015b; Roux et al. 2013).

Morphology and image capture

Spore stages, such as aeciospores, urediniospores and teliospores, were removed from host material with a scalpel, then mounted in clear lactic acid (100% v/v) on a microscope slide and gently heated. Slides were examined with a Leica DM 2500 compound microscope using differential interference microscopy and images were taken with a Leica DFC550 camera. Measurements of each examined spore stage were made from a minimum of 20 spores per specimen.

The approach to stacking multiple images follows that of Shivas et al. (2014). Composite images were made with image stacking software Helicon Focus (Helicon Soft, Kharkov). For example, teliospores shown on the website are montaged from two to four images taken through different focal planes. Images of spore stages with ornamented walls were captured in two focal planes, one through the equator of the spores, and the other through the upper surface of the wall. The roll-over Java Script used by Shivas et al. (2014), to simulate focusing through a microscope, was incorporated for spore stages with ornamented walls.

Host symptoms were photographed with hand-held digital cameras, for example a Coolpix Nikon S9300. Host symptoms of fresh leaf material were scanned on an Epson Perfection V700 flatbed scanner with a minimum resolution of 300 dpi. Images that were finally used for the website were selected based on their quality and diagnostic potential.

Key development

An interactive key, the *Rust Fungi of Southern Africa*, was built using Lucid 3.5.32 (http://www.lucidcentral.org). The dataset used for rust fungi had 93 features and 320 character states, which included the morphological features of all spore stages present on the examined specimens.

Results

The key has been made publicly available at the following URL: http://collections.daf.qld.gov.au/web/key/africarust.

There are 50 taxa uploaded to the website. Two of these are species of *Ravenelia* that may represent new taxa. There are 18 genera on the website, of which *Aecidium* and *Uredo* are anamorphic genera used for species with unknown telial stages that have uncertain phylogenetic positions. The website contains 190 images, of which 38 are field shots, 48 are scanned host symptoms and 104 are spore stages taken from a light microscope.

A comprehensive list of rust fungi reported in southern Africa since Doidge (1950) is included in the 'references and records' page of the website. The list includes references that have described or reported new taxa, and changed taxonomic names of rust fungi in southern Africa.

One taxon included in the *Rust Fungi of Southern Africa* is a new addition for the region. *Puccinia porri*, which was taxonomically resolved by McTaggart et al. (2016a), was found on *Allium porrum* in South Africa. This identification was confirmed by an ITS-LSU sequence that had 100% identity over 1646 characters to specimens on GenBank identified as *P. porri* by McTaggart et al. (2016a). This sequence has been deposited in GenBank (KY849820) and the specimen can be viewed on the *Rust Fungi of Southern Africa* (collections.daff.qld.gov.au/web/key/africarust/Media/Html/pucciniaporri.html). Rust fungi on species of *Allium* in South Africa were previously identified as *P. allii* (Doidge 1950), which is a species complex.

Discussion

Identification of rust fungi is challenging for a number of reasons, including their complex lifecycles, multiple species on one host, multiple hosts and the fact that there

are few contemporary resources with information about their biology and morphology. Furthermore, identification based on a molecular barcode is not always possible, as many species have not been sequenced. The *Rust Fungi of Southern Africa* is a web-based, interactive resource that allows users to identify taxa based on host range and morphology. The identification is supported by comparison to images of symptoms and spore stages made from reference specimens. It further acts as a real-time list of rust fungi in southern Africa.

Berndt (2008b) recorded about 546 species of rust fungi in Botswana, Namibia and South Africa. The literature indicates that there are 572 species of rust fungi in southern Africa, which we have listed in the *Rust Fungi of Southern Africa*. Many of these species will certainly represent the same organism, for example, independently described aecial or uredinial stages of teleomorphic species (Berndt 2008b). There are 90 species of *Aecidium* and 53 species of *Uredo* in the list of taxa, and these will likely belong to other genera such as *Puccinia* (discussed by McTaggart and Shivas in Marin-Felix et al. 2017).

Further diversity may be expected from cryptic species, which have been found in multiple genera of rust fungi on hosts in the Annonaceae (Beenken 2014), Fabaceae (Doungsa-ard et al. 2015; McTaggart et al. 2015a) and Poaceae (Demers et al. 2017; Liu and Hambleton 2013). Doidge (1950) recorded one species of rust, *Uromyces aloës*, on 18 different host species, and this may represent a taxon with cryptic diversity.

Two rust fungi were recently described in southern Africa from agricultural and forestry hosts, namely *Macruropyxis fulva* on *Saccharum* and *Phakopsora myrtacearum* on *Eucalyptus* (Maier et al. 2015; Martin et al. 2017). It is interesting that two new rusts were found on introduced, well-studied plants in southern Africa. Host jumps were found to be one of the main drivers of speciation for rust fungi (McTaggart et al. 2016b), and host shifts or jumps from native plant species in South Africa to introduced species may explain the observed new taxa on exotic, well-studied hosts.

The Rust Fungi of Southern Africa is the second publicly released Lucid key to identify rust fungi. The Rust Fungi of Australia (available at: http://collections.daff.qld.gov.au/web/key/rustfungi) currently contains 122 species (Shivas et al. 2014). The broader scientific and non-scientific communities are invited to contribute images and specimens to the authors and help build these resources. Submissions for the resource will be acknowledged as a contribution on the home page of the website.

Acknowledgements

We thank the members of the Tree Protection Co-operative Programme (TPCP), the THRIP initiative of the Department of Trade and Industry, and the Department of Science and Technology (DST) / National Research Foundation (NRF) Centre of Excellence in Tree Health Biotechnology (CTHB) for financial assistance that made this study possible. The authors have no conflict of interest to declare.

References

Beenken L (2014) Pucciniales on *Annona* (Annonaceae) with special focus on the genus *Phakopsora*. Mycological Progress 13: 791–809. https://doi.org/10.1007/s11557-014-0963-5

Beenken L, Wood AR (2015) *Puccorchidium* and *Sphenorchidium*, two new genera of Pucciniales on Annonaceae related to *Puccinia psidii* and the genus *Dasyspora*. Mycological Progress 14: 1–13. https://doi.org/10.1007/s11557-015-1073-8

Berndt R (2008a) The rust fungi (Uredinales) on ferns in South Africa. Mycological Progress 7: 7–19. https://doi.org/10.1007/s11557-007-0548-7

Berndt R (2008b) The rust mycobiota of southern Africa: Species richness, composition, and affinities. Mycological Research 112: 463–471. https://doi.org/10.1016/j.mycres.2007.05.005

Berndt R (2009) New species of rust fungi (Uredinales) from South Africa and new observations on known species. Mycological Progress 8: 99–114. https://doi.org/10.1007/s11557-008-0582-0

Crous PW, Hawksworth DL, Wingfield MJ (2015) Identifying and naming plant-pathogenic fungi: past, present, and future. Annual Review of Phytopathology 53: 247–267.

Demers JE, Liu M, Hambleton S, Castlebury LA (2017) Rust fungi on *Panicum*. Mycologia: 1–17. https://doi.org/10.1080/00275514.2016.1262656

Doidge EM (1926) A preliminary study of South African rust fungi. Bothalia 2: 1–228.

Doidge EM (1928) South African rust fungi. Part II. Bothalia 2: 473–474.

Doidge EM (1939) South African rust fungi. Part III. Bothalia 3: 487–512.

Doidge EM (1941) South African rust fungi. Part IV. Bothalia 4: 229–236.

Doidge EM (1948a) South African rust fungi. Part V. Bothalia 5: 895–918.

Doidge EM (1948b) South African rust fungi. Part VI. The species of *Uromyces* on Iridaceae. Bothalia 5: 919–937.

Doidge EM (1950) The South African fungi and lichens to the end of 1945. Bothalia 5: 1–1094

Doungsa-ard C, McTaggart AR, Geering ADW, Dalisay TU, Ray J, Shivas RG (2015) *Uromycladium falcatarium* sp. nov., the cause of gall rust on *Paraserianthes falcataria* in south-east Asia. Australasian Plant Pathology 44: 25–30. https://doi.org/10.1007/s13313-014-0301-z

Little KM, Payn RG (2016) Screening of fungicides for the management of wattle rust (*Uromycladium acaciae*) in *Acacia mearnsii* plantations, South Africa. Southern Forests 78: 151–158.

Liu M, Hambleton S (2013) Laying the foundation for a taxonomic review of *Puccinia coronata s.l.* in a phylogenetic context. Mycological Progress 12: 63–89. https://doi.org/10.1007/s11557-012-0814-1

Maier W, McTaggart AR, Roux J, Wingfield MJ (2015) *Phakopsora myrtacearum* sp. nov., a newly described rust (Pucciniales) on eucalypts in eastern and southern Africa. Plant Pathology 65: 189–195. https://doi.org/10.1111/ppa.12406

Marin-Felix Y, Groenewald JZ, Cai L, Chen Q, Marincowitz S, Barnes I, Bensch K, Braun U, Camporesi E, Damm U, De Beer ZW, Dissanayake A, Edwards J, Giraldo A, Hernández-Restrepo M, Hyde KD, Jayawardena RS, Lombard L, Luangsa-ard J, McTaggart AR, Rossman AY, Sandoval-Denis M, Shen M, Shivas RG, Tan YP, van der Linde EJ, Wingfield MJ, Wood AR, Zhang JQ, Zhang Y, Crous PW (2017) Genera of phytopathogenic fungi: GOPHY 1. Studies in Mycology 86: 99–216. https://doi.org/10.1016/j.simyco.2017.04.002

Martin LA, Lloyd Evans D, Castlebury LA, Sifundza JT, Comstock JC, Rutherford RS, McFarlane SA (2017) *Macruropyxis fulva* sp. nov., a new rust (Pucciniales) infecting sugarcane in southern Africa. Australasian Plant Pathology 46: 63–74. https://doi.org/10.1007/s13313-016-0460-1

McTaggart AR, Doungsa-ard C, Geering ADW, Aime MC, Shivas RG (2015a) A co-evolutionary relationship exists between *Endoraecium* (Pucciniales) and its *Acacia* hosts in Australia. Persoonia 35: 50–62. https://doi.org/10.3767/003158515X687588

McTaggart AR, Doungsa-ard C, Wingfield MJ, Roux J (2015b) *Uromycladium acaciae*, the cause of a sudden, severe disease epidemic on *Acacia mearnsii* in South Africa. Australasian Plant Pathology 44: 637–645. https://doi.org/10.1007/s13313-015-0381-4

McTaggart AR, Shivas RG, Doungsa-ard C, Weese TL, Beasley DR, Hall BH, Metcalf DA, Geering AD (2016a) Identification of rust fungi (Pucciniales) on species of *Allium* in Australia. Australasian Plant Pathology 45: 581–592. https://doi.org/10.1007/s13313-016-0445-0

McTaggart AR, Shivas RG, van der Nest MA, Roux J, Wingfield BD, Wingfield MJ (2016b) Host jumps shaped the diversity of extant rust fungi (Pucciniales). New Phytologist 209: 1149–1158. https://doi.org/10.1111/nph.13686

Mostert L, Bester W, Coertze S, Wood AR (2008) First report of daylily rust caused by *Puccinia hemerocallidis* in the Western Cape Province of South Africa. Plant Disease 92: 1133. https://doi.org/10.1094/PDIS-92-7-1133A

Mostert L, Bester W, Jensen T, Coertze S, van Hoorn A, Le Roux J, Retief E, Wood A, Aime MC (2010) First report of leaf Rust of blueberry caused by *Thekopsora minima* on *Vaccinium corymbosum* in the Western Cape, South Africa. Plant Disease 94: 478–478. https://doi.org/10.1094/pdis-94-4-0478c

Pretorius ZA, Bender CM, Visser B (2015) The rusts of wild rye in South Africa. South African Journal of Botany 96: 94–98. doi:https://doi.org/10.1016/j.sajb.2014.10.005

Roux J, Granados GM, Shuey L, Barnes I, Wingfield MJ, McTaggart AR (2016) A unique genotype of the rust pathogen, *Puccinia psidii*, on Myrtaceae in South Africa. Australasian Plant Pathology 45: 645–652. https://doi.org/10.1007/s13313-016-0447-y

Roux J, Greyling I, Coutinho TA, Verleur M, Wingfield MJ (2013) The Myrtle rust pathogen, *Puccinia psidii*, discovered in Africa. IMA Fungus 4: 155–159

Shivas RG, Beasley DR, McTaggart AR (2014) Online identification guides for Australian smut fungi (Ustilaginomycotina) and rust fungi (Pucciniales). IMA Fungus 5: 195–202.

Trench TN, Baxter AP, Churchill H (1988) First Report of *Melampsora medusae* on *Populus deltoides* in Africa. South African Forestry Journal 144: 6–9. https://doi.org/10.1080/00382167.1988.9630310

Visser B, Herselman L, Park RF, Karaoglu H, Bender CM, Pretorius ZA (2011) Characterization of two new *Puccinia graminis* f. sp. *tritici* races within the Ug99 lineage in South Africa. Euphytica 179: 119–127. https://doi.org/10.1007/s10681-010-0269-x

Wood AR, Lutz M, Bauer R, Oberwinkler F (2014) Morphology and phylogenetics of *Stomatisora*, including *Stomatisora psychotriicola* sp. nov. Mycological Progress 13: 997. doi:DOI 10.1007/s11557-014-0997-8

Wood AR, Morris MJ (2007) Impact of the gall-forming rust fungus *Uromycladium tepperianum* on the invasive tree *Acacia saligna* in South Africa: 15 years of monitoring. Biological Control 41: 68–77.